Properties of Nuclear Levels in a Number of Odd-A Nuclei ($151 \leq A \leq 191$)

B. HARMATZ AND T. H. HANDLEY
Oak Ridge National Laboratory, Oak Ridge, Tennessee*

AND

J. W. MIHELICH†
University of Notre Dame, Notre Dame, Indiana

(Received June 29, 1962)

In order to obtain more evidence on the systematic behavior of nuclear energy levels in the deformed region, a number of neutron-deficient odd-mass activities were studied with internal conversion electron spectrographs. Some scintillation counter measurements were made. Level schemes are postulated for decays leading to the following odd-neutron nuclei: $Pm^{151} \rightarrow Sm^{151}$, $Tb^{151} \rightarrow Gd^{151}$, $Tb^{153} \rightarrow Gd^{153}$, $Tb^{155} \rightarrow Gd^{155}$, $Eu^{157} \rightarrow Gd^{157}$, $Tm^{163} \rightarrow Er^{163}$, $Tm^{165} \rightarrow Er^{165}$, $Ho^{167} \rightarrow Er^{167}$, $Re^{183} \rightarrow W^{183}$, $Ir^{185} \rightarrow Os^{185}$, $Ir^{187} \rightarrow Os^{187}$, and $Ir^{189} \rightarrow Os^{189}$. As a corollary, data are presented for the odd-proton nuclei populated in the decays of $Pt^{189} \rightarrow Ir^{189}$ and $Pt^{191} \rightarrow Ir^{191}$. The proposed states are described using the Mottelson and Nilsson predictions. Some conclusions may be drawn concerning such properties of these orbitals as moments of inertia, $M1/E2$ mixing ratios, and positions of the intrinsic excitations. Ratios of gamma-ray transition probabilities from the various states are given. Previously published studies of odd-A nuclei in the region of odd-N numbers 99–107 are incorporated in the energy-level systematics.

I. INTRODUCTION

IT has become clear that the majority of the large number of levels observed in the radioactive decay of the odd-mass nuclei in the deformed rare-earth region may be described by the unified model,[1] incorporating the intrinsic levels as calculated by Nilsson (see Fig. 1)[2] with rotational excitatnio of these levels. In general, the low-lying nuclear level structure of the odd-A rare earths is fairly well known, although many details are still to be investigated. The emphasis, theoretically, is to try to explain the observed phenomena with more detailed models, as have Nilsson and Prior,[3] who have calculated the moments of inertia and collective gyromagnetic ratios for even-even nuclei, taking into account pairing correlation. For odd-mass nuclei, the properties of a rotational band will depend on the details of the odd-particle orbital as well.

Mottelson and Nilsson[4] have performed analyses of the intrinsic states of odd-A rare-earth nuclei having an ellipsoidal equilibrium shape. They have used a set of asymptotic quantum numbers $[Nn_z\Lambda]$ and K to characterize the different single-particle states in the limit where the nuclear potential becomes an anisotropic harmonic oscillator. In this limit, the quantum numbers are N, the total number of nodes in the wave function; n_z, the number of nodal planes perpendicular to the symmetry axis; Λ, the projection of orbital angular momentum on the symmetry axis; and K, the projection of total angular momentum on the symmetry axis.

Mottelson and Nilsson[4] have classified a large number of experimentally observed levels which agree with their predictions. We have previously presented experimental evidence[5] for the level ordering of odd-A nuclei having odd-neutron numbers in the range of 99 to 107. The systematic behavior of the low-energy excitation spectra was quite striking and may be correlated with theoretical predictions. The situation, experimentally at least, is most clear in the middle of the deformed rare-earth region.

With this in mind, a number of odd-neutron nuclei have been investigated in the rare-earth region extending from Sm^{151} ($N=89$) to Os^{189} ($N=113$), with an aim to classify more completely the low-lying excitation spectra. Two of the odd-proton nuclei of Ir ($A=189$ and 191) were studied primarily to examine the behavior of excited states at the upper end of the deformed region. In general, we are trying to determine the positions and movements of the base or primary levels of possible rotational bands; for example, the $\frac{3}{2}-[521]$ base state reappears in nuclei between Sm^{151} and Yb^{167}, ranging in neutron numbers from 89 to 97. Checks have been made on the validity of the proposed state assignments, employing the quantitative description of any rotational excitation of these levels and the details of the electromagnetic de-excitation or feeding of these levels.

Essentially, this has been a high-resolution conversion electron study of electron-capture activities. The experimental procedure has been described previously.[6] Separated isotopes were irradiated in the ORNL 86-in. cyclotron with proton beams of 70 μA and varying in energy from 12 to 22 MeV. With rare-earth targets, a

* Operated for the U. S. Atomic Energy Commission by Union Carbide Corporation.

† Oak Ridge National Laboratory Consultant.

[1] A. Bohr and B. R. Mottelson, Kgl. Danske Videnskab. Selskab, Mat.-fys. Medd. **27**, No. 16 (1953).

[2] S. G. Nilsson, Kgl. Danske Videnskab. Selskab, Mat.-fys. Medd. **29**, No. 16 (1955).

[3] S. G. Nilsson and O. Prior, Kgl. Danske Videnskab. Selskab, Mat.-fys. Medd. **32**, No. 16 (1960).

[4] B. R. Mottelson and S. G. Nilsson, Kgl. Danske Videnskab. Selskab, Mat.-fys. Medd. **1**, No. 8 (1959).

[5] B. Harmatz, T. H. Handley, and J. W. Mihelich, Phys. Rev. **119**, 1345 (1960).

[6] B. Harmatz, T. H. Handley, and J. W. Mihelich, Phys. Rev. **114**, 1082 (1959).

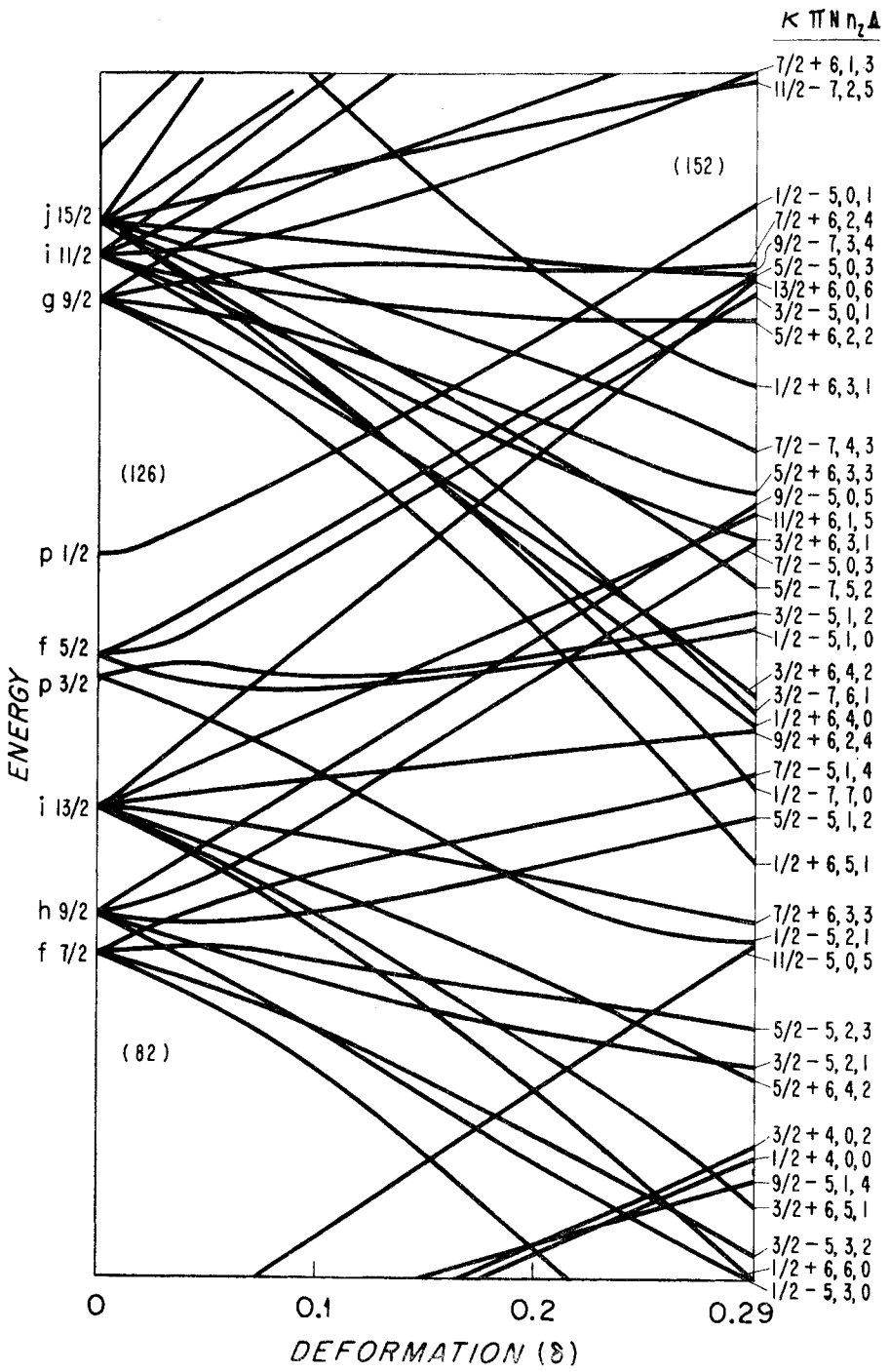

FIG. 1. The Nilsson representation for odd-neutron states in deformed nuclei (reference 4). The abscissa is the prolate deformation (δ), and the ordinate indicates the energy of the various levels designated by $K\pi[Nn_z\Lambda]$.

two-stage ion exchange separation was used to isolate the desired activity. This procedure was applicable to conversion electron spectroscopy with weak Eu^{157} and Ho^{167} activities produced by (p,α) reactions.

The iridium targets were fused with KOH and KNO_3 (50–50) and dissolved in HCl.[7] The Ir and Pt activity were reduced with stannous chloride followed by extraction of the Pt with ethyl acetate. The ethyl acetate was removed by evaporation and the Pt taken up in dilute HCl for plating on a wire source.

The osmium targets were dissolved in dilute nitric acid and the Os removed from the Ir activity by several distillations. The residue from distillation was placed in a quartz tube and evaporated in HCl just to dryness.

[7] G. W. Leddicotte, in *The Radiochemistry of Platinum* (National Academy of Sciences—National Research Council Publication No. 3044, Washington, D. C., 1962).

The quartz tube was heated to a bright redness and the iridium activity caught on a cold finger. The Ir was taken up in HCl with a small amount of NaCl added. Following evaporation of the HCl, the product was dissolved in water for electroplating onto 10-mil Pt wires.

The energies and intensities of a large number of converted transitions were obtained on Eastman "AA" x-ray film. Transition energies were determined precisely by a direct comparison of internal conversion lines with Auger lines and with other well-established energy measurements. The spectra are generally not monoisotopic. The isotopic assignment is based on relative activation yield with enriched isotopes and on the decay rate of the lines observed in a series of exposures.

The electron lines which cover a wide range of intensities were read on a series of spectrograms which must be normalized to each other. Only peak heights (corrected for radius of orbit and film response) of the photometrically determined intensities were measured. The errors which should be assigned to our measurements have been discussed previously.[5,6] For the lowest electron energies (~10 keV), the uncertainties are greatest, depending mainly on the quality of the source in the spectrograph.

TABLE I. Conversion electron data for decay of Tb^{151}(17 h) → Gd^{151}.

Transition energy (keV)	K	L_I	L_{II}	L_{III}	M	Remarks[a]
108.1	>1 000	170	180	165	100	$M1/E2=1.6$
180.1[b]	160	24		w	5.5	$M1$
183.2[b]	~1.5					
192.0	44	7				$M1$
251.8	155	21		w	5	$M1$
287.2	110	15		w	4	$M1$
318.5	1.0					
380.1[b]	1.7					
384.6[b]	2.3					
395.2	9	1.4				
416.0[b]	2.8	0.4				
426.4[b]	6.0	1.1				
443.8	11	1.6			0.4	
479.2	8	1.2			0.4	
499.8[b]	0.35					
511.7	0.35					
587.5	4.2	0.65				
604.8[b]	0.4					
703.9[b]	1.4	0.2				
731.7	1.3	0.2				
794.3[b]	~0.06					
798.8	~0.06					
805.5[b]	0.28	w				
906.0	0.17					
938.8[b]	~0.04					
979.5[b]	0.054					
1009.5[b]	~0.04					

Energy (keV)	K	Energy (keV)	K
1025.5[b]	0.035	1170.8[b]	0.075
1053.0[b]	w	1249.5[b]	w
1090.0[b]	0.043	1308.4[b]	0.055
1096.6[b]	~0.04	1311.7[b]	0.075

[a] Multipole assignments are based on K/L and L-subshell ratios. Intensity data are internally consistent. "w" indicates weak line.
[b] Not placed in decay scheme.

TABLE II. Intensity and multipolarity assigned to transitions depopulating levels shown in decay scheme of Tb^{151}(17 h) → Gd^{151} (Fig. 2).

Proposed excited states (keV)	π	De-exciting transitions (keV)	Multipole[a] assignment	Photon intensities Calculated[b]	Photon intensities Experimental[c]
108.1	(−)	108.1	$M1/E2=1.6$	1270	1600
395.2	(−)	287.2	$M1$	1130	980
		395.2	$M1$	228	~180
587.3	(−)	192.0	$M1$	163	~200
		479.2	($M1$)	320	
		587.5	$M1$	277	~120
839.0	(−)	251.8	$M1$	1125	1125
		443.8	($M1$)	380	
		731.7	($M1$)	154	

[a] Multipolarities are assigned either from conversion electron ratios or from conversion coefficients where photon intensity measurements are available. Assignments in parentheses are uncertain.
[b] Estimates of photon intensity are based on conversion electron data and theoretical conversion coefficients.
[c] Relative gamma-ray intensity data are normalized to the 251.8-keV ($M1$) transition.

In the tables of conversion electron data, multipole orders are based on a comparison of experimental K/L ratios and L- and M-subshell ratios with theoretical values of Rose.[8] In some cases, dipole radiation is classified as magnetic rather than electric due to the absence of an L_{III} conversion electron line. Values of $M1/E2$ mixtures (of photon intensities) are usually based on L-subshell ratios. In these conversion electron spectra, it is expected that $E1$ transitions are more likely to be unobserved as a result of their small conversion coefficients.

In the tables of suggested decay schemes, a number of multipolarities are proposed (if photon data are available) based on internal conversion coefficients. The multipole character of other transitions is often predictable, either from assignment to a rotational band or from angular momentum selection rules. The total transition intensities are subsequently deduced by applying the relevant theoretical internal conversion coefficient. For transitions close to K-electron binding energies, a more accurate estimate of transition intensity may be obtained from use of L-subshell values. One may roughly estimate the fraction of electron-capture decay directly to the ground state, using the estimate of K x-ray intensity calculated from the KLL Auger line intensity.[5]

The experimental decay schemes proposed are subject, of course, to the uncertainties which must always be considered. The energies, spins, and parities of the levels, properly determined, will be independent of the model attempting to explain them. The classifications of low-energy excited states are, in the main, based on considerable interlocking data. The uncertainties be-

[8] M. E. Rose, *Internal Conversion Coefficients* (North-Holland Publishing Company, Amsterdam, 1958).

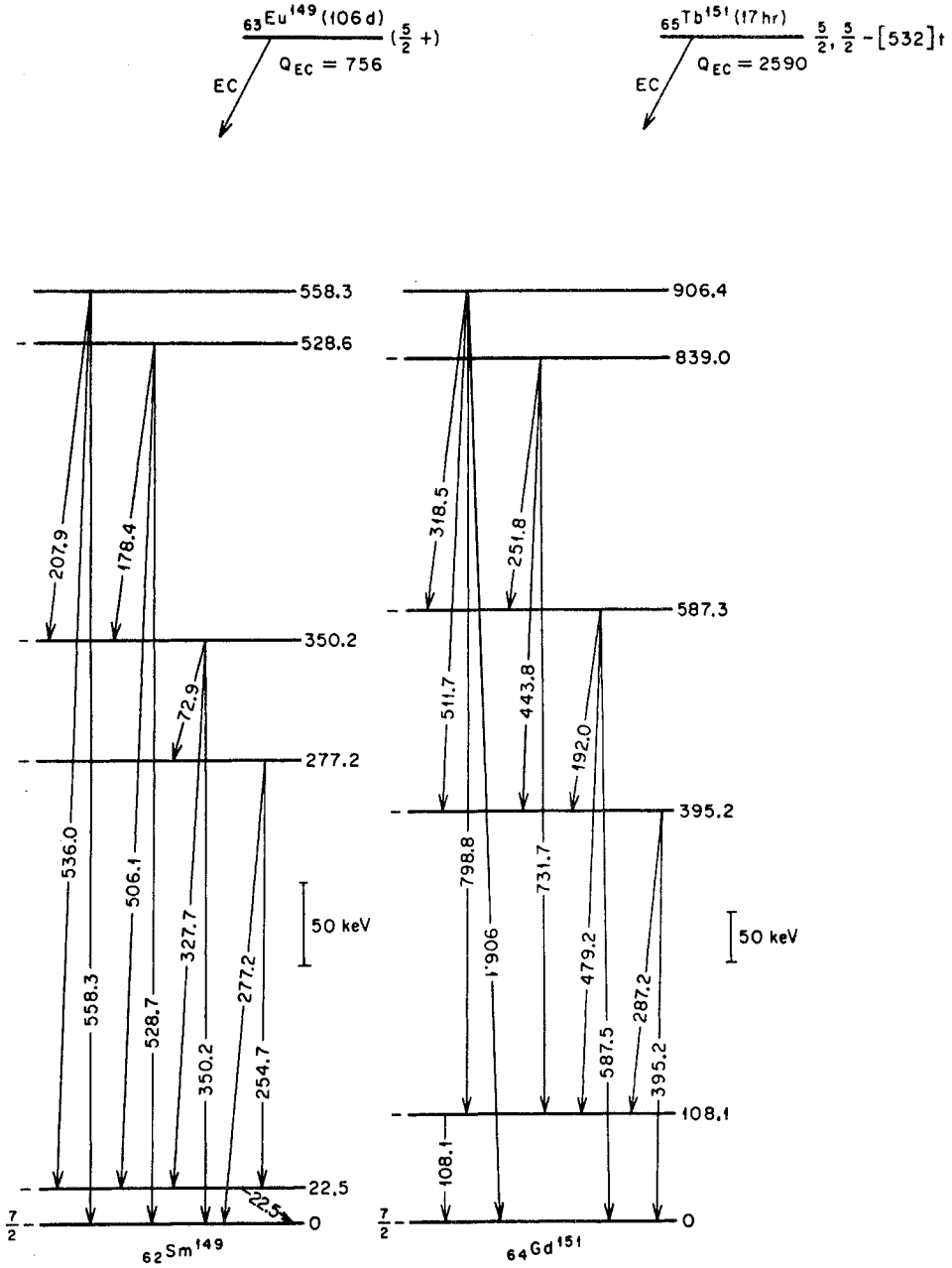

FIG. 2. Electron-capture (EC) decay schemes of Sm^{149} and Gd^{151}, nuclei with $N=87$. Independent linear energy scales are used. Level and transition energies are given in keV, including estimates of disintegration energy (Q_{EC}) taken either from Nuclear Data Sheets (reference 17) or from P. Seeger, Nuclear Phys. **25**, 1 (1961).

come greater if the level structures are affected by an appreciable decrease of the nuclear deformation or by a perturbation due to Coriolis coupling of states. One is also faced with the difficulty of establishing the nature or character of the high-lying states where rotational structures are not identifiable, and one must rely mainly on electromagnetic transition probabilities and on the systematic behavior of analogous states in neighboring nuclei. Where included, data on the strength of electron-capture branches and log(ft) estimates[9] may allow a test of state assignments. The classification of these branches derived from selection rules of Alaga[10] follows the notation: allowed (a), first-forbidden (1), unique first-forbidden (1*), hindered (h), and unhindered (u). Very few of the complex level schemes have been studied rigorously; however, the direction of future experiments is indicated.

II. DATA AND RESULTS

A. Tb^{151}(17 h) → Gd^{151}

The conversion electron spectrum of a source of Tb^{151}, produced by proton irradiation of Gd^{152}, has been re-

[9] S. A. Moszkowski, Phys. Rev. **82**, 35 (1951).

[10] G. Alaga, Phys. Rev. **100**, 432 (1955); Nuclear Phys. **4**, 625 (1957).

TABLE III. Intensity and multipolarity assigned to transitions depopulating levels shown in decay scheme of Eu^{149}(106 day) → Sm^{149} (Fig. 2).

Proposed excited states (keV)	π	De-exciting transitions (keV)	Multipole[a] assignment	Photon intensities Calculated[b]	Photon intensities Experimental[c]
22.5	(−)	22.5	$M1/E2=90$	150	
277.2	(−)	254.7	$(M1)$	210	
		277.2	$M1$	1190	1145
350.2	(−)	72.95	$M1+E2$	4	
		327.7	$M1$	1296	1135
		350.2	$M1$	74	<90
528.6	(−)	178.4	$M1$	7	<30
		506.1	$(M1)$	122	
		528.7	$(M1)$	98	

[a] Multipolarities are consistent with conversion electron ratios and available conversion coefficients. Assignments in parentheses are uncertain.
[b] Estimates of photon intensity are based on conversion electron data and theoretical conversion coefficients.
[c] Relative gamma-ray intensity data are normalized to agree with the $E2$ conversion coefficient of the 439-keV gamma ray belonging to Eu^{150}. Radiations which belong to long-lived Eu^{150} (e.g., 334 and 439 keV) are also present in the spectra.

examined.[11] Gd^{151} has 87 neutrons, the same as Sm^{149} which has been discussed in a previous publication.[12] The spin of Gd^{151} is perhaps $\frac{7}{2}-$, in analogy with Sm^{149}. The Tb^{151} parent is tentatively assigned as a $\frac{5}{2}-[532]$[13] state, corresponding to a deformation of $\delta<0.18$.

Tables I and II list our $Tb^{151} \rightarrow Gd^{151}$ conversion electron data as well as some γ-ray scintillation counter measurements. In Table II, the multipolarities of a few transitions were deduced from the internal conversion coefficients. The partial decay scheme constructed from these data, as well as the apparently similar level structure of Sm^{149}, is shown in Fig. 2. Note that different linear energy scales are employed in the chart. There is a striking similarity in the sequence of energies of excited states for the two isotones. The postulated states appear to be arranged in doublets with relatively small energy spacings. Likewise, the parities of the first five levels are the same, presumably negative. The levels in Sm^{149} populated by electron-capture decay of Eu^{149} are probably of relatively low spin ($I \leq \frac{7}{2}$). For the sake of completeness, we list in Table III the recently published $Eu^{149} \rightarrow Sm^{149}$ transition data[12] relevant to the decay scheme.

Many transitions of weaker intensity are present in the Tb^{151} spectrum, so that the complete decay scheme is considerably more complex than shown. Additional levels at 811.6, 1444, and 1566 keV are possible, based on energy sums. The unassigned 180.1-keV ($M1$) γ ray may originate at a 575-keV level and terminate at the 395.2-keV level according to the studies of Strigachev *et al.*[14]

Neither the Nilsson model nor the shell model[15] have been used to attempt to explain the level structures of Sm^{149} and Gd^{151}, in the absence of spin assignments.

B. Pm^{151}(28 h) → Sm^{151}

Little is known about particle and rotational states in odd-A, odd-N nuclei at the lower edge of the strongly deformed region. A marked change in nuclear structure occurs between the isotopes Eu^{151} and Eu^{153} (88 and 90 neutrons, respectively). Eu^{153} shows[16] a well-developed rotational structure; there is no apparent rotational pattern in Eu^{151}.[17]

One may question the propriety of assigning asymptotic quantum numbers to $N=89$ nuclei; e.g., Sm^{151} and Gd^{153}. The density of low-energy, low-spin states is high and the rotational bands built on particle states are unusual. As a result, some of the level assignments are not unique, and certainly further experiments are needed to confirm and complete the decay schemes.

The evidence available on the properties of rotational spectra for nuclei of $N=89$ are compared with the values for $N=91$, 93, 95, ··· in Table IV. In Table V, theoretical values for the ratios of reduced transition probabilities are compared with results found experimentally in the above odd-neutron nuclei. All transitions are K allowed.

The energy levels of Sm^{151} were studied from the β^- decay of Pm^{151}. The activity was produced by irradiating Nd^{150} with slow neutrons and extracting the Pm^{151} daughter by ion-exchange chemistry.

Internal conversion data for 60 transitions in Sm^{151} have been compiled in Table VI. There were difficulties in the measurement of intensities of high-energy lines due to the β^- background. Figure 3 shows the energy levels of Sm^{151} populated by decay of Pm^{151}. The ground-state spin of Pm^{151} ($N=90$) has been measured by Cabezas *et al.*[18] to be $\frac{5}{2}$; the $\frac{5}{2}-[532]$ orbital is predicted[4] for a deformation ($\delta \geq 0.2$. The $\frac{3}{2}+[651]$ configuration is assigned to the ground state of Sm^{151}, in analogy with isotone Gd^{153} and odd-A, $Z=89$ isotopes.

The postulated levels in Fig. 3 are consistent with transition energies, intensities, and multipolarities of

[11] J. W. Mihelich, B. Harmatz, and T. H. Handley, Phys. Rev. **108**, 989 (1957).
[12] B. Harmatz, T. H. Handley, and J. W. Mihelich, Phys. Rev. **123**, 1758 (1961).
[13] The notation used is $K\pi[Nn_z\Lambda]$. In the following discussion, this denotes the "primary" level of intrinsic nature, as contrasted to the collective state above it which is due to rotational excitation of the "primary" state.
[14] A. T. Strigachev, L. S. Novikov, A. A. Sorokin, V. A. Khalkin, N. V. Tsvetkova, and V. S. Shpinel. Izvest. Akad. Nauk. S.S.S.R., Ser. Fiziol. **25**, 813 (1961).
[15] M. G. Mayer and J. H. D. Jensen, *Elementary Theory of Nuclear Shell Structure* (John Wiley & Sons, New York, 1955).
[16] T. Suter, P. Reyes-Suter, S. Gustafsson, and I. Marklund, Nuclear Phys. **29**, 33 (1962).
[17] *Nuclear Data Sheets*, National Research Council, compiled by K. Way, F. Everling, G. H. Fuller, N. B. Gove, J. B. Marion, R. Nakasima, and C. L. McGinnis (U. S. Government Printing Office, Washington, D. C., 1958 to 1961).
[18] A. Cabezas, I. Lindgren, R. Marrus, and W. Nierenberg, University of California Radiation Laboratory Report UCRL-9225, 1960 (unpublished).

TABLE IV. Empirical constants for rotational bands and $M1/E2$ ratios ($89 \leq N \leq 107$).[a]

N	Nucleus	Assigned orbital $K\pi[Nn_z\Lambda]$	$E(I_0)$ (keV)	$3\hbar^2/\mathcal{I}$ (keV)	B (keV)	a	$I_0+1 \rightarrow I_0$ (keV)	$I_0+1 \rightarrow I_0$ $M1/E2$[b]
89	$_{64}Gd^{153}$	$\frac{3}{2}-[532]$	212.0	45.0			37.4	
89	$_{62}Sm^{151}$	$\frac{1}{2}+[660]$	4.85				64.8	pure $M1$
91	$_{64}Gd^{155}$	$\frac{1}{2}+[660]$	247.0	20.8		+0.88		
89	$_{64}Gd^{153}$	$\frac{3}{2}+[651]$	0	52.2	−0.077		41.6	15
91	$_{64}Gd^{155}$	$\frac{3}{2}+[651]$	86.5	37.7			31.4	pure $E2$
89	$_{64}Gd^{153}$	$\frac{3}{2}-[521]$	303.5	78.1				
91	$_{64}Gd^{155}$	$\frac{3}{2}-[521]$	0	72.7	+0.024		60.0	26
93	$_{64}Gd^{157}$	$\frac{3}{2}-[521]$	0	65.0	+0.01		54.5	29
95	$_{66}Dy^{161}$	$\frac{3}{2}-[521]$	74.5	68.6			57.1	32
95	$_{68}Er^{163}$	$\frac{3}{2}-[521]$	104.3	71.9	+0.01		60.2	18
97	$_{68}Er^{165}$	$\frac{3}{2}-[521]$	242.7	63.8			53.2	22
89	$_{64}Gd^{153}$	$\frac{5}{2}+[642]$	129.0	46.5			54.3	
93	$_{64}Gd^{157}$	$\frac{5}{2}+[642]$	64.0	44.4			51.8	34
95	$_{66}Dy^{161}$	$\frac{5}{2}+[642]$	0	37.5			43.8	24
95	$_{66}Dy^{161}$	$\frac{5}{2}-[523]$	25.6	66.9	−0.01		77.4	0.9
95	$_{68}Er^{163}$	$\frac{5}{2}-[523]$	0	72.0			83.9	0.12
97	$_{66}Dy^{163}$	$\frac{5}{2}-[523]$	0	63				
97	$_{68}Er^{165}$	$\frac{5}{2}-[523]$	0	66.2			77.2	pure $E2$
99	$_{70}Yb^{169}$	$\frac{5}{2}-[523]$	570.5	66.8				
99	$_{68}Er^{167}$	$\frac{5}{2}-[523]$	585.4	71.5			83.4	~7
99	$_{68}Er^{167}$	$\frac{7}{2}+[633]$	0	52.9			79.3	
99	$_{70}Yb^{169}$	$\frac{7}{2}+[633]$	0	47.2			70.9	14
101	$_{70}Yb^{171}$	$\frac{7}{2}+[633]$	95.2	48.2			72.3	14
103	$_{70}Yb^{173}$	$\frac{7}{2}+[633]$	351.2	53.0				
105	$_{72}Hf^{177}$	$\frac{7}{2}+[633]$	747.2	67.9				
95	$_{68}Er^{163}$	$\frac{1}{2}-[521]$	345.7	79.7		+0.47		
97	$_{68}Er^{165}$	$\frac{1}{2}-[521]$	297.2	76.0		+0.56	59.1	1.4
99	$_{68}Er^{167}$	$\frac{1}{2}-[521]$	207.8	67.2	+0.001	+0.70	57.1	7
99	$_{70}Yb^{169}$	$\frac{1}{2}-[521]$	24.3	70.4	−0.008	+0.79	62.8	1.9
101	$_{70}Yb^{171}$	$\frac{1}{2}-[521]$	0	72.4	−0.004	+0.85	66.7	2.1
101	$_{72}Hf^{173}$	$\frac{1}{2}-[521]$	0	77.1	−0.009	+0.82	69.8	1.3
103	$_{72}Hf^{175}$	$\frac{1}{2}-[521]$	125.9	81.0	−0.010	+0.75	70.5	1.1
107	$_{74}W^{181}$	$\frac{1}{2}-[521]$	746.1	90.2		+0.59		
99	$_{70}Yb^{169}$	$\frac{5}{2}-[512]$	191.4	75.4	−0.010		87.4	15
101	$_{70}Yb^{171}$	$\frac{5}{2}-[512]$	122.4	73.5	−0.005		85.5	
101	$_{72}Hf^{173}$	$\frac{5}{2}-[512]$	107.2	77.6	−0.007		90.2	
103	$_{70}Yb^{173}$	$\frac{5}{2}-[512]$	0	67.6	−0.003		78.7	20
103	$_{72}Hf^{175}$	$\frac{5}{2}-[512]$	0	70.0	−0.004		81.5	17
105	$_{72}Hf^{177}$	$\frac{5}{2}-[512]$	508.9	82.6			96.4	
107	$_{74}W^{181}$	$\frac{5}{2}-[512]$	365.5	94.6			110.3	
101	$_{70}Yb^{171}$	$\frac{7}{2}-[514]$	835.6	76.0				
103	$_{72}Hf^{175}$	$\frac{7}{2}-[514]$	348.8	86.0	−0.034		126.6	~2
105	$_{72}Hf^{177}$	$\frac{7}{2}-[514]$	0	76.4	−0.004		113.0	<0.1

[a] The energy constants within a rotational band are given by

$$E_I = E^0 + (\hbar^2/2\mathcal{I})[I(I+1) + a(-1)^{I+\frac{1}{2}}(I+\tfrac{1}{2})] + B[I(I+1) + a(-1)^{I+\frac{1}{2}}(I+\tfrac{1}{2})]^2,$$

where E_I is the energy of state of spin I, $\mathcal{I}$ is the moment of inertia, E^0 is a constant, and "a" is the decoupling parameter which is nonzero only for $K=\frac{1}{2}$, $I_0=\frac{1}{2}$ cases.

[b] Ratios (of photon intensities) obtained from L-subshell ratios.

Table VII; however, a prominent low-energy transition of 4.8 keV was not observed, due to a cutoff in film sensitivity below 9 keV. The 4.8-keV energy-level spacing agrees with the precisely measured energy difference between seven pairs of intense transitions. The 4.8-keV ($M1$) radiation may connect single-particle states $\frac{1}{2}+[660] \rightarrow \frac{3}{2}+[651]$ and is allowed unhindered (*au*) in the asymptotic quantum numbers.

There is a possible rotational level at 65.8 keV ($\frac{5}{2}+$) based on either the $\frac{3}{2}+[651]$ or $\frac{1}{2}+[660]$ primary states. This level is depopulated by a 65.8-keV γ ray ($M1/E2 \approx 30$) and by a 2% γ ray ($E2$) branch to the 4.8-keV ($\frac{1}{2}+$) state. A 69.7-keV ($\frac{3}{2}+$) rotational state could be associated with the $\frac{1}{2}+[660]$ band based at 4.8 keV. The rotational energy spacing $\frac{3}{2} \rightarrow \frac{1}{2}$ appears larger than might be expected for this orbital. The perturbation may perhaps be due to a Coriolis interaction which couples states which have the same spin

TABLE V. Ratios of reduced transition probabilities in de-excitation of levels in Sm, Gd, Dy, and Er ($151 \leq A \leq 165$).

Nucleus	Initial state $I(K\pi[Nn_z\Lambda])$	Initial state (keV)	Assumed multipolarity	Final states $I, I+1, I+2(K\pi[Nn_z\Lambda])$	Reduced transition[a] probability, exper.
Gd^{155}	$\frac{1}{2}(\frac{1}{2}+[400])$	588.0	$M1$	$\frac{1}{2}, \frac{3}{2}(\frac{1}{2}+[660]\dagger)$[c]	6.6/1
Er^{165}	$\frac{1}{2}(\frac{1}{2}+[651])$	507.1	$E1$	$\frac{1}{2}, \frac{3}{2}(\frac{1}{2}-[521])$	0.58/1
					0.5/1(theor.)[b]
Sm^{151}	$\frac{3}{2}(\frac{3}{2}+[402])$	104.85	$M1$	$\frac{1}{2}, \frac{3}{2}, \frac{5}{2}(\frac{1}{2}+[660]\dagger)$[c]	$\sim 15/1/\cdots$
Sm^{151}	$\frac{3}{2}(\frac{3}{2}-[532]\dagger)$	344.7	$E1$	$\frac{1}{2}, \frac{3}{2}, \frac{5}{2}(\frac{1}{2}+[660]\dagger)$[c]	$1.6/1/\cdots$
Gd^{155}	$\frac{3}{2}(\frac{3}{2}+[402])$	367.7	$M1$	$\frac{1}{2}, \frac{3}{2}, \frac{5}{2}(\frac{1}{2}+[660]\dagger)$[c]	0.02/1/0.4
					1.2/1/0.25(theor.)[b]
Er^{165}	$\frac{3}{2}(\frac{1}{2}+[651])$	589.4	$E1$	$\frac{1}{2}, \frac{3}{2}, \frac{5}{2}(\frac{1}{2}-[521])$	$4.2/w/1$
					0.6/0.1/1(theor.)[b]
Gd^{155}	$\frac{3}{2}(\frac{1}{2}+[660]\dagger)$	266.6	$M1$	$\frac{3}{2}, \frac{5}{2}(\frac{3}{2}+[651]\dagger)$[c]	1.6/1
Er^{163}	$\frac{3}{2}(\frac{1}{2}-[521])$	404.2	$M1$	$\frac{3}{2}, \frac{5}{2}(\frac{3}{2}-[521])$	0.54/1
Er^{165}	$\frac{3}{2}(\frac{1}{2}-[521])$	356.3	$M1$	$\frac{3}{2}, \frac{5}{2}(\frac{3}{2}-[521])$	0.35/1
					0.67/1(theor.)[b]
Gd^{155}	$\frac{5}{2}(\frac{1}{2}+[660]\dagger)$	268.6	$M1$	$\frac{3}{2}, \frac{5}{2}, \frac{7}{2}(\frac{3}{2}+[651]\dagger)$[c]	$3.4/1/\cdots$
Er^{163}	$\frac{5}{2}(\frac{1}{2}-[521])$	439.7	$M1$	$\frac{3}{2}, \frac{5}{2}, \frac{7}{2}(\frac{3}{2}-[521])$	0.12/1/1.3
Er^{165}	$\frac{5}{2}(\frac{1}{2}-[521])$	384.1	$M1$	$\frac{3}{2}, \frac{5}{2}, \frac{7}{2}(\frac{3}{2}-[521])$	$0.17/1/\cdots$
					0.15/1/1(theor.)[b]
Sm^{151}	$\frac{3}{2}(\frac{3}{2}-[521])$	167.8	$E1$	$\frac{3}{2}, \frac{5}{2}(\frac{3}{2}+[651]\dagger)$[c]	1.9/1
Gd^{153}	$\frac{3}{2}(\frac{3}{2}-[532]\dagger)$	212.1	$E1$	$\frac{3}{2}, \frac{5}{2}(\frac{3}{2}+[651]\dagger)$[c]	2.3/1
Gd^{153}	$\frac{3}{2}(\frac{3}{2}+[402])$	109.8	$M1$	$\frac{3}{2}, \frac{5}{2}(\frac{3}{2}+[651]\dagger)$[c]	9/1
Gd^{155}	$\frac{3}{2}(\frac{3}{2}+[651]\dagger)$	86.5	$E1$	$\frac{3}{2}, \frac{5}{2}(\frac{3}{2}-[521])$	3.7/1
Er^{165}	$\frac{3}{2}(\frac{3}{2}+[402])$	1427.0	$E1$	$\frac{3}{2}, \frac{5}{2}(\frac{3}{2}-[521])$	1.5/1
					1.5/1(theor.)[b]
Gd^{153}	$\frac{5}{2}(\frac{3}{2}-[532]\dagger)$	249.6	$E1$	$\frac{3}{2}, \frac{5}{2}(\frac{3}{2}+[651]\dagger)$[c]	2.4/1
Gd^{155}	$\frac{5}{2}(\frac{3}{2}+[651]\dagger)$	118.0	$E1$	$\frac{3}{2}, \frac{5}{2}(\frac{3}{2}-[521])$[c]	0.015/1
					1/1(theor.)[b]
Dy^{161}	$\frac{5}{2}(\frac{3}{2}-[521])$	132.1	$M1$	$\frac{5}{2}, \frac{7}{2}(\frac{5}{2}-[523])$	0.1/1
Er^{163}	$\frac{5}{2}(\frac{3}{2}-[521])$	164.5	$M1$	$\frac{5}{2}, \frac{7}{2}(\frac{5}{2}-[523])$	0.26/1
Er^{165}	$\frac{5}{2}(\frac{3}{2}-[521])$	295.9	$M1$	$\frac{5}{2}, \frac{7}{2}(\frac{5}{2}-[523])$	0.46/1
					0.4/1(theor.)[b]
Gd^{153}	$\frac{5}{2}(\frac{5}{2}+[642])$	129.2	$M1$	$\frac{3}{2}, \frac{5}{2}(\frac{3}{2}+[651]\dagger)$[c]	0.2/1
Gd^{155}	$\frac{5}{2}(\frac{5}{2}+[642])$	105.3	$E1$	$\frac{3}{2}, \frac{5}{2}(\frac{3}{2}-[521])$	1.1/1
Gd^{155}	$\frac{5}{2}(\frac{5}{2}-[523])$	286.8	$M1$	$\frac{3}{2}, \frac{5}{2}(\frac{3}{2}-[521])$	0.9/1
Gd^{153}	$\frac{5}{2}(\frac{5}{2}\pm)$	945.9	$M1$ or $E1$	$\frac{3}{2}, \frac{5}{2}(\frac{3}{2}+[651])$	1.5/1
Er^{165}	$\frac{5}{2}(\frac{5}{2}-[512])$	608.0	$M1$	$\frac{3}{2}, \frac{5}{2}(\frac{3}{2}-[521])$	0.6/1
					2.3/1(theor.)[b]
Gd^{153}	$\frac{5}{2}(\frac{5}{2}\pm)$	945.9	$M1$ or $E1$	$\frac{5}{2}, \frac{7}{2}(\frac{5}{2}+[642])$	1.7/1
Yb^{169}	$\frac{5}{2}(\frac{5}{2}-[523])$	570.5	$M1$	$\frac{5}{2}, \frac{7}{2}(\frac{5}{2}-[512])$	2.1/1
					2.5/1(theor.)[b]
Dy^{161}	$\frac{7}{2}(\frac{5}{2}-[523])$	103.2	$E1$	$\frac{5}{2}, \frac{7}{2}(\frac{5}{2}+[642])$	0.46/1
Yb^{169}	$\frac{7}{2}(\frac{5}{2}-[523])$	648.4	$M1$	$\frac{5}{2}, \frac{7}{2}(\frac{5}{2}-[512])$	0.44/1
					0.5/1(theor.)[b]
Gd^{153}	$\frac{7}{2}(\frac{3}{2}+[651]\dagger)$	93.4	$E2$	$\frac{3}{2}, \frac{5}{2}(\frac{3}{2}+[651]\dagger)$	0.32/1
					0.67/1(theor.)[b]
Dy^{161}	$\frac{9}{2}(\frac{5}{2}-[523])$	201.3	$E2$	$\frac{5}{2}, \frac{7}{2}(\frac{5}{2}-[523])$	1/2.7
					1/3.0(theor.)[b]

[a] Experimental reduced gamma-ray intensity is obtained by dividing the K-electron intensity by the theoretical K-conversion coefficient and by the energy dependent term, E^{2L+1}.

[b] The theoretical relation is given by the square of the ratio of Clebsch-Gordan coefficients compiled by A. H. Wapstra, G. J. Nijgh, and R. Van Lieshout, *Nuclear Spectroscopy Tables* (North-Holland Publishing Company, Amsterdam 1959).

[c] Retardation effects and deviations from theoretical transition intensity rules are expected between states involving changes in nuclear deformation († designates relatively weak δ).

and parity and with $\Delta K=1$. This situation arises in W^{183} where a $K=\frac{1}{2}$ ground state and a $K=\frac{3}{2}$ excited state are 208 keV apart. Kerman[19] has shown that the discrepancies in the W^{183} band structure can be attributed to the Coriolis term.

Supplementary data on γ and β^- radiation in the decay $Pm^{151} \rightarrow Sm^{151}$ have recently been published by Chéry.[20] Components of the β^- spectra proceed to levels at 0 keV ($\frac{7}{2}-$), 165 keV ($\frac{7}{2}+$), 340 keV ($\frac{7}{2}-$), 440 keV, and 815 keV. A 38% β^- component (of 1.3 MeV) decays to the ground state. His half-life measurements for two additional levels at 65 keV ($\frac{9}{2}-$) and 100 keV ($\frac{9}{2}-$) are $\leq 5\times 10^{-10}$ and $\leq 10^{-9}$ sec, respectively. In addition, β-γ and γ-γ coincidences were investigated, as well as angular correlations. Spin assignments above, in parentheses, for the low-lying levels are attributed to Chéry. The ground state of Sm^{151} is described as $h_{9/2}$ or $f_{7/2}$ in the framework of Mayer and Jensen's shell model.[15]

It is suggested that the 104.8-keV ($\frac{3}{2}+$) level is a single-particle state corresponding to the $\frac{3}{2}+[402]$ Nilsson orbital. This level is forced to de-excite via forbidden dipoles ($\Delta n_z=5$ or 6) which may account for

[19] A. Kerman, Kgl. Danske Videnskab. Selskab, Mat.-fys. Medd. **30**, No. 15 (1956).

[20] R. Chéry, J. phys. radium **22**, 665 (1961).

TABLE VI. Conversion electron data for decay of Pm^{151}(28 h) → Sm^{151}.

Transition energy (keV)	K	L_I	L_{II}	L_{III}	M	N	Remarks[a,b]
25.6		d	~60[c]	d	~60	15	$E1$
35.15		~10	70	80	35	10	$M1/E2=2$
58.6[e]			25	25	d		$E2$
61.0			~13	13	w		$E2$
64.85	>1000	400	w	d	100	30	$M1$
65.8	>700	~280[d]	70	60	80	20	$M1/E2\approx30$
69.7	>300	85	~8	d	25		$M1$
76.2	>100	~17	105	115	70	12	$E2$
77.2	20	d					
89.0[e]	8	w					
100.05	1000	<250[d]		w	50	15	$M1$
101.9	80	13	c	~6	w		$E1$
104.85	~1250[d]	210	17	7	50	12	$M1$
105.8[e]	~15						
109.6[e]	~10	w					
112.05[e]	~12						
139.4	<250[d]	~20			w		
143.2	27	8					
149.6[e]	~8						
156.25[e]	20	~6		w			
163.0	14	c					
163.6	200	30	c	~5	d		$E1$
167.8	175	23		d	d		
168.4	130	19		d	d		
177.2	390	58	c		18		$M1$
186.4[e]	~5	w					
188.1[e]	~5	w		w			

Energy (keV)	K	L_I	L_{II}	L_{III}	M	Remarks[a,b]
208.9	120	20	c		6	$M1$
219.5[e]	w					
232.35[e]	70	13				$M1$
236.8[e]	15	d				
239.9	45	~9		d		
251.1[e]	w					
257.5[e]	w					
275.05	55	8		w		
280.0[e]	~11[d]	w				
290.8	3.3					
323.7[e]	9					
339.65	100	15		w		
344.4	11	w				

Energy (keV)	K	Energy (keV)	K	Energy (keV)
358.8	w	447.3[e]	3.5	547.0
394.5	~5	459.0		555.5[e]
422.9[e]	~5	464.3		715.3[e]
433.6[e]	~4.5	467.8[e]		833.4
440.1	~5	498.1[e]		838.2
445.0	12	542.0		850.7[e]

[a] Multipole assignments are based in K/L and L-subshell ratios.
[b] Intensity data are normalized to 1250 units for the most prominent line. "w" indicates weak line.
[c] Conversion line is partially resolved.
[d] Conversion line is a composite of two different lines
[e] Not placed in decay scheme.

the measurable lifetime. A questionable level of odd parity is indicated at 91.5 keV.

Levels shown at 167.8 keV ($\frac{3}{2}-$) and 168.4 keV ($\frac{1}{2}-$) decay possibly by $E1$ radiation to ground ($\frac{3}{2}+$) and 4.8-keV ($\frac{1}{2}+$) states. The relatively intense photon peak for the 170-keV transition indicates it is of $E1+(M2)$? multipolarity. From the experimental L ratio for the 163.6-keV radiation ($L_I/L_{III}=6$), the multipole character may be $E1$.

Very intense transitions may depopulate a proposed 344.7-keV ($\frac{3}{2}-$[532]) state. The 177.2-keV de-excitation to the 167.8-keV ($\frac{3}{2}-$) state is designated as $M1$ from ratios of K/L and L-subshell intensities. Other transitions proceeding from the 344.7-keV level (of 239.9, 275.0, 339.7, and 344.3 keV) are classified as $E1$ based on estimates of conversion coefficients. A 27% β^- branch was observed to feed the 344.7-keV state.[20] The rather small ft value tends to identify this level with the $\frac{3}{2}-$[532] orbital, which is fed by allowed unhindered beta transitions.

Three even-parity states are possible at 209.0 keV ($I=\frac{5}{2}$), 237.0 keV ($I=\frac{1}{2}$), and 463.9 keV. A number of states in the higher energy region (at 838.2, 547.0, and 445.0 keV) may de-excite by a pair of gamma rays of 4.8-keV energy difference as well as by other transitions.

C. Tb^{153}(62 h) → Gd^{153}

The 62-h activity of Tb^{153} was produced by the reaction $Gd^{154}(p,2n)Tb^{153}$. Impurities of Tb^{154} and Tb^{155} were present and had to be subtracted in the analysis of the spectra. Table VIII lists our internal conversion data; the number of transitions is in excess of 80. A decay scheme of Tb^{153} to Gd^{153} is shown in Fig. 4. Table IX correlates the transition intensity and multipolarity data with the decay scheme. Log(ft) values have been calculated, assuming the intensity of the branching component to the ground state (first-forbidden hindered) is not appreciable.

Tb^{153} ($Z=65$) with 88 neutrons probably has a deformation (δ)$\leq$0.18. Assuming this eccentricity, one may identify the ground state of Tb^{153} with the orbital $\frac{5}{2}-$[532]. The ground state of Gd^{153} ($N=89$) is probably in a $\frac{3}{2}+$[651] state of smaller nuclear deformation, as has been suggested by Mottelson and Nilsson.[4] The configuration $\frac{3}{2}+$[651] has a $\frac{5}{2}+$ rotational member at 41.6 keV and a $\frac{7}{2}+$ member at 93.4 keV. The small inertial parameter, $3\hbar^2/\mathcal{I}=52.2$ keV, may be characteristic of this orbital. $M1/E2$ mixing ratios for the rotational transitions are ($\frac{5}{2}\rightarrow\frac{3}{2}$)15 and ($\frac{7}{2}\rightarrow\frac{5}{2}$)50. Table V displays branching ratios within the $K=\frac{3}{2}+$ rotational band. The experimental ratio of the $B(E2)$ for the crossover transition to the $B(E2)$ for the cascade transition is 0.32 as compared to the theoretical value of 0.67.

A 109.8-keV state of even parity is depopulated by intense $M1$ radiation to the ground ($\frac{3}{2}+$) state with an 8% branching to the 41.6-keV ($\frac{5}{2}+$) level. This may be the intrinsic $\frac{3}{2}+$[402] orbital; no rotational excitation of the particle state is observed.

It is probable that the spin and parity of the 129.2-keV level are $\frac{5}{2}+$ and the $\frac{5}{2}+$[642] assignment is most likely. A rotational excitation of orbital $\frac{5}{2}+$[642] is indicated at 183.5 keV ($\frac{7}{2}+$). As shown in Table IV, the inertial terms and $M1/E2$ ratios obtained for $\frac{5}{2}+$[642] bands are of similar magnitude, but are quite different

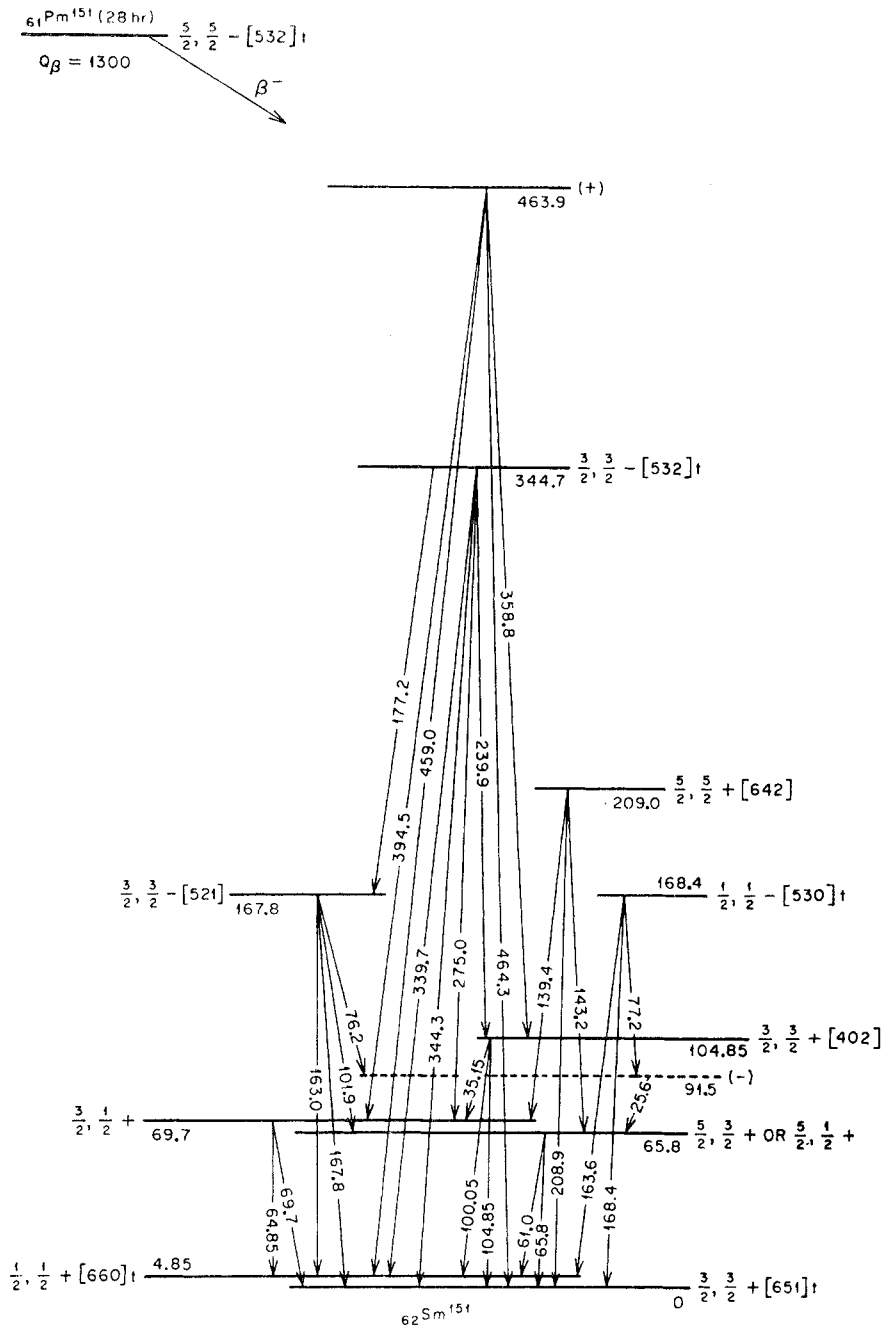

FIG. 3. Levels in Sm^{151} excited by β^- decay of Pm^{151}. States associated with smaller nuclear deformation are denoted by †. The convention employed in the designation of intrinsic states is I, $K\pi[Nn_z\Lambda]$, as for all succeeding figures. Excited states which are very uncertain are shown as dashed lines.

from values for $\frac{5}{2}-[523]$ bands which occur in this region.

The 212.1- and 249.6-keV levels might correspond to a rotational band built on the $\frac{3}{2}-[532]$ configuration. From the 212.1-keV $(\frac{3}{2}-)$ state, γ rays of $E1$ multipolarity (on the basis of $L_I/L_{II}/L_{III}$ ratios) proceed to states of $I=\frac{3}{2}+$ and $\frac{5}{2}+$, and no feeding to $\frac{7}{2}+$ levels was observed. The ratio of reduced $E1$ transition probabilities from the 212.1-keV level to the members of the $K=\frac{3}{2}$ rotational band at 0 and 41.6 keV is 2.3, which is consistent with the predicted value of 1.5 for a $K=\frac{3}{2}$ assignment to the 212.1-keV state. The relatively intense electron capture to the $\frac{3}{2}-[532]$ band (73% of the total) is consistent with the allowed unhindered transitions expected from Tb^{153}, which was assigned as $\frac{5}{2}-[532]$.

A 91.5-keV transition from the 303.5-keV level to the 212.1-keV $(\frac{3}{2}-)$ state is $M1$ with some $E2$ admixture. The 303.5-keV level decays to four other low spin states of $I\leq\frac{5}{2}$. This level may be described as the $\frac{3}{2}-[521]$

TABLE VII. Intensity and multipolarity assigned to transitions depopulating levels shown in decay scheme of Pm^{151}(28 h) → Sm^{151} (Fig. 3).

Proposed excited states $(I,K\pi)$	(keV)	De-exciting transitions (keV)	Multipole[a] assignment	Calculated relative intensities $N_\gamma+N_{ce}$	N_γ[b]	Photon data of Chéry N_γ[c]
$(\frac{3}{2},\frac{3}{2}+)$	0					
$(\frac{5}{2}+)$	65.8	61.0	$E2$	50	3	
		65.8	$M1/E2\approx30$	2650	500	
$(\frac{1}{2},\frac{1}{2}+)$	4.85	...	...			2500
$(\frac{3}{2},\frac{1}{2}+)$	69.7	64.85	$M1$	3600	665	
		69.7	$M1$	820	177	
$(\frac{3}{2},\frac{3}{2}+)$	104.85	35.15	$M1/E2=2$	205	3	
		100.05	$M1$	1920	690	
		104.85	$M1$	2550	1000	4100
$(\frac{3}{2},\frac{3}{2}-)$	167.8	101.9	$E1$	470	365	
		76.2	$E2$	580	80	
		163.0	$(E1)$	245	226	
		167.8	$(E1)$	3280	3070	<7100[d]
$(\frac{3}{2},\frac{3}{2}-)$	344.7	177.2	$M1$	1820	1345	
		239.9	$(E1)$	2080	2025	<2850[e]
		275.0	$(E1)$	3545	3480	3480
		339.7	$(E1)$	10 760	10 640	12 500
		344.3	$(E1)$	1225	1210	
$(\frac{5}{2},\frac{5}{2}+)$	209.0	139.4	$(M1)$	~285	~140	
		143.2	$(M1)$	85	50	
		208.9	$M1$	765	620	
$(-)$	91.5	25.6	$E1$	480	160	
$(\frac{1}{2},\frac{1}{2}-)$	168.4	77.2	$(M1)$	30	7	
		163.6	$E1$	3470	3225	<7100[d]
		168.4	$(E1)$	2435	2280	

[a] Multipolarities are assigned either from conversion electron ratios of Table VI or from consistency with angular momentum selection rules; latter assignments are in parentheses and are shown unmixed since we have no way of estimating mixing ratios.
[b] Estimates of photon intensity are obtained from internal conversion electron data and theoretical conversion coefficients.
[c] Photon data of R. Chéry (reference 20) are normalized to the 275.0-keV transition, assuming pure $E1$ multipolarity.
[d] Composite photon peak of 163.0-, 163.6-, 167.8-, 168.4-, and 177.2-keV transitions.
[e] Composite photon peak of 232.3-, 236.8-, and 239.9-keV transitions.

particle state, with an allowed hindered electron-capture branch [$\log(ft)=7.4$] proceeding to it. The 368.6-keV level is perhaps a $\frac{5}{2}-$ rotational excitation of the 303.5-keV state; the above level spacing ($3\hbar^2/\mathcal{I}=78$ keV) is expected of $\frac{3}{2}-[521]$ configurations.

A pair of levels at 448.2 and 548.7 keV are observed to de-excite to all three levels of the ground-state $\frac{3}{2}+[651]$ band as well as to higher levels. On the basis of energy sums, there is perhaps a level at 320.0 keV which is not shown in Fig. 4.

The decay scheme shows an excited state at 945.9 keV populating six even-parity levels of spins $I=\frac{3}{2}, \frac{5}{2}, \frac{7}{2}$. Assuming the decay mode is pure dipole, the reduced γ-ray branching ratios to $I=\frac{3}{2}, \frac{5}{2}, \frac{7}{2}$ levels of the ground-state band are experimentally 1.5/1/1 to be compared with the theoretical ratios 2.3/1/0.2 for $I_i=K_i=\frac{5}{2}$. Similarly, the experimental branching ratio to the $I=\frac{5}{2}$ and $\frac{7}{2}$ levels of the $\frac{5}{2}+[642]$ band yields 1.7 while the theoretical relationship is 2.5 for $I_i=K_i=\frac{5}{2}$. In the absence of photon data, the parity of the 945.9-keV state could not be determined. The $\frac{5}{2}-[523]$ Nilsson orbital is available, as well as vibrational excitations, but the data do not permit any further specification.

D. Tb^{155}(5.6 day) → Gd^{155}

The levels in Gd^{155} up to 105-keV excitation have been studied extensively[17] in the past, by employing beta-active sources of Eu^{155}. The situation for the low-lying states in Gd^{155} has been reviewed by Mottelson and Nilsson,[4] and a decay scheme based on the available data is in the Nuclear Data Sheets. Electron-capturing Tb^{155} is able to populate higher lying levels in Gd^{155} than is Eu^{155} in its β^- decay.[17] The radiations of Tb^{155} decay have previously been analyzed[11] using the descendant of 10-h Dy^{155} in order to obtain isotopically pure sources. A more complete study was subsequently carried out by Ward,[21] including gamma ray and coincidence measurements.

New and more precise information on the Tb^{155} conversion electron spectrum are compiled in Table X. This allows one to construct a more elaborate decay scheme (see Fig. 5) which is consistent with the new data and information already available. A detailed analysis of the data is presented in Table XI where the

[21] T. J. Ward, thesis, University of Notre Dame, 1957 (unpublished).

TABLE VIII. Conversion electron data for decay of Tb^{153}(62 h) → Gd^{153}.

Transition energy (keV)	K	L_I	L_{II}	L_{III}	M	Remarks[a,b]
16.4					*w*	
19.4			80	100	*c*	*E*2
37.4		4.4	*w*			*M*1
41.6		810	720	820	~660	*M*1/*E*2=15
46.5[e]		70			*d*	
51.8		110	28	23	35	*M*1/*E*2=50
54.3	*w*					
68.2	~100[e]	*c*	6	4	8	*M*1+(*E*2)
82.8	185	25	5.5	10	*d*	*E*1
87.6	335	45	4.5	*d*	8	*M*1
90.2	*c*					
91.5	*d*	5	4.5	4.5	*d*	*M*1/*E*2=2.7
93.4	12	2	7	7.5	*d*	*E*2
102.3	170	19	3	5.5		*E*1
106.9[e]	8.4					
109.7	1000	150	15	3.5	35	*M*1
126.1[e]	9	~2				
129.2	60	8.5			2	*M*1
132.6[e]	~8[d]					
139.8	~9[d]					
141.9	~13[d]	*d*				
166.9[e]	3					
170.5	44	*d*		*w*	~2	
174.4	34	5		*w*	1.5	
183.5	~7[d]	*c*				
185.9[e]	1.4					
186.9[e]	1.1					
193.6	2.8					
195.2[e]	24	3.2				
208.1	14	*d*				
210.1	~3[e]	*w*				
212.1	113	15.5[c]	*c*	2.5	4	*E*1

Energy (keV)	K	L	Energy (keV)	K	L
249.6	36	4.5	496.4[e]	~0.55[d]	
258.8	1.2		502.5[e]	0.3	
262.1	*d*		507.0	~0.55[e]	*d*
266.6[e]	0.9		525.5[e]	0.14	
275.1	2.9	~0.3	530.5[e]	0.33	
278.4	1.2	*d*	548.8	~0.24[d]	*w*
299.4	1.4	0.25	566.1[e]	0.2	*w*
303.4	2.0	*c*	570.9[e]	0.31	
315.05[e]	4.6	*d*	599.2[e]	0.27	
318.85	~0.3		629.4[e]	0.32	*w*
320.0	2.5	*d*	636.2[e]	0.2	
327.0	1.6	~0.35	665.2[e]	0.2	
332.6[e]	0.7	*w*	740.4[e]	~0.1[d]	
340.3[e]	2.2	*d*	754.1[e]	~0.1	
348.6[e]	~0.27		762.4	~0.13	
354.8	1.5		785.8[e]	0.18	
361.5[e]	~1.1[d]	~0.18	816.3	0.24	*d*
392.7[e]	~0.4	*c*	836.1	0.25	
406.6	~0.3	*d*	843.4[e]	~0.05	
436.1[e]	2.1	0.45	846.9[e]	0.1	
441.0[e]	~0.25		852.5	0.12	
448.2	0.4		858.3[e]	0.20	
455.3	1.3	*d*	904.4	0.12	*d*
466.9[e]	1.05	*c*	907.0[e]	0.09	
918.9[e]	0.08		974.0[e]	0.07	
946.0	0.2		992.5[e]	0.2	

[a] Multipole assignments are based on K/L and L-subshell ratios.
[b] Intensity data are internally consistent. "*w*" indicates weak line.
[c] Conversion line is partially resolved.
[d] Conversion line is a composite of two different lines.
[e] Not placed in decay scheme.

transitions are grouped according to the postulated initial level. The level scheme suggests ten Nilsson orbital assignments, three of which exhibit rotational excitation.

The experimental magnetic moment ($\mu=-0.3$ nm) and spin ($I_0=\frac{3}{2}$) of Gd^{155} identify the ground-state orbital as $\frac{3}{2}-[521]$, in accord with the predictions of Mottelson and Nilsson.[4] The rotational structure associated with the ground state shows a positive interaction term ($B=+0.024$ keV) which is characteristic of band mixing; however, no evidence exists for another odd-parity configuration near to ground.

TABLE IX. Intensity and multipolarity assigned to transitions depopulating levels shown in decay scheme of Tb^{153}(62 h) → Gd^{153} (Fig. 4).

Proposed excited states $(I,K\pi)$	(keV)	De-exciting transitions (keV)	Multipole[a] assignment	Calculated relative intensities $N_\gamma+N_{ce}$	N_γ[b]
$(\frac{3}{2},\frac{3}{2}+)$	0				
$(\frac{5}{2},\frac{3}{2}+)$	41.6	41.6	*M*1/*E*2=15	3550	340
$(\frac{7}{2},\frac{3}{2}+)$	93.4	51.8	*M*1/*E*2=50	880	80
		93.4	*E*2	42	9
$(\frac{3}{2},\frac{3}{2}+)$	109.8	16.4	(*E*2)	*w*	*w*
		68.2	*M*1+(*E*2)	160	20
		109.7	*M*1	1965	750
$(\frac{5}{2},\frac{5}{2}+)$	129.2	19.4	*E*2	255	<1
		87.6	*M*1	525	130
		129.2	*M*1	143	72
$(\frac{7}{2},\frac{5}{2}+)$	183.5	54.3	(*M*1)	*w*	*w*
		90.2	(*M*1)	...	...
		141.9	(*M*1)	36	20
		183.5	(*E*2)	45	35
$(\frac{3}{2},\frac{3}{2}-)$	212.1	82.8	*E*1	690	450
		102.3	*E*1	940	733
		170.5	(*E*1)	800	745
		212.1	*E*1	3505	3370
$(\frac{5}{2},\frac{3}{2}-)$	249.6	37.4	*M*1	7	1.3
		139.8	(*E*1)	100	90
		208.0	(*E*1)	417	400
		249.6	(*E*1)	1678	1635
$(\frac{3}{2},\frac{3}{2}-)$	303.5	91.5	*M*1/*E*2=2.7	65	22
		174.4	(*E*1)	648	607
		193.6	(*E*1)	69	66
		262.1	(*E*1)	...	...
		303.4	(*E*1)	150	148
$(\frac{5}{2},\frac{3}{2}-)$	368.6	258.8	(*E*1)	62	60
		275.1	(*E*1)	173	170
		327.0	(*E*1)	147	145
$(\frac{5}{2},\frac{5}{2}\pm)$	945.9	762.4	(*E*1) or (*M*1)	≤ 79	≤ 79
		816.3	(*E*1) or (*M*1)	≤≤166	≤≤166
		836.1	(*E*1) or (*M*1)	≤≤181	≤≤181
		852.5	(*E*1) or (*M*1)	≤≤ 90	≤≤ 90
		904.4	(*E*1) or (*M*1)	≤≤101	≤≤101
		946.0	(*E*1) or (*M*1)	≤≤182	≤≤182

[a] Multipolarities are assigned either from conversion electron ratios of Table VIII or from consistency with angular momentum selection rules; latter assignments are in parentheses and are shown unmixed since we have no way of estimating mixing ratios.
[b] Estimates of photon intensity are based on internal conversion electron data and theoretical conversion coefficients (reference 8).

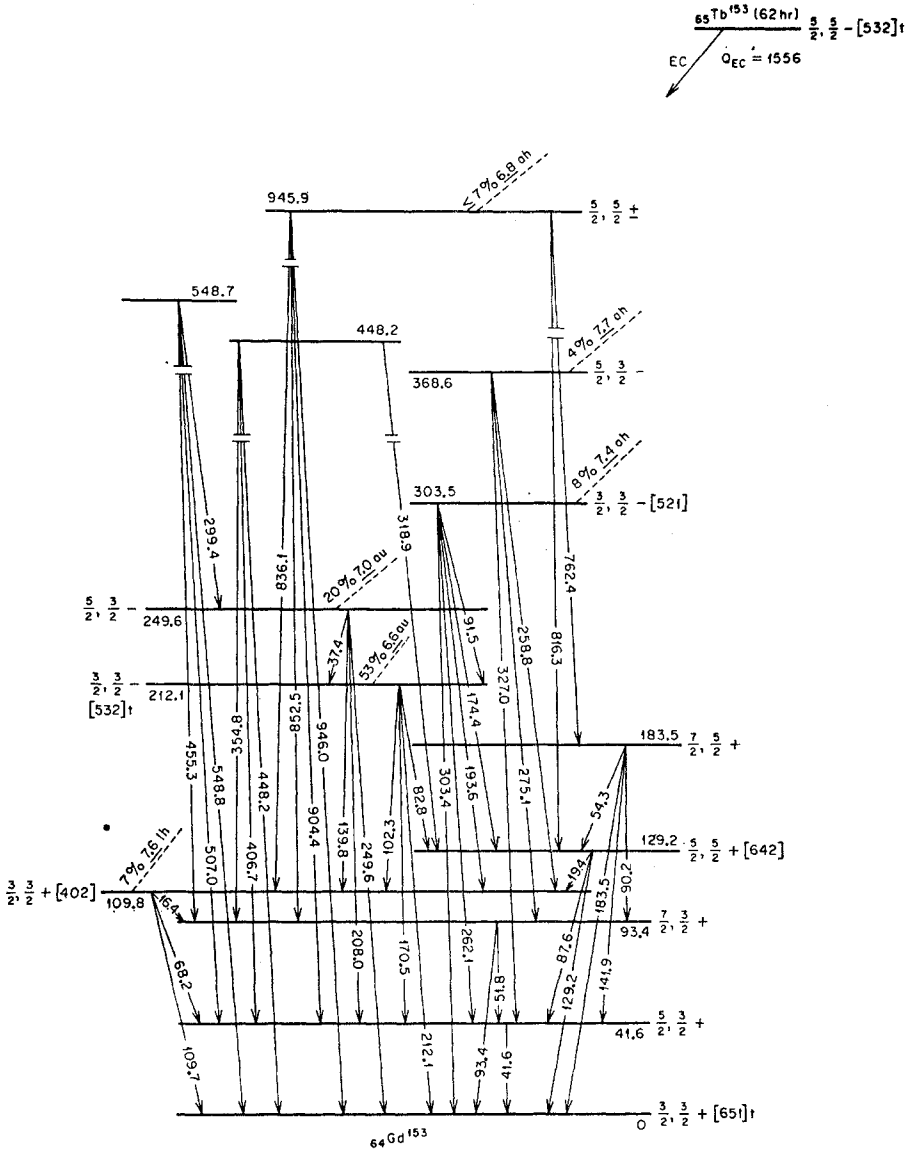

FIG. 4. Proposed decay scheme of Tb^{153}(62 h) to Gd^{153}. Rotational sequences are aligned vertically. Electron-capture branches to various levels are shown by dashed arrows with relative intensities in percent and log(ft) values underlined. The classification of these branches follows the notation of Mottelson and Nilsson (reference 4). Note that the EC branch to 945-keV level should be $\leq 7\%$, ≥ 6.8.

There exists some ambiguity as to the most consistent assignment of the orbitals $\frac{3}{2}+[651]$ and $\frac{5}{2}+[642]$ to excited states at 86.5 and 105.3 keV. Using γ-γ angular correlations, Rao[22] recently designated the 105.3-keV level as $\frac{3}{2}+$. Deutch *et al.*[23] prefer instead the lower spin assignment for the 86.5-keV state. Their preference is based on a correlation of electromagnetic lifetimes of the states with the Nilsson model predictions. Our studies of the properties of nuclear states in Gd^{155} indicate agreement with the interpretation of Deutch *et al.*

Evidence of the rotational character of the 118.0-keV ($\frac{5}{2}+$) state is listed in Table IV. Intensity rules in Table V indicate that the ground-state transition depopulating the 118.0-keV level is highly retarded. A 12.7-keV ($M1$) transition de-exciting the 118.0-keV state is incorporated in the decay scheme in order to achieve an intensity balance. This radiation was not detected and requires confirmation.

Another rotational sequence is possibly based on a $\frac{1}{2}+[660]$ level at 247.0 keV with rotational excitations at 266.6 keV ($\frac{3}{2}+$) and 268.6 keV ($\frac{5}{2}+$). This band is depopulated by transitions of known multipolarity which establish the spins and parities of the levels. It may be remarked that the available coincidence data are in agreement with the decay scheme as shown.

One may identify the 286.8-keV level by the asymptotic quantum numbers $\frac{5}{2}-[523]$; this configuration

[22] B. N. Subba Rao, Nuclear Phys. **28**, 503 (1961).
[23] B. I. Deutch, F. R. Metzger, and F. J. Wilhelm, Nuclear Phys. **16**, 81 (1960).

TABLE X. Conversion electron data for decay of Tb^{155}(5.6 day) → Gd^{155}.

Transition energy (keV)	K	L_I	L_{II}	L_{III}	M	N	Remarks[a]
18.75[b]		100	330	450	320	75	$M1/E2 \approx 17$
21.0			70	100	~45	16	$E2$[e]
26.55[b]		20	~8[c]	*d*	~10	*w*	$E1$
31.43[b]			35	45	~20	6	$E2$[e]
39.8[f]		4.5	*w*	*w*			
40.7[b]		*w*					
45.3[b]		57	22	29	25	6	$E1$
58.0	*w*	4.6	1.3	*d*			$E1$
60.0[b]	>400	210	58	52	65	24	$M1/E2=26$
60.3		*d*	~5[c]	5.5	*d*		$E2$
79.2	~4	*w*					
80.9	~2.8						
86.0[b]	~10	*c*					Coulomb excited
86.5[b]	1480	210	55	70	75	22	$E1$
99.0	28	4	~1.5	*w*			$M1+E2$
101.15	65	10	*c*	*w*			$M1$
101.6[f]	*w*						
105.3[b]	1000	130	25	32	38	14	$E1$
118.0[b]	~0.9						
120.5	~1.6						
138.2[f]	~3.5	*d*					
146.0	*w*						Coulomb excited
148.65	290	44	*c*	1.4	12	3.5	$M1/E2=60$
150.6	~2						
158.6[f]	~4						
160.5	65	8.2			*c*		
161.3	230	34	*c*	*w*	9.3		$M1+E2$
163.3	390	55	*c*	1.1	14.5	3.5	$M1/E2 \approx 150$
175.2[f]	3	*w*					
180.1	490	75	*c*	2.8	19	5	$M1/E2=30$
181.6	~7[c]	~1.5[d]					
182.05	~7[c]						
208.0	8.5	1.3			0.3		
220.0	~3[c]						
220.6	21	*d*			<3.5[d]	0.3	
226.8	6.2	<3.5[d]					
239.45	8.5	4.2[d]					
262.45	130	18	*c*		4		$M1$
268.7	<3.5[d]	*d*					
281.1	<4.2[d]	*c*					
286.9	5.9	0.8					
321.8	1.8	0.4					
340.8	12	1.7			0.4		
367.6	3.5	0.43					
371.0[f]	1.9	0.22					
402.3[f]	0.6	~0.1					
451.3	~0.15						
454.8	*w*						
501.8	0.15						
505.9[f]	0.07						
559.9[f]	0.46	*w*					
588.2	~0.2						
592.8	0.6	0.1					
615.5	0.075						
706.2[f]	~0.07						
715.3[f]	~0.05						
KLL Auger	730[g]						

[a] Electron intensity data are internally consistent for lines of the same activity. "*w*" indicates a weak line. Multipole assignments are based on K/L and L-subshell ratios.
[b] Transitions are observed also in decay of Eu^{155}(1.7 yr) → Gd^{155}.
[c] Conversion line is partially resolved.
[d] Conversion line is a composite of two different lines.
[e] Relative magnitudes of M-subshell lines (i.e., the absence of appreciable M_{IV} and M_V) makes an $E2$ assignment preferable to $E3$. A small admixture of $M1$ cannot be excluded on the basis of L-subshell ratio.
[f] Not placed in decay scheme.
[g] Total intensity of KLL Auger-electron lines is tabulated. The Auger-electron spectrum is used to estimate the fraction of electron-capture decay directly to the ground state, in conjunction with an intensity balance made on the basis of the decay scheme.

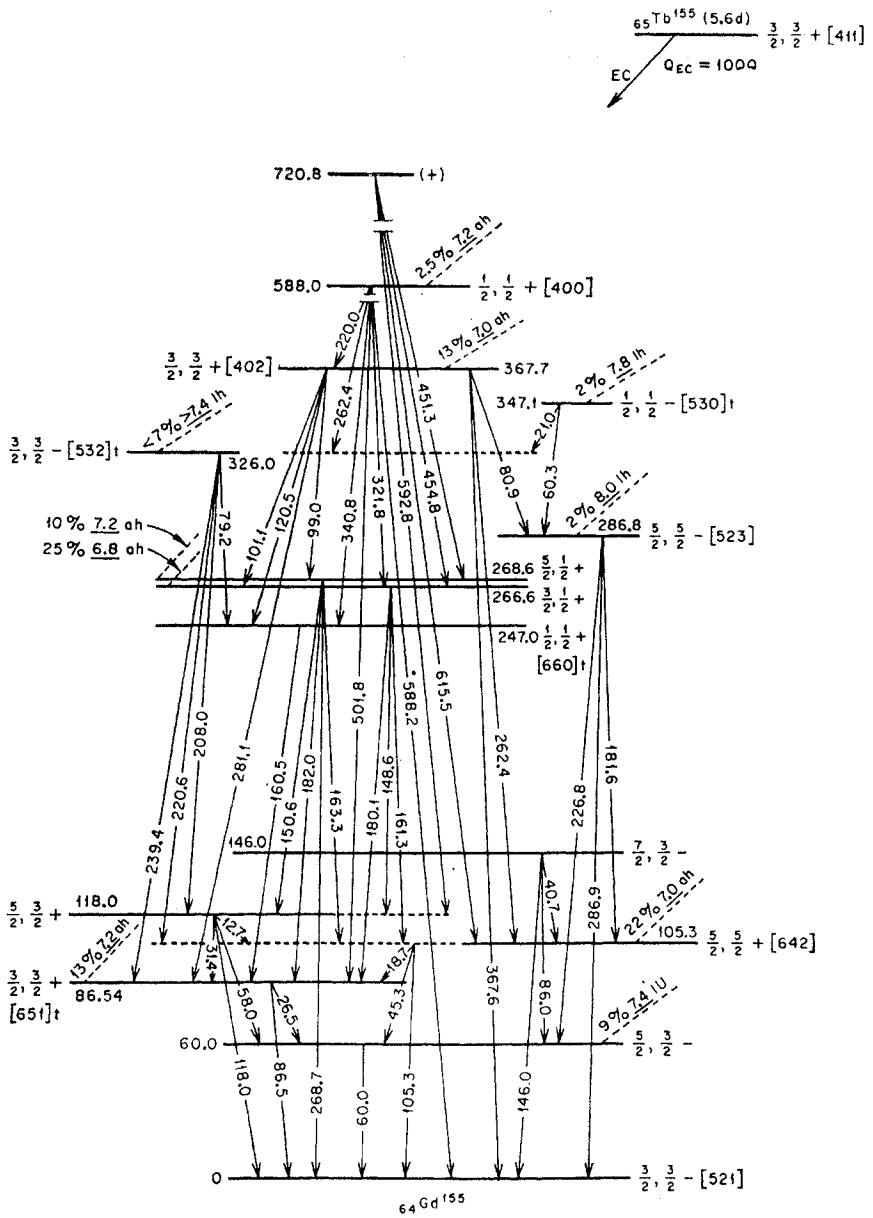

FIG. 5. Levels in Gd^{155} populated by decay of Tb^{155}(5.6 day), based partly on studies of β^- decay of Eu^{155} (reference 17).

will reappear as the ground state of Er^{163}, Er^{165}, and Dy^{163} and will be discussed later. The branching ratio from this state to the $\frac{3}{2}-[521]$ band is 0.9, experimentally, as compared to the theoretical value 2.3, assuming pure $M1$ radiation. It appears that the $\frac{5}{2}-[523]$ state does not populate levels associated with smaller deformation as was predicted by Mottelson and Nilsson.[4] This behavior between levels involving a change in nuclear eccentricity is apparent in the de-excitation of the 326.0-keV ($\frac{3}{2}-[532]$) and 347.1-keV ($\frac{1}{2}-[530]$) states, both of which arise from a smaller nuclear deformation.

The de-excitation spectrum of the 367.7-keV state consists of seven dipoles proceeding to states of spins $I=\frac{3}{2}$ and $\frac{5}{2}$. Even parity is required and $I=\frac{3}{2}$ is most likely for the above level. The particle state $\frac{3}{2}+[402]$ is available; it arises originally from a spherical state below the 82 neutron shell.

A low spin for the 588.0-keV state is implied by the evidence its decay to six states of spins $I\leq\frac{3}{2}$. Even parity for this state is consistent with $M1$ multipolarity (derived from conversion coefficients) of the 340.8-keV de-exciting gamma ray. At 720.8 keV is situated a weakly populated level which decays mainly to states of $I=\frac{5}{2}+$. This level is tentatively assigned as relatively high spin, even parity.

The total transition intensities given in Table XI are consistent with the decay scheme shown in Fig. 5. The value of K x-ray intensity listed in column $N\gamma$ (obtained

TABLE XI. Intensity and multipolarity assigned to transitions depopulating levels shown in decay scheme of Tb^{155}(5.6 day) → Gd^{155} (Fig. 5).

Proposed excited states $(I,K\pi)$	(keV)	De-exciting transitions (keV)	Multipole[a] assignment	Calculated relative intensities $N_\gamma+N_{ce}$	N_γ[b]	Data of Ward N_γ[c]
$(\frac{3}{2},\frac{3}{2}-)$	0					
$(\frac{5}{2},\frac{3}{2}-)$	60.0	60.0	$M1/E2=26$	2050	240	470
$(\frac{7}{2},\frac{3}{2}-)$	146.0	40.7	$(E1)$	w	w	
		86.0	$M1$	16	4	
		146.0	$E2$	w	w	
$(\frac{3}{2},\frac{3}{2}+)$	86.54	26.55	$E1$	93	32	
		86.5	$E1$	6022	4110	6600
$(\frac{5}{2},\frac{3}{2}+)$	118.0	12.7	$(M1)$		unobserved	
		31.43	$E2$	106	0.3	
		58.0	$E1$	90	48	
		118.0	$(E1)$	6.5	5.5	
$(\frac{5}{2},\frac{5}{2}+)$	105.3	18.75	$M1/E2\approx17$	1280	5	
		45.3	$E1$	465	326	
		105.3	$E1$	5784	4545	4545
$(\frac{1}{2},\frac{1}{2}+)$	247.0	160.5	$(M1)$	225	149	
$(\frac{3}{2},\frac{1}{2}+)$	266.6	148.65	$M1/E2=60$	875	525	540
		180.1	$M1/E2=30$	2170	1580	1380
		161.3	$M1+E2$	806	529	1510
$(\frac{5}{2},\frac{1}{2}+)$	268.6	163.3	$M1/E2\approx150$	1400	935	
		150.6	$(M1)$	6	3.8	
		182.05	$(M1)$	31	22	
		268.7	$(E1)$	98	96	
$(\frac{3}{2},\frac{3}{2}-)$	326.0	79.2	$(E1)$	14	9	
		208.0	$(E1)$	253	243	
		220.6	$E1$	713	688	400
		239.45	$(E1)$	357	347	
$(\frac{5}{2},\frac{5}{2}-)$	286.8	181.6	$(E1)$	148	140	
		226.8	$(M1)$	43	34	
		286.9	$(M1)$	69	62	
$(\frac{1}{2},\frac{1}{2}-)$	347.1	21.0	$E2$	300	0.1	
		60.3	$E2$	15	1	
$(\frac{3}{2},\frac{3}{2}+)$	367.7	80.9	$(E1)$	10	6.5	
		99.0	$M1+E2$	50	15	
		101.15	$M1$	117	38	
		120.5	$(M1)$	3.5	1.5	
		262.45	$M1$	1218	1065	1170
		281.1	$(M1)$	34	30	
		367.6	$E1$	431	427	670
$(\frac{1}{2},\frac{1}{2}+)$	588.0	220.0	$(M1)$	19	15	
		262.45[d]	$(E1)$	...	...	
		321.8	$(M1)$	29	26.5	
		340.8	$M1$	223	208	265
		501.8	$(M1)$	7	7	
		588.2	$(E1)$	70	70	
$(+)$	720.8	451.3	$(M1)$	5.5	5.3	
		454.8	$(M1)$	w	w	
		592.8	$(M1)$	41	40	
		615.5	$(M1)$	6.0	5.8	
K x-ray intensity					19 000[e]	

[a] Multipolarities are assigned either from conversion electron ratios (Table X), as a member of a rotational band, from conversion coefficients, or from consistency with angular momentum selection rules; latter assignments are in parentheses and are shown unmixed since we have no way of estimating mixing ratios.

[b] Estimates of photon intensity are based on conversion electron intensity results (Table X) and theoretical conversion coefficients (reference 8).

[c] Photon data of Ward (reference 21) are normalized to the 105.3-keV transition, assuming pure $E1$ radiation.

[d] Recurring transition energy is previously listed.

[e] An extrapolation from KLL Auger-electron intensity data to K x-ray intensity is based on K-fluorescence yield of 0.94 and total K Auger intensity of 1.66 times the KLL Auger intensity. The adopted values are obtained from the compilation by A. H. Wapstra, G. J. Nijgh, and R. Van Lieshout, *Nuclear Spectroscopy Tables* (North-Holland Publishing Company, Amsterdam, 1959).

from the *KLL* Auger-electron intensity data) indicates that no electron capture proceeds directly to the ground state. In calculating the log(ft) values, a total decay energy of 1 MeV is obtained from Nuclear Data Sheets, 1959. Allowed hindered [log(ft)=7.0±0.2] electron capture to 6 different levels accounts for essentially 80% of the decay. A 9% electron-capture branch proceeds to the 60.0-keV state with a first-forbidden unhindered [log(ft)=7.4] transition. Electron-capture decay to three of the remaining states is $1h$, and the corresponding log(ft) values are estimated as ~7.9.

E. Eu^{157}(15 h) → Gd^{157}

Early studies[17] of 15-h Eu^{157} have established that the β^- decay populated relatively high-lying states as well as the ground state (Nuclear Data Sheets, 1959). Coulomb excitation experiments have indicated states at 55 and 131 keV, presumably rotational levels based on the $\frac{3}{2}-[521]$ ground state. In the region of 93 neutrons (Gd^{157}), the $\frac{5}{2}+[642]$ and $\frac{5}{2}-[523]$ orbits are also expected to be populated by the decay of Eu^{157}. The Eu^{157} ground state probably corresponds to the $\frac{5}{2}+[413]$ orbital.[4]

The preparation of Eu^{157} by the reaction $Gd^{160}(p,\alpha)$-Gd^{157} yielded a relatively weak source. Table XII presents the conversion line energy and intensity measurements. One may construct with these incomplete data the ground-state $\frac{3}{2}-[521]$ rotational band (see Fig. 6) since the intraband transitions, both cascade and crossover, have been observed. The radiations of Eu^{157} observed in the scintillation spectrum were not well

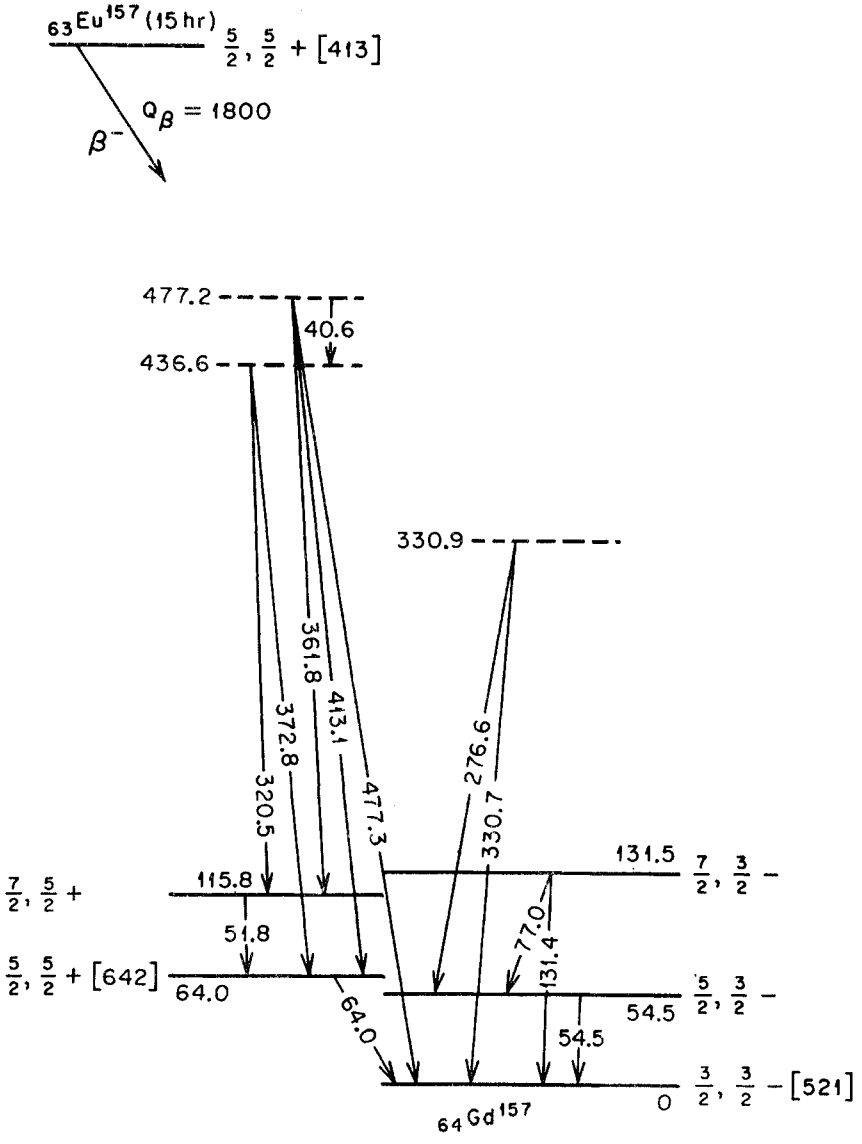

FIG. 6. Partial decay scheme for Eu^{157}(15 h) to Gd^{157}.

resolved. Relative photon intensities are as follows:

$$623\gamma/413\gamma/373\gamma/(320+330)\gamma \approx 1/8/4/2.$$

At 64.0 keV above ground, there may be the expected $\frac{5}{2}+[642]$ state with a rotational excitation of 115.8 keV $(\frac{7}{2}+)$ superimposed. The $\frac{5}{2}+$ assignment for the 64.0-keV level is supported by the $E1$ character of the de-exciting radiation to ground $(\frac{3}{2}-)$. The inertial parameter for the odd-neutron $\frac{5}{2}+[642]$ state in Gd^{157} is $3\hbar^2/\mathcal{I}=44$ keV, which is reasonable (compare e.g., Gd^{153} and Dy^{161} with $3\hbar^2/\mathcal{I}=46.5$ and 37.5 keV, respectively).

The energy differences of transitions to the lowest bands indicate tentative levels at 330.9, 436.6, and 477.2 keV.

TABLE XII. Conversion electron data for $Eu^{157}(15\text{ h}) \rightarrow Gd^{157}$.

Transition energy (keV)	K	L_I	L_{II}	L_{III}	M	Remarks[a]
40.6		w				
51.8		370	~120	105	>110	$M1/E2=34$
54.5		1000	300	275	~450	$M1/E2=29$
64.0	>1000	325	130	160	~125	$E1$
77.0	>100	65	w	w		$M1+E2$
131.4	w		w	w		$E2$
276.6	w					
320.5	20					
330.7	w					
361.8	w					
372.8	25					
413.1	160	30				
477.3	w					
527.0[b]	15					
623.3[b]	w					
687.5[b]	w					
727.4[b]	w					

[a] Electron intensity data are separately consistent for high- and low-energy ranges; transitions >200 keV could not be normalized to those <200 keV. "w" indicates a weak line. Multipole assignments are based on K/L and L-subshell ratios.
[b] Not placed in decay scheme.

F. $Tm^{163}(2\text{ h}) \rightarrow Er^{163}$

The experimental basis of the level scheme of Dy^{161} as populated by the decay of Ho^{161} (2.5 h) has been previously published.[6] The theoretical interpretation of the decay scheme was performed by Bes.[24] The distinct properties of the odd-nucleon orbitals assigned to Dy^{161} ($N=95$) are incorporated in Tables IV and V.

By use of mass-free activities of Tm^{163}, it has been possible to record radiations converting in Er^{163} as listed in Table XIII. Only the low-energy portion of the de-excitation spectrum is reported. The mass tables of Seeger[25] predict an energy of 2.3 MeV is available for electron capture of Tm^{163}. The decay scheme that is drawn in Fig. 7 is consistent with transition intensity

[24] D. R. Bès, Nuclear Phys. **6**, 645 (1958).
[25] P. A. Seeger, Nuclear Phys. **25**, 1 (1961).

TABLE XIII. Conversion electron data for decay of $Tm^{163}(2\text{ h}) \rightarrow Er^{163}$.

Transition energy (keV)	K	L_I	L_{II}	L_{III}	M	Remarks[a, b]
22.2		15	c	10	9	$E1$
60.2		55	c	18	20	$M1/E2=18$
69.2	>60	33	c	12	10	$E1$
80.5	d	11				
83.9	30	5.5	40	42		$M1/E2=\frac{1}{8}$
85.1	30	d				
104.3	1200	230	30	8	70	$M1$
145.3	2.6					
164.4	28	5				
165.4	1.2					
190.1	32	7				
239.7	65	11				
241.5	140	22				

Energy (keV)	K	L	Energy (keV)	K	L
249.2	w		505.1[e]	1.8	w
275.3	26	4	531.0	~0.7[e]	
299.9	37	6	549.9[e]	2.7	w
335.4	3.3		579.9[e]	2.6	
345.6	5	c	613.0	c	
393.5	5.3		655.5[e]	1.2	
404.2	2.2		671.1[e]	1.8	
471.2	3.8	w			

[a] Multipole assignments are based on K/L and L-subshell ratios.
[b] Intensity data are normalized to 1200 units for the most prominent line. "w" indicates weak line.
[c] Conversion line is partially resolved.
[d] Conversion line is a composite of two different lines.
[e] Not placed in decay scheme.

TABLE XIV. Intensity and multipolarity assigned to transitions depopulating levels shown in decay scheme of $Tm^{163}(2\text{ h}) \rightarrow Er^{163}$ (Fig. 7).

Proposed excited states $(I,K\pi)$	(keV)	De-exciting transitions (keV)	Multipole[a] assignment	Calculated relative intensities $N_\gamma+N_{ce}$	N_γ[b]
$(\frac{5}{2},\frac{5}{2}-)$	0				
$(\frac{7}{2},\frac{5}{2}-)$	83.9	83.9	$M1/E2=\frac{1}{8}$	178	28
$(\frac{3}{2},\frac{3}{2}-)$	104.3	104.3	$M1$	2100	545
$(\frac{5}{2},\frac{3}{2}-)$	164.5	60.2	$M1/E2=18$	465	42
		80.5	$(M1)$	96	21
		164.4	$(M1)$	82	47
$(\frac{7}{2},\frac{3}{2}-)$	249.5	85.1	$M1+E2$	45	8
		145.3	$(E2)$	10.5	6.5
		165.4	$(M1)$	3.5	2
		249.2	$(M1)$	w	w
$(\frac{1}{2},\frac{1}{2}-)$	345.7	241.5	$(M1)$	836	667
		345.6	$(E2)$	151	145
$(\frac{3}{2},\frac{1}{2}-)$	404.2	239.7	$(M1)$	382	302
		299.9	$(M1)$	367	322
		404.2	$(M1)$	45	42
$(\frac{5}{2},\frac{1}{2}-)$	439.7	190.1	$(M1)$	121	80
		275.3	$(M1)$	208	177
		335.4	$(M1)$	43	39
$(\frac{5}{2},\frac{5}{2}+)$	22.2	22.2	$E1$	63	18
$(\frac{3}{2},\frac{3}{2}+)$	415.1	69.2	$E1$	515	265
		393.5	$(M1)$	103	96

[a] Multipolarities are assigned either from conversion electron ratios of Table XIII, as a member of a rotational band or from consistency with angular momentum selection rules; latter assignments are in parentheses and are shown unmixed since we have no way of estimating mixing ratios.
[b] Estimates of photon intensity are obtained from internal conversion electron data and theoretical conversion coefficients.

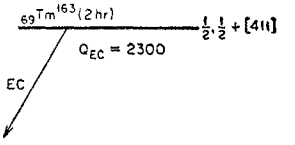

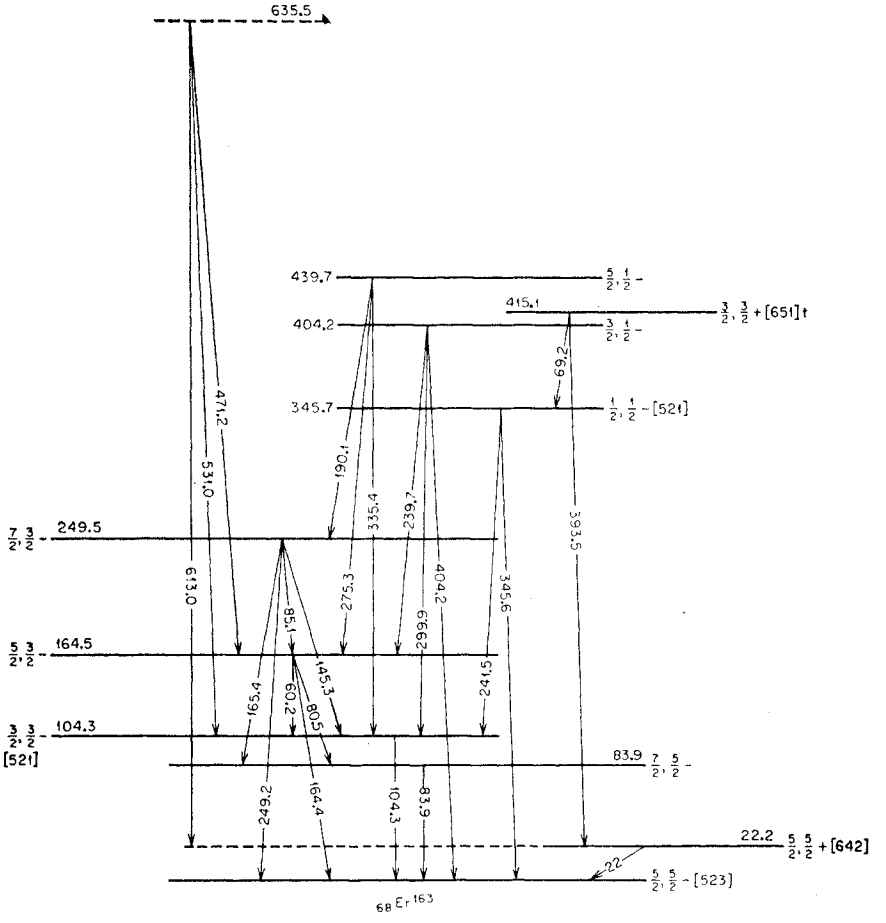

FIG. 7. Proposed level diagram o $Tm^{163}(3\ h) \rightarrow Er^{163}$.

and multipole order determinations summarized in Table XIV.

The Tm^{163} ground state is expected to be $\frac{1}{2}+[411]$, as for the other Tm isotopes; therefore, the levels directly populated in Er^{163} should be of relatively low spin. One may identify the ground state of Er^{163} with the $\frac{5}{2}-[523]$ orbital. This assignment is consistent with the rotational interpretation of the 83.9-keV ($I=\frac{7}{2}$) level. The experimental moment of inertia and the $M1/E2$ mixture for the rotational transition (see Table IV) are characteristic of $\frac{5}{2}-[523]$ bands. The low-lying intrinsic $\frac{5}{2}+[642]$ excitation in Er^{163} at 22.2 keV occurs as the ground state in the isotone, Dy^{161}.

The development of the $\frac{3}{2}-[521]$ band, consisting of levels at 104.3, 164.5, and 249.5 keV, is based on considerable interlocking data. The energy levels are rather well fixed, having a total of 16 transitions beginning or ending with them. The data indicate the populating of a $\frac{7}{2}-$ state (at 249.5 keV) of the proposed $K=\frac{3}{2}$ band for which the rotational energy constants $3\hbar^2/\mathcal{I}$ and B are, respectively, 71.9 and +0.01 keV. The experimental branching ratio from the 164.5-keV ($\frac{5}{2}-$) level to the

$\frac{5}{2}-[523]$ band is

$$B(M1: \tfrac{5}{2} \rightarrow \tfrac{5}{2})/B(M1: \tfrac{5}{2} \rightarrow \tfrac{7}{2}) = 0.26,$$

assuming pure $M1$ radiation. The predicted ratio is 0.4.

At 345.7 keV above ground, there appears a probable $\frac{1}{2}-[521]$ state which could be the base for a rotational sequence extending to $I=\frac{5}{2}$ at 439.7 keV. The energies of the states in the $K=\frac{1}{2}$ band have been fitted to the rotational energy formula (see Table IV). The value obtained for $3\hbar^2/\mathcal{I}$ is 79.7 keV and for a is $+0.47$, which are in accord with the known systematics of the $\frac{1}{2}-[521]$ orbital.

The $K=\frac{1}{2}$ band is observed to de-excite mainly to the $\frac{3}{2}-[521]$ configuration. This is indicative of allowed unhindered transitions between states having the same asymptotic quantum numbers. Reduced transition probabilities for gamma rays (assumed pure $M1$) between bands $K_i=\frac{1}{2}$, $K_f=\frac{3}{2}$ are compared as follows:

experimental 0.54/1, theoretical 0.67/1 for the 404.4-keV ($\frac{3}{2}$) state; and

experimental 0.12/1/1.3, theoretical 0.15/1/1 for the 439.7-keV ($\frac{5}{2}$) state.

It is possible to interpret the available data on the 415.1-keV excited level as indicating the $\frac{3}{2}+[651]$ state. The positive parity assignment is consistent with the observed $E1$ de-excitation to the 345.7-keV ($\frac{1}{2}-$) state. It would appear that a spin $\frac{3}{2}$ is preferable on the assumption of dipole radiation proceeding to the 22.2-keV ($\frac{5}{2}+$) level. The evidence for level ordering of $\frac{3}{2}+[651]$ states serves to establish the 415.1-keV level assignment as reasonable.

G. Tm^{165}(29 h) $\rightarrow$ Er^{165}

Some data have been available[6] regarding the levels of $Er^{165}(N=97)$ which are populated by the electron-capture decay of Tm^{165}. The existence of $\frac{3}{2}-[521]$ and $\frac{5}{2}+[642]$ states at 243 and 47 keV, respectively, has been discussed previously.[5] Additional data have since been published by Gromov *et al.*[26] and Staehle *et al.*[27] Using more intense sources in the present study, over 90 transitions have been measured (see Table XV), and an attempt was made to classify some of the higher energy transitions according to their conversion coefficients (see Table XVI). The data allow one to expand the decay scheme (see Fig. 8). Checks have been made on the validity of the proposed scheme employing the rotational energy criteria as well as the ratio of intensities of de-exciting transitions.

The parent, Tm^{165}, is most likely in a $\frac{1}{2}+[411]$ state with a disintegration energy of ~ 2 MeV.[17] In the decay scheme of Fig. 8, the rotational excitation of the $\frac{5}{2}-$ ground state is situated at 77.2 keV. The character o the intraband transition is $E2$ and the moment, $3\hbar^2/\mathcal{I}$, is 66.2 keV which are characteristic of $\frac{5}{2}-[523]$ configurations. The above rotational interpretation was suggested by Mottelson and Nilsson.[4]

A few remarks are in order for some of the multipolarity assignments in Table XV. It is concluded that the 15.4-keV radiation is $E2$ on the basis of observed conversion in M_{II}, M_{III}, N_{II}, and N_{III} shells; however, a small admixture of $M1$ cannot be excluded on the basis of experimental data. The $E1$ multipole assignment for the 47.1-keV transition is made on the basis of L-subshell ratio data. The experimental ratio is $1.5/<1/1$ as compared to the theoretical ratio[8] of 1.6/0.7/1. The 297.2-keV radiation appears to be $E2$ from conversion line data, as well as from conversion coefficient values.

The designation of the 47.2-keV state as $\frac{5}{2}+[642]$ is partly based on $E1$ radiation proceeding to ground ($\frac{5}{2}-$), and on a 30-keV ($E1$) gamma ray originating from the 77.2-keV ($\frac{7}{2}-$) level. A study[5] of the levels of Yb^{167}, an isotone of Er^{165}, established the $\frac{5}{2}+[642]$ orbital at 29.7 keV.

A 117.7-keV ($\frac{7}{2}+$) state may de-excite to the 47.2-keV ($\frac{5}{2}+$) level by a 70.5-keV ($M1/E2=140$) transition, and has been assigned as the $\frac{7}{2}+[633]$ orbital. An intrinsic level is somewhat preferable since a 70.5-keV rotation of the $\frac{5}{2}+[642]$ state would yield higher values for the inertial term and $M1/E2$ ratio than are usually obtained for this orbital.

In the decay scheme of Fig. 8, an anomalous rotational sequence is shown based at 297.2 keV ($\frac{1}{2}-[521]$), which de-excites preferentially to both levels of a band based at 242.7 keV ($\frac{3}{2}-[521]$). This is expected of allowed transitions between configurations having the same asymptotic quantum numbers and $\Delta K=1$. The branching ratio of the rotational 356.3-keV ($\frac{3}{2}-$) level to the members of the 242.7-keV band yields $B(M1: \frac{3}{2} \rightarrow \frac{3}{2})/B(M1: \frac{3}{2} \rightarrow \frac{5}{2}) = 0.35$, to be compared with the theoretical value of 0.67. The analogous branching from the 384.1-keV level ($K=\frac{1}{2}$, $I=\frac{5}{2}$) gives $B(M1: \frac{5}{2} \rightarrow \frac{3}{2})/B(M1: \frac{5}{2} \rightarrow \frac{5}{2}) = 0.17$, in agreement with the predicted value of 0.15.

The energy constants for the three excited levels of the $K=\frac{1}{2}-$ sequence are $3\hbar^2/\mathcal{I}=76$ keV and $a=+0.56$. The $M1/E2$ ratio for the 59.1 keV ($\frac{3}{2} \rightarrow \frac{1}{2}$) transition is 1.4. Certain regularities appear in the properties of $\frac{1}{2}-[521]$ bands in the region of odd-N numbers 95 to 107 (see Table IV). The $M1/E2$ mixing ratios for rotational transitions between $\frac{3}{2} \rightarrow \frac{1}{2}$ states are low (1.6 ± 0.5) except for the case of Er^{167} where $M1/E2=7$. Figure 9 presents experimental decoupling parameters for the $\frac{1}{2}-[521]$ configuration. There is a smooth variation observed in "a" as a function of mass number, indicating a maximum of $+0.85$ for Yb^{171}. The occurrence of a maximum was predicted by Mottelson and

[26] K. Ya. Gromov, Meng-hua Kang, B. S. Dzhelepov and V. Zvol'skia, Izvest. Akad. Nauk. S.S.S.R., Ser. Fiz. **25**, 1092 (1961).

[27] G. G. Staehle, R. G. Wilson, and M. L. Pool, Bull. Am. Phys. Soc. **6**, 238 (1961); and private communication.

TABLE XV. Conversion electron data for decay of Tm^{165}(29 h) → Er^{165}.

Transition energy (keV)	K	L_I	L_{II}	L_{III}	M	N	Remarks[a]
15.45					~80	20	$E2$
27.75		9	w		w		$M1+E2$
30.05		3.3	2.3	3.3	w		$E1$
35.2[b]		10	6	8	w		$E1$
47.15		260	<175[d]	175	c	30	$E1$
53.2		140	50	d	d	14	$M1/E2=22$
54.45		~1500	d	d	460	115	$M1$
59.15		8	30	d			$M1/E2=1.4$
60.4		135	d	d	33	8	$M1$
70.55	>40	27	2.7	1.3		1.3	$M1/E2=140$
77.2	>80	15	190	200	110	22	$E2$
82.25	3.4	~0.7	1	1			$M1/E2\approx 2$
86.9	w		2.4	<5[d]	1		$E2$
88.2	14	<5[d]			1		
113.6	400	60	6	1.8	14	3.3	$M1/E2=100$
141.4	2.5	w					
150.8	7.6	w					
156.0[b]	1.1						
165.5	7.5	c	2[e]	1.9	c		$E2$
175.7[b]	1.2						
181.5[b]	1.2						
195.6	4.9						
197.2[b]	1.0						
205.2	2.7						
209.9	5.0						
218.6	165	25	c	0.8	5.5	<2.9[d]	$M1$
221.5[b]	~2						
223.9	1.2						
233.2	d						
234.6[b]	3.1						
242.7	1270	185			45	12	$M1$
248.9	5						
249.7[b]	4.5						
264.4	d						
275.6[b]	<2.9[d]						
279.1	7	c	1.7	0.56	1		$E2$
286.1[b]	<1.6[d]						
292.3	13	2.2					
295.9	83	c			c		
297.2	125	~16[e]	c	d	8		$E2$
306.9	2.8	d					
312.1	10	1.5			0.5		
330.5	2.9	0.4					
346.6	33	5			1.1		$M1$
356.3	22	3.6			0.9		

Energy (keV)	K	L	Energy (keV)	K	L
365.3	6.2	1	605.6[b]	<0.37[d]	
384.1	1.4	w	608.1	~0.4[e]	
389.2[b]	4.5	0.6	622.8	~0.5[e]	
400.2[b]	1.5	d	664.6[b]	1.0	w
420.7[b]	1.4	w	677.3	0.33	
426.9[b]	0.5		680.5[b]	~0.15[e]	
429.9[b]	0.4		698.6[b]	1.4	<0.4[d]
442.4[b]	2.2	0.25	747.4[b]	<0.4[d]	
448.1[b]	1.8		791.0[b]	0.26	
456.0	6.6	0.75	806.8	14	2.1
459.9	11.7	2.1	821.2[b]	0.18	
471.8	2.0	~0.3	826.9[b]	~0.2[d]	
477.7[b]	2.2		837.7	0.7	0.1
487.0[b]	5.2	0.8	892.8[b]	0.8	
513.5[b]	1.5		907.8[b]	w	
526.8	2.0	d	932.4[b]	0.11	
530.9	w		952.8[b]	0.14	
542.2	4.8	d	1045.7[b]	w	
558.3	1.0	<0.37[d]	1131.0	0.28	0.04
563.7	8.7	1.3	1184.5	0.44	0.07
573.8	1.2	d	1246.4[b]	w	
577.3[b]	0.5		1379.5	0.16	
589.4	3.0	0.45	1426.9	0.11	

[a] Intensity data are internally consistent. "w" indicates weak line. Multipole assignments are based on theoretical K/L and L-subshell ratios of M. E. Rose, *Internal Conversion Coefficients* (North-Holland Publishing Company, Amsterdam, 1958).
[b] Not assigned in decay scheme.
[c] Conversion line is partially resolved.
[d] Conversion line is a composite of two different lines.

TABLE XVI. Intensity and multipolarity assigned to transitions depopulating levels shown in decay scheme of Tm^{165}(29 h) → Er^{165} (Fig. 8).

Proposed excited states $(I,K\pi)$	(keV)	De-exciting transitions (keV)	Multipole[a] assignment	Calculated relative intensities $N_\gamma+N_{ce}$	N_γ[b]	Photon data of Gromov *et al.* N_γ[c]
$(\frac{5}{2},\frac{5}{2}-)$	0					
$(\frac{7}{2},\frac{5}{2}-)$	77.2	30.05	$E1$	19	7	
		77.2	$E2$	760	82	
$(\frac{5}{2},\frac{5}{2}+)$	47.15	47.15	$E1$	2280	1530	
$(\frac{7}{2},\frac{7}{2}+)$	117.7	70.55	$M1/E2=140$	227	33	
$(\frac{3}{2},\frac{3}{2}-)$	242.7	165.5	$E2$	12	2.7	
		195.6	$(E1)$	110	104	
		242.7	$M1$	7720	6200	4300
$(\frac{5}{2},\frac{3}{2}-)$	295.9	53.2	$M1/E2=22$	345	73	
		218.6	$M1$	802	604	
		248.9	$(E1)$	202	196	
		295.9	$(M1)$	790	690	<4300[d]
$(\frac{1}{2},\frac{1}{2}-)$	297.2	297.2	$E2$	2570	2400	
		54.45	$M1$	3110	833	
$(\frac{3}{2},\frac{1}{2}-)$	356.3	59.15	$M1/E2=1.4$	142	9	
		60.4	$M1$	1100	100	
		113.6	$M1/E2=100$	715	230	
		279.1	$E2$	117	113	
		356.3	$(M1)$	341	314	<1370[e]
$(\frac{5}{2},\frac{1}{2}-)$	384.1	27.75	$M1+E2$	16	8	
		86.9	$E2$	8	1.8	
		88.2	$(M1)$	21	4	
		141.4	$(M1)$	6	3	
		306.9	$(M1)$	29	25	
		384.1	$(M1)$	25	24	
$(\frac{3}{2},\frac{1}{2}+)$	589.4	15.45	$E2$	420	<1	
		82.25	$M1/E2\approx2$	8	1	
		205.2	$(E1)$	67	64	
		233.2	$(E1)$	...	...	
		292.3	$(E1)$	781	765	*d*
		471.8	$(E2)$	135	133	
		542.2	$(M1)$	198	192	*f*
		589.4	$(E1)$	918	915	
$(\frac{1}{2},\frac{1}{2}+)$	507.1	150.8	$(E1)$	91	82	
		209.9	$(E1)$	136	130	
		459.9	$(E2)$	744	730	980
$(\frac{5}{2}$ or $\frac{7}{2}+)$	573.9	456.0	$(M1)$	183	176	
		526.8	$(M1)$	72	70	
		573.8	$(E1)$	346	345	
$(\frac{5}{2},\frac{5}{2}-)$	608.0	223.9	$(M1)$	6	4.6	
		312.1	$(M1)$	108	96	
		365.3	$(M1)$	101	94	*e*
		530.9	$(M1)$	*w*	*w*	
		608.1	$(M1)$	21	21	
$(\frac{3}{2},\frac{3}{2}+)$	853.9	264.4	$(M1)$	...	...	
		346.6	$M1$	473	434	*e*
		806.8	$(M1)$	1607	1590	1590
		558.3	$(E1)$	275	274	<900[f]
$(\frac{1}{2}$ or $\frac{3}{2}-)$	920.0	563.7	$(M1)$	397	387	
		330.5	$(E1)$	235	232	
		622.8	$(M1)$	28	28	
		677.3	$(M1)$	23	23	
$(\frac{3}{2},\frac{3}{2}+)$	1427.0	837.7	$(M1)$	89	89	
		1131.0	$(E1)$	297	297	815
		1184.5	$(E1)$	512	512	
		1379.5	$(M1)$	67	67	190
		1426.9	$(E1)$	177	177	

[a] Multipolarities are assigned either from conversion electron ratios of Table XV or from consistency with angular momentum selection rules; latter assignments are in parentheses and are shown unmixed since we have no way of estimating mixing ratios.
[b] Estimates of photon intensity are obtained from internal conversion electron data and theoretical conversion coefficients.
[c] Photon data of K. Ya. Gromov *et al.* (reference 26) are normalized to the 806.8-keV transition.
[d] Composite photon peak of 292.3-, 295.9-, and 297.2-keV transitions.
[e] Composite photon peak of 346.6-, 356.3-, and 365.3-keV transitions.
[f] Composite photon peak of 542.2-, 558.3-, and 563.7-keV transitions.

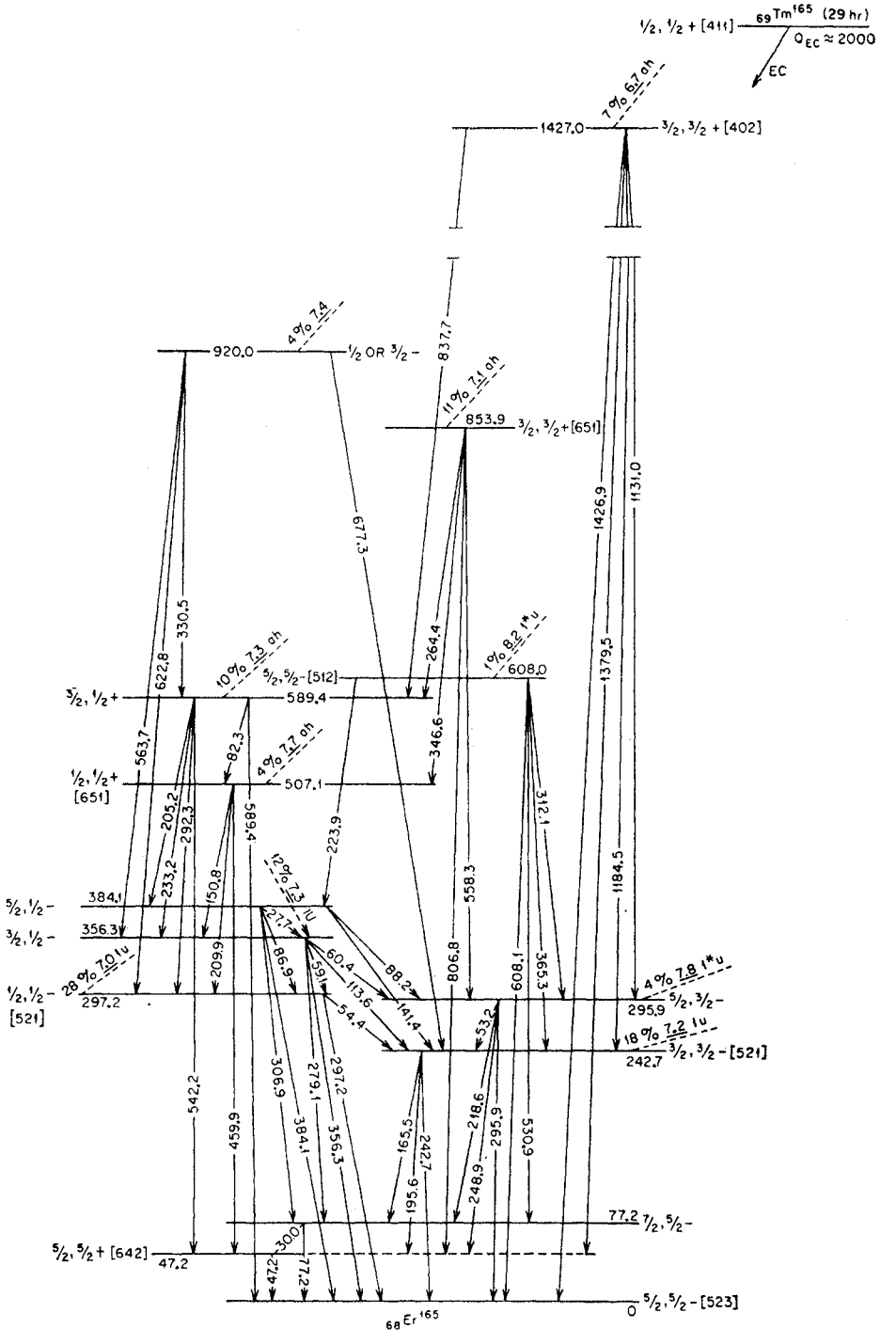

FIG. 8. Levels in Er^{165} following Tm^{165} (29 h) decay. In a previous paper (reference 5), the $\frac{3}{2}-[521]$ and $\frac{5}{2}+[642]$ states were postulated at 243 and 47 keV, respectively. There may be a level at 117.7 keV $(\frac{7}{2}+[633])$ which de-excites to the $\frac{5}{2}+[642]$ state by a 70.5-keV transition.

Nilsson.[4] The empirical data on the relevant values of $3\hbar^2/\mathcal{I}$ are also shown in Fig. 9 in order to examine the correspondence between the two parameters.

The 53.2-keV collective excitation $(\frac{5}{2}\rightarrow\frac{3}{2})$ of the $\frac{3}{2}-[521]$ particle state at 242.7 keV appears to have the $M1/E2$ mixing ratio and energy similar to those observed in neighboring odd-A nuclei. The branching ratio of the rotational 295.9-keV $(\frac{5}{2}-)$ level to the ground-state band gives $B(M1:\frac{5}{2}\rightarrow\frac{5}{2})/B(M1:\frac{5}{2}\rightarrow\frac{7}{2})=0.46$, in agreement with the theoretical value of 0.4.

Although the interpretation of the high-energy part of the Er^{165} spectrum must be considered tentative, the spin and parity state assignments seem reasonable. The levels excited at 507.1 keV $(\frac{1}{2}+)$ and 589.4 keV $(\frac{3}{2}+)$

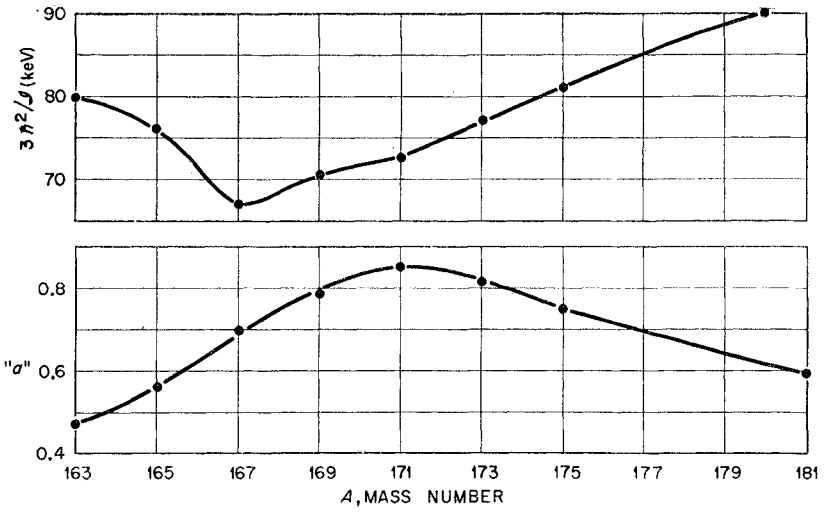

FIG. 9. Empirical constants for anomalous rotational sequences based on the $\frac{1}{2}-[521]$ configuration in odd-A nuclei (see Table IV). Note that $3\hbar^2/\mathcal{I}=90$ keV for W^{181}.

are connected by an 82.3-keV transition ($M1/E2=2$) of possible rotational character. A strong 460-keV radiation of $E2$ multipole order may proceed between the 507-keV $(\frac{1}{2}+)$ and 47-keV $(\frac{5}{2}+)$ states. The branching ratio between the 507.1-keV state and the $\frac{1}{2}-[521]$ band is in agreement with the predicted value where $I_i=K_i=\frac{1}{2}$ and pure $E1$ radiation are postulated. Quantitatively, the comparison is 0.58 (experimental) and 0.5 (theoretical). In the analogous branching from the 589.4-keV $(\frac{3}{2}+)$ level to the $I=\frac{1}{2}, \frac{3}{2}, \frac{5}{2}$ members of the $K=\frac{1}{2}$ band, the ratios are more consistent for assuming $K_i=\frac{1}{2}$ than for $K_i=\frac{3}{2}$. In the Nilsson diagram of Fig. 1, there is no intrinsic $K=\frac{1}{2}+$ state in the region of neutron number 97. However, the asymptotic state $\frac{1}{2}+[651]$, which originates from the $g_{9/2}$ state of the spherical potential beyond the 126-neutron shell, is close to the $\frac{5}{2}-[512]$ orbital for $\delta=0.3$.

A level at 608.0 keV is observed to populate five odd-parity states of spins $\frac{3}{2}, \frac{5}{2}, \frac{7}{2}$, and is designated as an intrinsic $\frac{5}{2}-[521]$ state. Intensity considerations and selection rules[9,10] indicate that a 1^*u electron-capture branch [$\log(ft)=8.2$] proceeds to it. For a level at 853.9 keV, an assignment of $\frac{3}{2}+[651]$ is preferred, representing an intrinsic excitation associated with smaller eccentricity. Under this assumption, the electron-capture branch is allowed hindered with $\log(ft)=7.1$. The postulation of the 920.0-keV state as $I=\frac{1}{2}$ or $\frac{3}{2}-$ is consistent with the observed feeding to states of $I\leq\frac{3}{2}$. A very tentative level at 573.9 keV ($\frac{5}{2}$ or $\frac{7}{2}+$) is not indicated in the decay scheme.

The fact that the 1427-keV level is de-excited by $E1$ radiation to the $\frac{3}{2}-[521]$ configuration, as well as to ground $(\frac{5}{2}-)$, suggests an assignment of $I=\frac{3}{2}+$ to the level in question. The assignment is supported by branching ratios to the members of the $\frac{3}{2}-[521]$ band, which are in exact agreement with theory where $I_i=K_i=\frac{3}{2}$. This level may correspond to the orbital $\frac{3}{2}+[402]$. Electron capture to the 1427-keV state should be ah and is observed to have $\log(ft)=6.7$.

The density of single-particle energy levels in Er^{165} appears to exceed the level density predicted by the Nilsson scheme. An alternative is to consider some of these levels as vibrational excitations of lower lying states, but there is no firm evidence for this possibility on the basis of the present data.

H. Ho^{167}(3 h) → Er^{167}

Since the existing evidence on the beta decay[28] of Ho^{167} to Er^{167} was incomplete, a detailed study of the

TABLE XVII. Conversion electron data for decay of Ho^{167}(3 h) → Er^{167}.

Transition energy (keV)	K	L_I	L_{II}	L_{III}	Remarks[a,b]
57.1[c]		50	45	45	$M1/E2=7$
73.7			20	20	$E2$
79.3	~250	50	w		$M1+(E2)$
83.4	~150	30	~15		$M1/E2\approx7$
133.4	w				
136.9	w				
150.4	w				
207.8[c]	90		75	40	$E3$
237.7	60	10			
241.1[d]	w				
260.2[d]	w				
266.5	w				
271.7[d]	w				
304.3	w				
320.7	80	15			
322.8	w				
331.0[d]	w				
347.7	35	6			
386.6	15				
403.4	w				
459.3[d]	w				
531.5[c]	w				

[a] Multipole assignments are made on the basis of K/L and L ratios.
[b] Intensity data are internally consistent; "w" indicates a weak line.
[c] Transitions are associated also with decay of Tm^{167}(9.6 day) → Er^{167}.
[d] Not assigned in decay scheme.

[28] T. Handley, W. S. Lyon, and E. L. Olson, Phys. Rev. 98, 688 (1955).

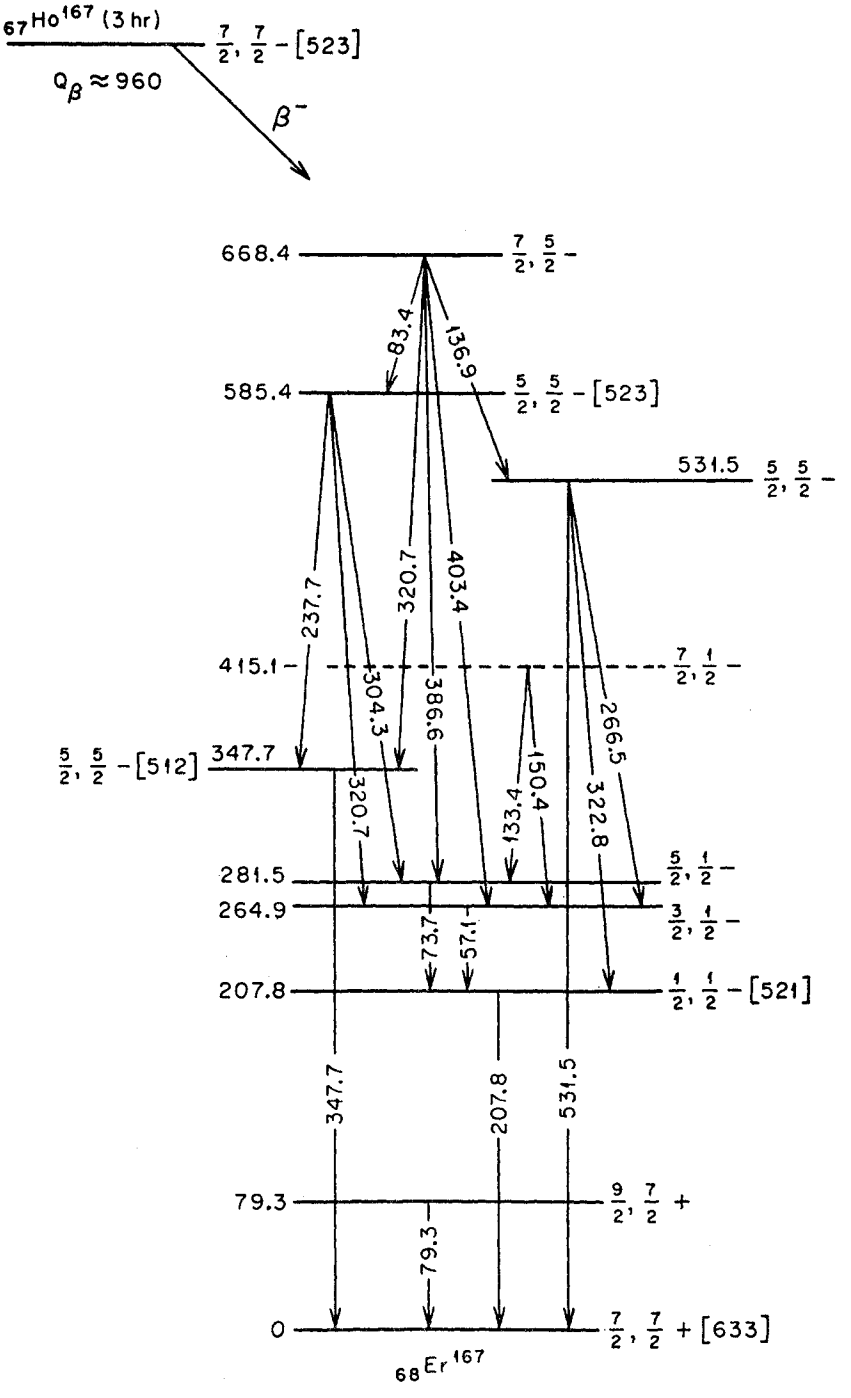

FIG. 10. A possible decay scheme for Ho^{167}(3 h) to levels in Er^{167}.

conversion electron spectrum was made. A level structure for Er^{167} populated by electron-capturing Tm^{167} has been previously proposed[4-6] on the basis of three transitions of 57 keV ($M1/E2=7$), 208 keV ($E3$), and 532 keV. The ground-state spin of Er^{167} has been measured as $\frac{7}{2}$ and is represented by Mottelson and Nilsson[4] as the $\frac{7}{2}+[633]$ configuration. The first excited intrinsic state was found at 208 keV ($T_{1/2}=2.5$ sec) and classified as $\frac{1}{2}-[521]$. A $\frac{3}{2}-$ rotational excitation at 265 keV and a possible spin $\frac{5}{2}$ state at 532 keV were also postulated in the decay of Tm^{167}.

The low yield of 3-h Ho^{167} produced from the $Er^{170}(p,\alpha)$ reaction tended to increase uncertainties in the experimental results reported in Table XVII. According to Fig. 10, Ho^{167} decay may excite those levels associated with electron-capture decay as well as

TABLE XVIII. Conversion electron data for decay of Re^{183}(68 day) → W^{183}.

Transition[a] energy (keV)	K	L_I	L_{II}	L_{III}	M	N	Remarks[b]
41.0		15					
46.5		3000	490	220	950	280	$M1/E2=135$
52.6		870	155	100	260	65	$M1/E2=70$
82.9	>50	27	27	d	~12		$M1/E2=3$
84.7	>250	<120[d]	9	~5[e]	20	5	
99.1	175	18	270	240	120	30	$E2$
101.9[e]	~8[e]						
102.5[e]	25						
103.1[e]	c						
107.9	470	70	d	d	19	~6	
109.7	530	80	10	d	20		$M1/E2=50$
120.4[e]	d						
142.1	d	~0.8					
144.1	13	1.9	w				
160.5	12		<9[d]	d	2.2		$E2$
161.4	24	<9[d]					
162.3	1300	220	~45[e]	21	58	17	$M1/E2=8$
192.6	8	1.6	~0.5	~0.3	0.5		$M1/E2\approx2.5$
203.3[e]	~0.6						
205.1	3.8	<0.8[d]			w		
208.8	100	18			4.8	1.3	
209.9	2.4		c	<1.4[d]	~0.6[d]		$E2$
210.3[e]	~0.5[e]		<1.4[d]	0.55			$E3$
244.3	3.4	c	c	<5.4[d]			$E2$
245.2	~6[e]	~0.8[e]					
246.1	29	<5.4[d]					
262.5[e]	<0.8[d]						
291.7	14	c	3.2[e]	1.6	1.5	0.45	$E2$
313.0	5.5	0.9			0.25		
354.0	4.4	0.8			0.2		
365.6	~0.25						
406.6	~0.04						
KLL Auger	400						

[a] Conversion line energy calibration is based on precise transition energy measurements of Ta^{183} decay (reference 30).
[b] Multipole assignments are made on the basis of K/L ratios and L-subshell ratios. Intensity data are normalized to 3000 units for the most prominent line; "w" indicates weak line.
[c] Conversion line is partially resolved.
[d] Conversion line is a composite of two different lines.
[e] Not previously observed in decay of Re^{183} (reference 31).

a number of new states. The ground state of Ho^{167} is expected to be the $\frac{7}{2}-[523]$ orbital, as is the case for the other odd Ho isotopes.

The first rotational level $(\frac{9}{2}+)$ based on the ground $\frac{7}{2}+[633]$ state is at 79.3 keV. This measurement resolves the existing ambiguity regarding the isotopic assignment of the first excited states in Er^{167} and Er^{170} by the Coulomb excitation process.[29]

The data suggest the development of the $K=\frac{1}{2}$ rotational sequence to $\frac{5}{2}-$ and possibly $\frac{7}{2}-$ levels at 281.5 and 415.1 keV, respectively. The experimental decoupling constant $(a=+0.70)$ and moment term $(3\hbar^2/\mathcal{I}=67.2$ keV) identify the orbital as $\frac{1}{2}-[521]$. There exists an anomalously high $M1/E2$ ratio for the 57-keV $(\frac{3}{2}\rightarrow\frac{1}{2})$ rotational transition.

Two possible $\frac{5}{2}-$ levels are placed at 347.7 and 531.5 keV; the latter was previously assigned[5] in connection with Tm^{167} decay. The level energy systematics of intrinsic states in this region suggests that the $\frac{5}{2}-[512]$ state is more likely to occur at 347.7 keV. This configuration occurs at an excitation energy of 191.4 keV in Yb^{169}, an isotone of Er^{167}. The 347.7-keV state is de-excited by $E1$ radiation to ground; the $E1$ assignment is consistent with the very intense photon peak observed at 340 keV. The relationship between intensities of the 340- and 208-keV photon peaks is 10 to 1.

Of interest is the rotational $\frac{5}{2}-[523]$ band based at 585.4 keV, which is characterized by $3\hbar^2/\mathcal{I}=71.5$ keV. The inertial term corresponds well with observed values in odd Dy and Er isotopes (see Table IV). The ratio $M1/E2\approx7$ for the 83.4-keV rotational transition $(\frac{7}{2}\rightarrow\frac{5}{2})$ is considerably higher than is usual for $\frac{5}{2}-[523]$ configurations.

Mottelson and Nilsson[4] have classified the Ho^{167} decay spectrum in the same manner as that shown in

[29] E. L. Chupp, J. W. M. DuMond, F. J. Gordon, R. C. Jopson, and H. Mark, Phys. Rev. **112**, 518 (1958).

Fig. 10. As they point out, the rather small log(ft) value for the 20% beta branch to a ~700-keV level is indicative of allowed unhindered transitions between $\frac{7}{2}-[523]$ and $\frac{5}{2}-[523]$ states.

III. RESULTS AND DATA FOR NUCLEI $183 \leq A \leq 191$

A. Re^{183}(68 day) $\rightarrow W^{183}$

This study of excited states in W^{183}, and subsequent studies with odd-A Os nuclei, are a natural extension of our previous research[5] which terminated at W^{181}. High-precision measurements with beta-active sources of Ta^{183} have been reported earlier by Murray *et al.*[30] The theoretical analysis of the W^{183} decay scheme was performed by Kerman,[19] who included a particle-rotation coupling (Coriolis interaction) between the $\frac{1}{2}-[510]$ and $\frac{3}{2}-[512]$ configurations to explain deviations of the rotational energy spacing. Kerman also calculated electromagnetic transition probabilities between admixed states, since the interaction has an important effect on branching intensity rules. Thulin *et al.*[31] studied the electron-capture decay of Re^{183} and, in general, their work was a confirmation of that of Murray *et al.*

More recently, Gallagher and Nielsen[32] investigated the 5.2-sec isomer of W^{183} which had been chemically separated from its parent, 5.2-day Ta^{183}. They concluded that the isomeric state at 309.5 keV was depopulated by the 102.5-keV ($M2$) γ ray first reported by Murray *et al.* This transition proceeds to the $\frac{7}{2}-$ state of the $K=\frac{1}{2}-$ band. Schmidt-Ott *et al.*[33] have reported a 210-keV ($E3$) γ ray competing with the 102.5-keV ($M2$) γ ray with an intensity of 3.5% of the total isomeric decay. The parity of the 309.5-keV state is certainly positive; the spin is either $\frac{9}{2}$[32] or 11/2.[33]

In the present experiment, the excited states of W^{183} ($N=109$) were investigated with sources of 68-day Re^{183}. The electron intensity data compiled in Table XVIII are sufficiently improved to allow further comparison with theoretical predictions of $M1/E2$ mixing ratios.[19] The agreement is quite close. Table XIX is a listing of transitions depopulating the various levels in W^{183} as presented in Fig. 11. Two transitions of 142 and 262 keV are shown to originate at a new rotational $(\frac{9}{2}-)$ state with 554.2-keV energy. The calculated energy value of 555.5 keV[19] for this high spin state in the $K=\frac{3}{2}-$ band tends to confirm the assignment.

The 309.4-keV isomeric excitation may also be observed in Re^{183} decay proceeding to members of the $K=\frac{1}{2}$ band via 102.5-keV ($M2$) and 210.3-keV ($E3$) radiation. A classification of $\frac{9}{2}+[624]$ for the 309.4-keV state seems more likely than $11/2+[615]$. According to the Nilsson diagram (see Fig. 1), $11/2+[615]$ is expected to occur in W^{183} at a higher excitation than the $\frac{7}{2}-[503]$ intrinsic state, which appears at 453.1 keV. One may observe an average energy displacement of 315 keV between $\frac{9}{2}+[624]$ and $\frac{1}{2}-[510]$ states in $N=107$ isotones (e.g., Yb^{177}, Hf^{179}, W^{181}, Os^{183}). This is approximately the energy difference for W^{183} ($N=109$). The assignment of $\frac{9}{2}+$ rather than $11/2+$ is, however, not consistent with the fact that the gamma rays are of higher multipolarity than might be expected from angular momentum selection rules.

In the figure, the log(ft) values for the different

TABLE XIX. Intensity and multipolarity assigned to transitions depopulating levels shown in decay scheme of Re^{183}(68 day) $\rightarrow W^{183}$ (Fig. 11).

Proposed excited states $(I,K\pi)$	(keV)	De-exciting transitions (keV)	Multipole[a] assignment	Calculated relative intensities $N_\gamma+N_{ce}$	N_γ[b]
$(\frac{3}{2},\frac{1}{2}-)$	46.5	46.5	$M1/E2=135$	5510	570
$(\frac{5}{2},\frac{1}{2}-)$	99.1	52.6	$M1/E2=70$	1690	240
		99.1	$E2$	1075	220
$(\frac{7}{2},\frac{1}{2}-)$	207.0	107.9	$(M1)$	725	150
		160.5	$E2$	65	40
$(\frac{9}{2},\frac{1}{2}-)$	308.9	101.9	$(M1)$	12	2
		209.9	$E2$	21	16
$(\frac{3}{2},\frac{3}{2}-)$	208.8	109.7	$M1/E2=50$	830	180
		162.3	$M1/E2=8$	3060	1400
		208.8	$(M1)$	320	194
$(\frac{5}{2},\frac{3}{2}-)$	291.7	82.9	$M1/E2=3$	290	36
		84.7	$(M1)$	720	90
		192.6	$M1/E2\approx2.5$	25	14
		245.2	$(M1)$	26	19
		291.7	$E2$	247	226
$(\frac{7}{2},\frac{3}{2}-)$	412.1	103.1	$(M1)$	...	...
		120.4	$(M1+E2)$	...	...
		203.3	$(E2)$	5	4
		205.1	$(M1)$	12	7
		313.0	$(M1)$	40	32
		365.6	$(E2)$	7.5	7.2
$(\frac{9}{2},\frac{3}{2}-)$	554.2	142.1	$(M1)$	10	4
		262.5	$(E2)$	...	...
$(\frac{7}{2},\frac{7}{2}-)$	453.1	41.0	$(M1)$	22	2
		144.1	$(M1)$	25	9
		161.4	$(M1)$	52	23
		244.3	$E2$	40	34
		246.0	$(M1)$	126	90
		354.0	$(M1)$	42	36
		406.6	$(E2)$	1.6	1.5
$(\frac{9}{2},\frac{9}{2}+)$	309.5	102.5	$(M2)$	34	1
		210.3	$E3$	4	1
K x-ray intensity[c]				10 450	

[a] Multipolarities are assigned either from conversion electron ratios of Table XVIII or from consistency with angular momentum selection rules; latter assignments are in parentheses and are shown unmixed since we have no way of estimating mixing ratios.
[b] Estimates of photon intensity are obtained from internal conversion electron data and theoretical conversion coefficients of Rose (reference 8).
[c] An extrapolation from KLL-Auger intensity data to K x-ray intensity is based on K-fluorescence yield of 0.94 and total K-Auger intensity at 1.66 times the KLL-Auger intensity.

[30] J. J. Murray, F. Boehm, P. Marmier, and J. W. DuMond, Phys. Rev. **97**, 1007 (1955).
[31] S. Thulin, J. O. Rasmussen, C. J. Gallagher, Jr., W. G. Smith, and J. M. Hollander, Phys. Rev. **104**, 471 (1956).
[32] C. J. Gallagher, Jr., and H. L. Nielsen, Nuclear Phys. **24**, 422 (1961).
[33] W. Schmidt-Ott, K. Hoffmann, I. Y. Krause, and A. Flammersfeld, Z. Physik **162**, 329 (1961).

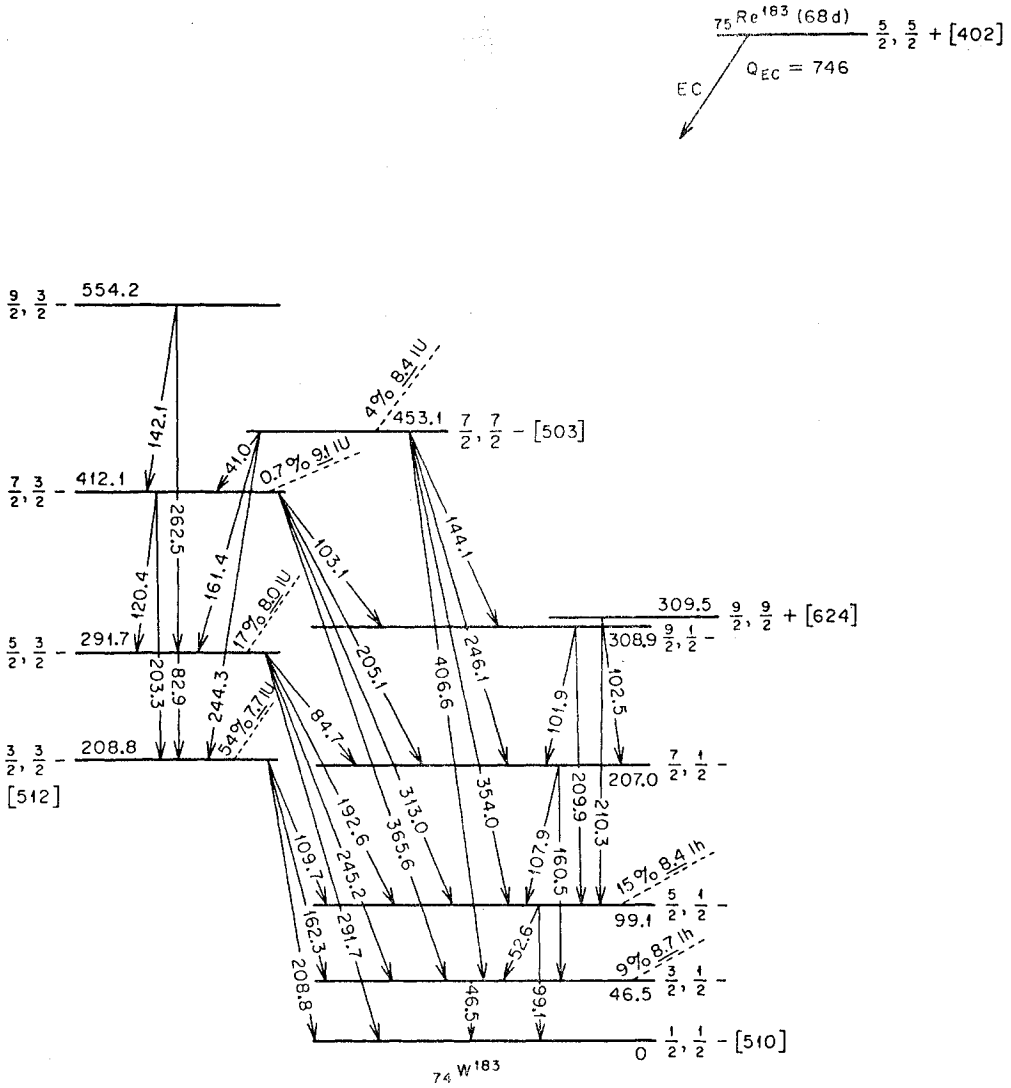

FIG. 11. Proposed decay scheme of Re^{183} (68 d) → W^{183}, based partly on studies of β^- decay of Ta^{183} (reference 30). *All* transitions are accounted for in the level scheme.

electron-capture transitions have been calculated, assuming the $\frac{5}{2}+[402]$ orbital for the Re^{183} ground state. Electron-capture decay totals about 70% to the $I=\frac{3}{2}$ and $I=\frac{5}{2}$ members of the rotational band associated with $\frac{3}{2}-[512]$. The transitions are thus classified as $1u$ and have log(ft)'s of 7.7 and 8.0, respectively. Weaker branches of 9% and 15% proceed to levels 46.5 keV ($\frac{3}{2}-$) and 99.1 keV ($\frac{5}{2}-$) of the $\frac{1}{2}-[510]$ configuration. These transitions are classified as $1h$ and are found to have log(ft) values of 8.7 and 8.4, respectively. The calculated number of K x rays is just sufficient to account for all electron-capture branches and K conversion. There is, therefore, no direct branching to the ground state, which is expected.

As will be shown below, the $\frac{1}{2}-[510]$ and $\frac{3}{2}-[512]$ configurations reappear as low-lying states in Os nuclei. Table XX is a compilation of the properties of the collective excitations (i.e., $3\hbar^2/\mathcal{I}$, B, a, and $M1/E2$ ratios) in this region. The effects of particle-rotation coupling are included in the empirical results. Only for W^{183} has the Coriolis coupling effect been subtracted (see Kerman)[19]; these values are enclosed in parentheses in Table XX. Likewise, the effects of band mixing on transition probabilities are included in the experimental branching ratios of Table XXI.

B. Ir^{185}(15 h) → Os^{185}

An investigation of the properties of nuclear levels in neutron deficient odd-Os isotopes was made with electron-capturing iridium activities. Our 15-h Ir^{185} source was produced by the (p,2n) reaction on a 19-mg Os target enriched to 60% Os^{186}. Table XXII presents, in the main, the low-energy portion of the de-excitation spectrum. Identification of the observed radiations with $A=185$ is based on relative measured yields from a systematic activation of several Os isotopes. It is possible to identify the character of the more intense

TABLE XX. Empirical constants for rotational bands and $M1/E2$ ratios ($181 \leq A \leq 193$).[a]

N	Nucleus	Assigned orbital $K\pi[Nn_z\Lambda]$	$E(I_0)$ (keV)	$3\hbar^2/\mathcal{I}$ (keV)	B (keV)	"a"	$I_0+1 \rightarrow I_0$ (keV)	$I_0+1 \rightarrow I_0$ $M1/E2$[b]
107	$_{74}W^{181}$	$\frac{1}{2}-[510]$	385.2	87.8		+0.48	65.0	15
109	$_{74}W^{183}$	$\frac{1}{2}-[510]$	0	(95.1)[c]		(+0.17)[c]		
109	$_{74}W^{183}$	$\frac{1}{2}-[510]$	0	78.1	−0.003	+0.19	46.5	135
109	$_{76}Os^{185}$	$\frac{1}{2}-[510]$	0	71.4	+0.074	+0.02	37.4	230
111	$_{76}Os^{187}$	$\frac{1}{2}-[510]$	0	48.5	+0.020	−0.60	9.8	···
113	$_{76}Os^{189}$	$\frac{1}{2}-[510]$	36.2				59.1	140
109	$_{74}W^{183}$	$\frac{3}{2}-[512]$	208.8	(84.3)[c]				
109	$_{74}W^{183}$	$\frac{3}{2}-[512]$	208.8	97.9	+0.05		82.9	3
109	$_{76}Os^{185}$	$\frac{3}{2}-[512]$	127.8	114.4	−0.035		94.5	1.4
111	$_{76}Os^{187}$	$\frac{3}{2}-[512]$	74.3	134.0	+0.06		113.1	0.3
113	$_{76}Os^{189}$	$\frac{3}{2}-[512]$	0	83.5			69.6	2.4
112	$_{77}Ir^{189}$	$\frac{3}{2}+[402]$	0	126.7	+0.33		113.7	7
114	$_{77}Ir^{191}$	$\frac{3}{2}+[402]$	0	143.7	+0.39		129.4	7
116	$_{77}Ir^{193}$	$\frac{3}{2}+[402]$	0	156.6	+0.34		139.0	
112	$_{77}Ir^{189}$	$\frac{1}{2}+[400]$	94.2	161.8		−0.015	82.1	pure $M1$
114	$_{77}Ir^{191}$	$\frac{1}{2}+[400]$	82.4	200.0		−0.035	96.5	pure $M1$
116	$_{77}Ir^{193}$	$\frac{1}{2}+[400]$	73					

[a] The energy constants within a rotational band are given by

$$E_I = E^0 + (\hbar^2/2\mathcal{I})[I(I+1) + a(-1)^{I+1/2}(I+\tfrac{1}{2})] + B[I(I+1) + a(-1)^{I+1/2}(I+\tfrac{1}{2})]^2,$$

where E_I is the energy of state of spin I, $\mathcal{I}$ is the moment of inertia, E^0 is a constant, and "a" is the decoupling parameter which is nonzero only for $K=\frac{1}{2}$, $I_0=\frac{1}{2}$ cases.

[b] Ratios (of photon intensities) obtained from L-subshell ratios.

[c] The effect of Coriolis mixing is included except for those values in parentheses which Kerman (reference 19) obtained for W^{183}.

TABLE XXI. Ratios of reduced transition probabilities in de-excitation of levels in W, Os, and Ir ($183 \leq A \leq 191$).

Nucleus	Initial state $I(K\pi[Nn_z\Lambda])$	(keV)	Assumed multipolarity	Final states $I, I+1, I+2(K\pi[Nn_z\Lambda])$	Reduced transition[a] probability ratios
W^{183}	$\frac{3}{2}(\frac{3}{2}-[512])$	208.8	$M1$	$\frac{1}{2}, \frac{3}{2}, \frac{5}{2}(\frac{1}{2}-[510])$	0.07/1/0.46
Os^{185}	$\frac{3}{2}(\frac{3}{2}-[512])$	127.8	$M1$	$\frac{1}{2}, \frac{3}{2}, \frac{5}{2}(\frac{1}{2}-[510])$	0.16/1/0.52
Os^{187}	$\frac{3}{2}(\frac{3}{2}-[512])$	74.3	$M1$	$\frac{1}{2}, \frac{3}{2}, \frac{5}{2}(\frac{1}{2}-[510])$	1.9/1/···
Os^{187}	$\frac{3}{2}(\frac{3}{2}-[501])$	501.4	$M1$	$\frac{1}{2}, \frac{3}{2}, \frac{5}{2}(\frac{1}{2}-[510])$	1.2/1/···
Os^{187}	$\frac{3}{2}(\frac{3}{2}-)$	987.8	$M1$	$\frac{1}{2}, \frac{3}{2}, \frac{5}{2}(\frac{1}{2}-[510])$	1.0/1/···
					1.25/1/0.25(theor.)[b]
Os^{189}	$\frac{3}{2}(\frac{3}{2}-[501])$	233.6	$E2$	$\frac{1}{2}, \frac{3}{2}(\frac{1}{2}-[510])$	2.1/1
					0.25/1(theor.)[b]
W^{183}	$\frac{5}{2}(\frac{3}{2}-[512])$	291.7	$M1$	$\frac{3}{2}, \frac{5}{2}, \frac{7}{2}(\frac{1}{2}-[510])$	0.9/1/100
Os^{185}	$\frac{5}{2}(\frac{3}{2}-[512])$	222.3	$M1$	$\frac{3}{2}, \frac{5}{2}, \frac{7}{2}(\frac{1}{2}-[510])$	6.5/1/110
					0.9/1/0.3(theor.)[b]
W^{183}	$\frac{7}{2}(\frac{3}{2}-[512])$	412.1	$M1$	$\frac{5}{2}, \frac{7}{2}, \frac{9}{2}(\frac{1}{2}-[510])$	1.3/1/w
Os^{185}	$\frac{7}{2}(\frac{3}{2}-[512])$	351.7	$M1$	$\frac{5}{2}, \frac{7}{2}, \frac{9}{2}(\frac{1}{2}-[510])$	1.5/1/0.9
					0.75/1/0.35(theor.)[b]
W^{183}	$\frac{5}{2}(\frac{1}{2}-[510])$	99.1	$E2$	$\frac{1}{2}, \frac{3}{2}(\frac{1}{2}-[510])$	2.6/1
Os^{185}	$\frac{5}{2}(\frac{1}{2}-[510])$	97.4	$E2$	$\frac{1}{2}, \frac{3}{2}(\frac{1}{2}-[510])$	1.9/1
Os^{187}	$\frac{5}{2}(\frac{1}{2}-[510])$	75.0	$E2$	$\frac{1}{2}, \frac{3}{2}(\frac{1}{2}-[510])$	0.4/1
					3.5/1(theor.)[b]
Os^{187}	$\frac{3}{2}(\frac{3}{2}-[501])$	501.4	$M1$	$\frac{3}{2}, \frac{5}{2}(\frac{3}{2}-[512])$	1.6/1
Os^{189}	$\frac{3}{2}(\frac{3}{2}-[501])$	233.6	$M1$	$\frac{3}{2}, \frac{5}{2}(\frac{3}{2}-[512])$	0.7/1
					1.5/1(theor.)[b]
Os^{189}	$\frac{3}{2}(\frac{1}{2}-[510])$	95.3	$M1$	$\frac{3}{2}, \frac{5}{2}(\frac{3}{2}-[512])$	2.4/1
Ir^{191}	$\frac{3}{2}(\frac{1}{2}+[400])$	179.0	$M1$	$\frac{3}{2}, \frac{5}{2}(\frac{3}{2}+[402])$	0.34/1
					0.67/1(theor.)[b]
Ir^{191}	$\frac{5}{2}(\frac{5}{2}+[402])$	539.3	$M1$	$\frac{3}{2}, \frac{5}{2}(\frac{3}{2}+[402])$	0.6/1
Ir^{189}	$\frac{5}{2}(\frac{5}{2}+[402])$	721.8	$M1$	$\frac{3}{2}, \frac{5}{2}(\frac{3}{2}+[402])$	0.6/1
					2.3/1(theor.)[b]
Os^{189}	$\frac{5}{2}(\frac{5}{2}-[503])$	275.9	$E2$	$\frac{3}{2}, \frac{5}{2}(\frac{3}{2}-[512])$	0.36/1
					0.67/1(theor.)[b]
Ir^{191}	$\frac{5}{2}(\frac{1}{2}+[400])$	351.4	$M1$	$\frac{3}{2}, \frac{5}{2}(\frac{3}{2}+[402])$	6.4/1
Ir^{189}	$\frac{5}{2}(\frac{1}{2}+[400])$	317.6	$M1$	$\frac{3}{2}, \frac{5}{2}(\frac{3}{2}+[402])$	1.3/1
					0.15/1(theor.)[b]
Os^{189}	$\frac{7}{2}(\frac{7}{2}-)$	216.7	$E2$	$\frac{3}{2}, \frac{5}{2}(\frac{3}{2}-[512])$	2.4/1
Os^{189}	$\frac{7}{2}(\frac{7}{2}-)$	219.4	$E2$	$\frac{3}{2}, \frac{5}{2}(\frac{3}{2}-[512])$	1.0/1
					1.5/1(theor.)[b]

[a] Experimental reduced gamma-ray intensity is obtained by dividing the K-electron intensity by the theoretical K-conversion coefficient and by the energy dependent term, E^{2L+1}. Coriolis interaction effects are not subtracted. All transitions are K-allowed.

[b] The theoretical relation is given by the square of the ratio of Clebsch-Gordan coefficients compiled by A. H. Wapstra, G. J. Nijgh, and R. Van Lieshout, *Nuclear Spectroscopy Tables* (North-Holland Publishing Company, Amsterdam, 1959).

TABLE XXII. Conversion electron data for decay of Ir^{185}(15 h) → Os^{185}.

Transition energy (keV)	K	L_I	L_{II}	L_{III}	M	N	Remarks[a,b]
24.2		12	~4	w	4		$M1+(E2)$
30.4		7			2		
33.85		3			1		
37.4		600	90	33	190	55	$M1/E2=230$
60.0		250	60	45	85	20	$M1/E2=30$
90.45	>50	18	3.5	d	c		$M1/E2=24$
94.5	>9	2.6	4	3.6	2		$M1/E2=1.4$
97.4	>26	d	95	85	47	12	$E2$
100.75	145	26	3.5	2.5	7	2.3	$M1/E2\approx30$
119.65	2	0.4					
124.95	1.2						
126.9[e]	~18[c]	3.2	~1	w			
127.9	23	4.5	w				
129.4	~0.5	c	1.1[c]	0.55	d		$E2+(M1)$
153.6	29	5.4	w		1.5		
158.3	~30[d]	4.6	w		1.4	d	$M1+(E2)$
160.75	5[c]	c	<5.9[d]	<5.8[d]	1.6	0.44	$E2$
185.0	8.6	1.3			w		
220.4	1.4	c	0.77[c]	<0.64[d]	0.25		$E2$
222.35	<5.9[d]	d	1.0[c]	<1.7[d]	0.35		$E2$
223.8	<5.8[d]	c	<1.7[d]	0.7	0.34		$E2$
254.4	50	8.5	c	0.2	2.2		$M1$
266.5[e]	0.35	d					
300.4[e]	0.25						
307.1[e]	0.28						
314.4	c	w					
321.5[e]	0.9	w					
339.2[e]	0.2						
352.4[e]	0.3						
377.7[e]	0.48	w					
406.8[e]	0.65	w					
419.1[e]	0.28						
431.4[e]	~0.25[c]						
507.0[e]	0.35						
513.7[e]	0.37						
539.4[e]	0.55[c]	w					
745.7[e]	w						
KLL Auger		70					

[a] Intensity data are normalized to 600 units for the 37.4-keV L_I-electron line; "w" indicates weak line.
[b] Multipole assignments are based on K/L ratios and L-subshell ratios.
[c] Conversion line is partly resolved.
[d] Conversion line is a composite of two different lines.
[e] Not placed in decay scheme.

transitions as $M1$, $E2$, or $M1+E2$ (see Table XXI). A number of transitions in the conversion electron spectrum have been previously reported.[34] The 15-h Ir^{185} parent appears to be represented by the $\frac{3}{2}+[402]$ configurations as are $Ir^{189,191}$.[4]

The spectra of Os^{185} consist of intrinsic states $\frac{1}{2}-[510]$ at ground and $\frac{3}{2}-[512]$ at 127.8 keV, with each of which is associated a rotational band (see Fig. 12). The interpretation of the intrinsic states, as implied by the rotational structures, is further supported by a comparison of the moments, $M1/E2$ ratios, and transition probabilities for the analogous states in the isotone, W^{183}. No attempt was made to estimate the contribution of the odd nucleon to the moment of inertia by an analysis of the ratio $\Delta\mathcal{I}/\mathcal{I}$ rigid, where $\Delta\mathcal{I}$ represents the increase in $\mathcal{I}$ for the odd-nucleon case over the value for the even-even nucleus with one less neutron. The rapid variation in the values of $3\hbar^2/\mathcal{I}$ for the $E2(2+\rightarrow 0+)$ transitions in even-A Os nuclei and the effect on $\mathcal{I}$ due to $K=\frac{1}{2}$ and $K=\frac{3}{2}$ band mixing would obscure such an analysis. The regularities in the energies of excited $\frac{7}{2}-[503]$ particle states may perhaps be an indication that the tentative 356.5-keV state is the same orbital.

The intraband transitions determine the four level spacings in the $\frac{1}{2}-[510]$ sequence of Os^{185} to within 0.1 keV. The energy of the $K=\frac{1}{2}$, $I=\frac{9}{2}$ level, using the parameters, is predicted to be 12 keV higher than the

[34] R. M. Diamond and J. M. Hollander, Nuclear Phys. 8, 143 (1958).

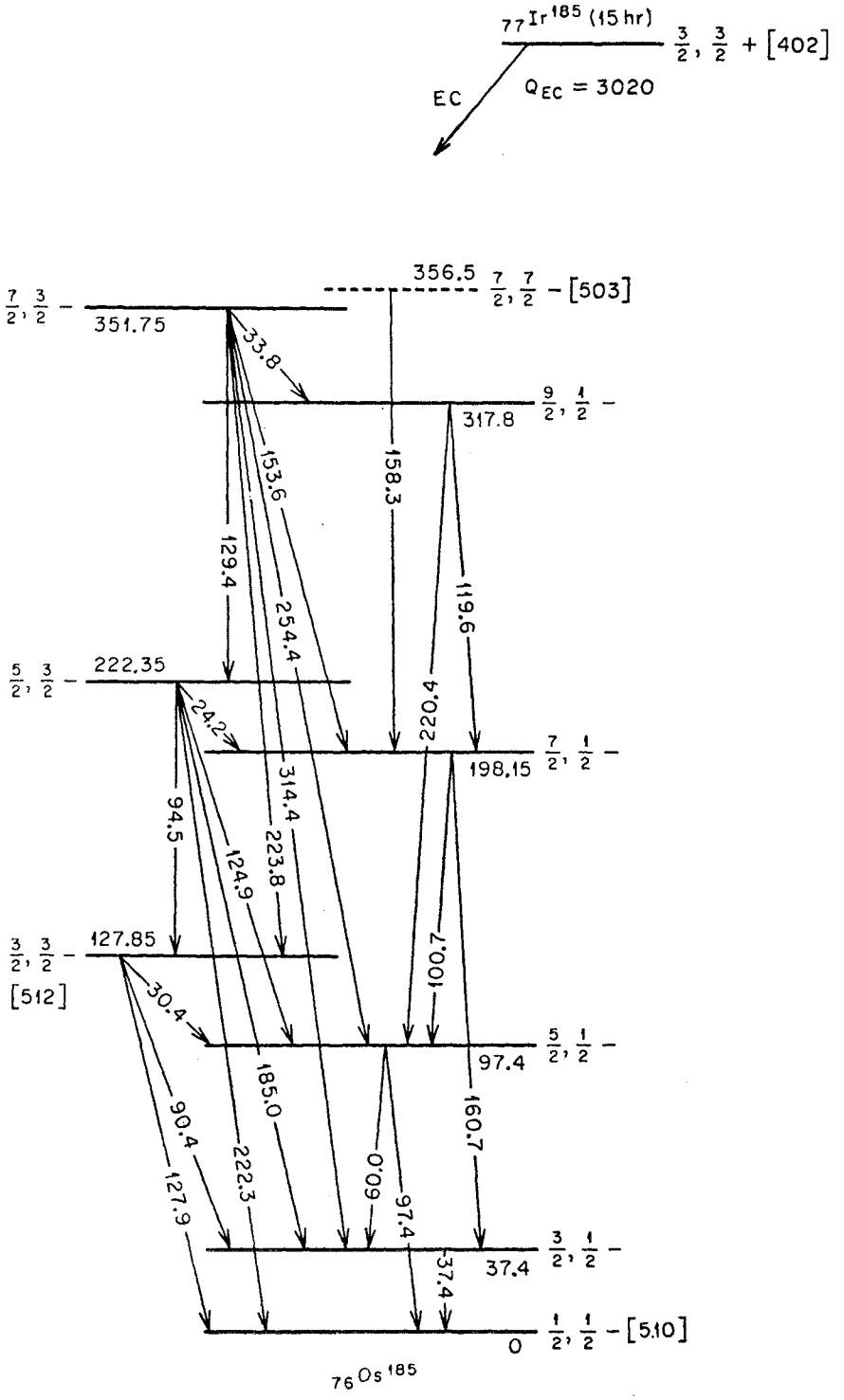

FIG. 12. Partial level scheme for electron-capture decay of Ir^{185}(15 h) to Os^{185}.

experimental value of 317.8 keV. In W^{183}, the empirical energy is about 8 keV less than the observed ($I=\frac{9}{2}$) energy state. For those transitions proceeding between levels of spin difference one, the multipolarities are $M1+E2$ ($M1/E2=230$, 30, 30), and all possible $E2$ crossovers are present, thus indicating the rotational character of the levels. Table XXI displays the experimental ratio of the value $B(E2)$ for the crossover transition to the $B(E2)$ for the cascade transition as 1.9. This is in better agreement with the ratio of 2.6 in W^{183} than with the prediction of 3.5.

Experimental decoupling parameters for postulated

TABLE XXIII. Conversion electron data for decay of Ir^{187}(13 h) → Os^{187}.

Transition energy (keV)	K	L_I	L_{II}	L_{III}	M	N	Remarks[a,b]
9.8			$N_I:N_{II}:N_{III}\approx 5:1:0.6$			>1000	$M1$
25.5		1700	250	50	630	190	$M1$
64.55		820	130	80	c	c	$M1/E2=60$
65.3		~100[c]	3900	3900	2000	540	$E2$
74.35		1500	160	50	380	100	$M1$
75.05		d	~1700[c]	1640	900	240	$E2$
84.9	>50	<80[d]			17		
87.1	w	~50[c]					
90.7	w		7	7	w		$E2$
112.4	w	c	~20[c]	~25[c]			$E2+(M1)$
113.15	155	~17[c]	80	60	35		$M1/E2=0.3$
115.65[e]	40	w					
150.5	w	c	~4.3	~3.9			$E2$
156.6[e]	125	d		~6	c		
162.8[e]	62	8					
163.5	36	d		d			
170.4[e]		c	~1.7	~1.7			
177.7	940	160	~34[c]	18.5	<105[d]		$M1/E2=6$
180.9[e]	25	c	10.5	7.5			$E2$
181.85[e]	10	c					
187.5	160	c	<105[d]	50	<64[d]		$E2$
189.2[e]	3						
198.7[e]	~22[d]	w					
206.9[e]	2.7						
224.4	~14[d]	w					
252.9[e]	11.5						
258.45[e]	<64[b]	6					

Energy (keV)	K	L_I	L_{II}	L_{III}	M	Remarks[a,b]
261.5[e]	32	c				
263.4[e]	3	w				
266.3[e]	5.4	w				
275.95	5.2	w				
276.6	w		w	w		$E2$
299.5[e]	25	3.6				
313.95	100	16		w	d	$M1$
344.6[e]	4.4	w				
348.2[e]	5	w				
370.1[e]	5.5	c				
395.6[e]	7.5	~1.3				
398.7	19	3				
400.7	67	c	14[c]	3	4.5	$E2$
426.4	d	d				
427.1	~175[d]	~27[d]				
447.6[e]	5.4	0.9				
486.1	9	c			w	
491.7	33	5.6			<8[d]	
501.4	39	<8[d]				
515.5[e]	10.5	<17[d]				
522.0[e]	7.5					
576.7	~15.5[d]	<5[d]			d	
586.7	4.6	d				
588.9[e]	3.6					
610.9	59	10			3	
636.8	<5[d]					
651.5	4	c				
654.35[e]	5	<3[d]				
715.9	<3[d]	w				
725.65	2.6	w				
747.4[e]	2.6					

[a] Multipole assignments are based on K/L and L-subshell ratios.
[b] Intensity data are normalized to 3900 units for the most prominent line. "w" indicates weak line.
[c] Conversion line is partially resolved.
[d] Conversion line is a composite of two different lines.
[e] Not placed in decay scheme.

TABLE XXIII (*continued*)

Energy (keV)	K	L_{I}	L_{II}	L_{III}	Remarks[a,b]
757.05[c]	2.4				
760.3[c]	~0.7				
800.2	6.6	1.3			
886.9	w				
903.1[c]	2.1				
912.8	23	4			
978.0	10.3	2			
987.9	10.7	2			
1102.8	w				
1112.1	1.5				

$\frac{1}{2}-[510]$ bands in Os^{185} and W^{183} disagree with each other and with predicted values for this orbital. $K=\frac{1}{2}-$ bands in Os^{185} and W^{183} are described by decoupling constants $a=+0.02$ and $+0.19$, as compared with $a_{\mathrm{theor}}=-0.17$ for the expected eccentricity, $\delta=0.2$. The experimental $3\hbar^2/\mathcal{I}$ values differ by 10%, the lower one belonging to Os^{185}. It is possible that the $3\hbar^2/\mathcal{I}$ term reflects a stronger Coriolis effect on Os^{185}, which is consistent with the decreased energy separation of the relevant levels. It is significant that Kerman[19] gives 95.1 keV as the "true" value of the $K=\frac{1}{2}$ inertial term in W^{183}, where the experimental value is 78.1 keV.

The members of the rotational band associated with intrinsic state $\frac{3}{2}-[512]$ at 127.8 keV are 222.3 keV $(\frac{5}{2}-)$ and 351.7 keV $(\frac{7}{2}-)$. Within the band, the cascade γ rays indicate strong $E2$ admixtures ($M1/E2=1.4$), which are found consistently in $\frac{3}{2}-[512]$ bands in this region. Of interest is the absence of feeding from $\frac{1}{2}-[510]$ to $\frac{3}{2}-[512]$ bands, although all three levels of the $K=\frac{3}{2}$ sequence proceed to all levels (where $\Delta I\leq 2$) of the ground-state $K=\frac{1}{2}$ band. As has been observed previously, levels de-excite preferentially towards K_0 (except for rotations), where K_0 is the K number assigned to ground.

The interpretation of Os^{185} states is supported by a comparison of interband transition probabilities between $K_i=\frac{3}{2}-$ and $K_f=\frac{1}{2}-$ states, with the results obtained in W^{183}. The reduced γ-ray branching ratios for $M1$ radiation in Os^{185} are

$E_i=127.8$ keV $(\frac{3}{2})$:
$127.9\gamma/90.4\gamma/30.4\gamma=0.16/1/0.52$,

$E_i=222.3$ keV $(\frac{5}{2})$:
$185.0\gamma/124.9\gamma/24.2\gamma=6.5/1/110$,

and

$E_i=351.7$ keV $(\frac{7}{2})$:
$254.4\gamma/153.6\gamma/33.8\gamma=1.5/1/0.9$.

The analogous branching ratios in W^{183} are

$E_i=208.8$ keV $(\frac{3}{2})$:
$208.8\gamma/162.3\gamma/109.7\gamma=0.07/1/0.46$,

$E_i=291.7$ keV $(\frac{5}{2})$:
$245.2\gamma/192.6\gamma/84.7\gamma=0.9/1/100$,

and

$E_i=412.1$ keV $(\frac{7}{2})$:
$313.0\gamma/205.1\gamma/103.1\gamma=1.3/1/w$.

The theoretical relationships are given by 1.25/1/0.25 for $I_i=\frac{3}{2}$, 0.9/1/0.3 for $I_i=\frac{5}{2}$, and 0.75/1/0.35 for $I_i=\frac{7}{2}$. The observation that comparable ratios of W^{183} and Os^{185} are in striking agreement among themselves but appear to disagree with predictions may be interpreted as evidence of band mixing.

C. Ir^{187}(13 h) $\rightarrow$ Os^{187}

Our experiments with Ir^{187} activity indicate the existence of at least 65 transitions of energies less than 1 MeV. It may be noted that all of the stronger radiation up to 400 keV, listed in Table XXIII, are classified as either $M1$, $E2$, or as a mixture of these. Conversion electron lines, attributed to a 9.8-keV $M1$ transition, are observed to convert in the N and O subshells. Gamma-ray scintillation spectra were studied, and Table XXIV lists the experimental photon intensities normalized relative to the 611-keV $M1$ conversion coefficient. The resulting conversion coefficients for the transitions of 912, 978, and 988 keV are consistent only with $M1$ multipolarity. Earlier work on this nuclide was done by Diamond and Hollander[34] who irradiated rhenium with α particles. An energy-level diagram which is compatible with experimental results is illustrated in Fig. 13.

The Ir^{187} ground state should correspond with the $\frac{3}{2}+[402]$ configuration just as for Ir^{189} and Ir^{191}. The lowest excited states of Os^{187} are found to be very similar to those proposed in W^{183}. The ground-state spins have been measured, and found to be $\frac{1}{2}$ for both nuclei, and the magnetic moments are identically 0.12 nm. The experimental deformation of Os^{187}, deduced from the measured intrinsic quadrupole moment, is 0.18 as compared with 0.21 for W^{183}.[4]

The development of the $\frac{1}{2}-[510]$ sequence, consisting of states at 0, 9.8, 75.0, and 100.5 keV, is based on five intraband transitions and twenty-one interband transitions populating the levels. The energies of the states have been fitted to the rotational energy formula. Thus,

TABLE XXIV. Intensity and multipolarity assigned to transitions depopulating levels shown in decay scheme of Ir^{187}(13 h) → Os^{187} (Fig. 13).

Proposed excited states $(I,K\pi)$	(keV)	De-exciting transitions (keV)	Multipole[a] assignment	Calculated relative intensities $N_\gamma+N_{ce}$	N_γ[b]	Photon data[c] N_γ
$(\frac{1}{2},\frac{1}{2}-)$	0					
$(\frac{3}{2},\frac{1}{2}-)$	9.8	9.8	$M1$	>5000	···	
$(\frac{5}{2},\frac{1}{2}-)$	75.05	65.3	$E2$	10 830	390	
		75.05	$E2$	5200	330	
$(\frac{7}{2},\frac{1}{2}-)$	100.55	25.5	$M1$	2880	60	
		90.7	$E2$	25	3.5	
$(\frac{3}{2},\frac{3}{2}-)$	74.35	64.55	$M1/E2=60$	1720	350	
		74.35	$M1$	10 700	1000	
$(\frac{5}{2},\frac{3}{2}-)$	187.5	87.1	$(M1)$	360	42	
		112.4	$E2+(M1)$	120	35	
		113.15	$M1/E2=0.3$	480	120	
		177.7	$M1/E2=6$	2440	1220	1700
		187.5	$E2$	1140	780	
$(\frac{7}{2},\frac{3}{2}-)$	351.0	163.5	$(M1+E2)$	75	32	
		275.95	$(M1)$	24	18	
		276.6	$E2$	w	w	
$(\frac{3}{2},\frac{3}{2}-)$	501.4	150.5	$E2$	42	23	
		313.95	$M1$	620	500	500
		400.7	$E2$	2400	2310	
		426.4	$(M1)$	d	d	3720
		427.1	$(M1)$	2300	2085	
		491.7	$(M1)$	600	555	1300
		501.4	$(M1)$	745	700	
$(\frac{1}{2},\frac{1}{2}-)$	725.8	224.4	$(M1)$	45	28	
		651.5	$(M1)$	145	140	
		715.9	$(M1)$	~93	~90	
		725.65	$(M1)$	120	117	
$(\frac{3}{2},\frac{3}{2}-)$	987.8	486.1	$(M1)$	160	150	
		636.8	$(E2)$	<500	<500	
		800.2	$(M1)$	398	390	
		886.9	$(E2)$	w	w	
		912.8	$(M1)$	1950	1920	1400
		978.0	$(M1)$	1030	1020	1800
		987.9	$(M1)$	1093	1080	
$(-)$	1112.3	610.9	$(M1)$	1810	1735	1735
		1102.8	$(M1)$	w	w	
		1112.1	$(M1)$	205	203	

[a] Multipolarities are assigned either from conversion electron ratios of Table XXIII or from consistency with angular momentum selection rules; latter assignments are in parentheses and are shown unmixed since we have no way of estimating mixing ratios.
[b] Estimates of photon intensity are obtained from internal conversion electron data and theoretical conversion coefficients.
[c] Photon data are normalized to the 610.9-keV transition, assuming pure $M1$ multipolarity.

the ground-state rotational band in Os^{187} is described by $3\hbar^2/\mathcal{I}=48.5$ keV and the decoupling constant $a=-0.60$, compared with $3\hbar^2/\mathcal{I}=71.4$ keV and $a=+0.02$ for Os^{185}. The theoretical value of a for $\frac{1}{2}-[510]$ bands is expected to increase with decreasing deformation, according to Mottelson and Nilsson,[4] which is opposite to the behavior of the experimental results. One may note that the decrease of the $(K=\frac{1}{2})$ inertial term in Os^{187}, as compared with Os^{185}, is consistent with the relatively small energy separation of the $\frac{3}{2}-[512]$ particle state. In postulating the 9.8-keV $(\frac{3}{2}-)$ excited state, it is presumed that the de-exciting transition is of sufficient intensity to at least balance the intensity of the electromagnetic radiation proceeding to it. Our intensity measurements are highly uncertain for such low electron energies. Electromagnetic transition probabilities for $E2$ radiation de-exciting the 75.0-keV $(\frac{5}{2}-)$ state show the effect of band mixing. Quantitatively, the experimental ratio of the crossover to the cascade transition is 0.4, while the simple theoretical relation gives 3.5.

The orbital assignment of $\frac{3}{2}-[512]$ for the 74.3-keV intrinsic state is consistent with the associated rotational excitations at 187.5 keV $(\frac{5}{2}-)$ and 351.0 keV $(\frac{7}{2}-)$ which characterize this configuration. The cross feeding between bands as well as within the band is extensive. For the 113-keV intraband transition, proceeding between levels of spin difference one, the multipolarity is $M1/E2=0.3$, and the $E2$ crossover is present, thus indicating the rotational character of the levels. The rotational energy parameter for this band is $3\hbar^2/\mathcal{I}=134$ keV, which is considerably larger than for neighboring

$N=109$ configurations. Compare, for example, W^{183} with $3\hbar^2/\mathcal{I}=97.9$ keV and Os^{185} with $3\hbar^2/\mathcal{I}=114.4$ keV. A displacement of energy levels due to the Coriolis effect would tend to increase the inertial term of the upper band. The relatively small energy separation between $K=\frac{1}{2}$ and $K=\frac{3}{2}$ levels in Os^{187} would be consistent with the rather marked effect. The positive signs of the empirical constant B (i.e., $B=+0.02$ for $K=\frac{1}{2}$ and

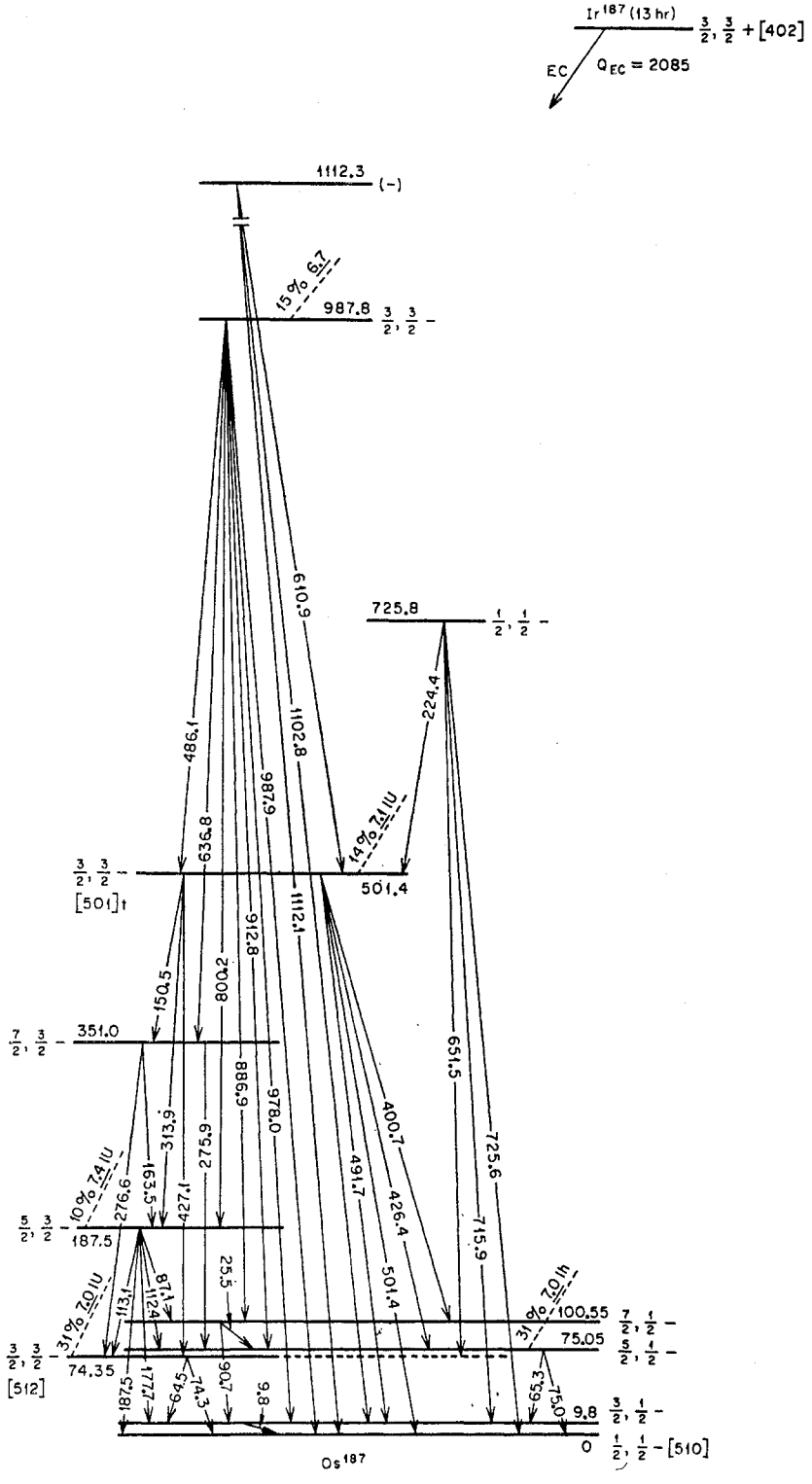

FIG. 13. Nuclear levels in Os^{187} populated by electron-capture decay of Ir^{187}(13 h). A tentative state at 586.4 keV is not shown.

TABLE XXV. Conversion electron data for decay of Ir^{189}(11 day) → Os^{189}.

Transition energy (keV)	K	L_I	L_{II}	L_{III}	M	N	Remarks[a,b]
25.7		15	w		w		$M1+(E2)$
30.8		33	w	180	95	25	$M3$
33.35			65	75	50		$E2$
36.23		360	50	13	140	45	$M1/E2=250$
56.5		39	5		10		$M1/E2=140$
59.1		350	45	d	110		$M1/E2=140$
59.3		~30[c]	6				$M1+E2$
69.6		490	830	780	570	180	$M1/E2=2.4$
95.2	~15[c]	d					
95.3	~75	45	13	8.5	16	5	$M1/E2=12$
97.8	d	1.6					
138.3	13	3.0	1.5	0.9	c		$M1/E2=3$
147.1	13	~2.5[d]	~2[c]	~1.5	<3[d]		$M1/E2\approx1$
149.9	6	c	3.5[c]	2.4	2.2		$E2$
164.0	11	1.5	w	w			$M1+(E2)$
180.5	3.2	w					
185.85	18	~2.5[c]	d	d	d		$M1+(E2)$
188.6	6.3	d	d	~0.6	d		$M1/E2\approx0.5$
197.4	8.5	d	~1.6[c]	c	d		$E2+(M1)$
206.3	4.6	c	~1.8[c]	d	c		$E2$
216.7	15	c	4.5[c]	3.1	2		$E2$
219.35	13	~1.5	4.5	2.4	2.1		$E2$
233.5	13	d	d	0.8	c		$M1/E2\approx0.5$
245.0	100	~15[c]	25[c]	18	14	4	$E2$
275.8	14	2.7	~1.3[c]	0.8	1		$M1/E2\approx0.6$
KLL Auger	230						

[a] Intensity data are normalized to 830 units for the 69.6-keV L_{II}-electron line; "w" indicates weak line.
[b] Multipole assignments are based on K/L and L ratios.
[c] Conversion line is not completely resolved.
[d] Conversion line is a composite of two different lines.

$B=+0.06$ for $K=\frac{3}{2}$ bands) also imply a substantial amount of interband mixing.

Decay branching from Ir^{187} is approximate and is meant to serve only as a guide; no data as to the existence of electron-capture branches to the 9.8-keV and ground states were obtained. The decays of Ir to the excited states (shown in Fig. 13) are first forbidden, and have log(ft) values ranging from 6.7 to 7.4.

A knowledge of the multipolarity of six transitions de-exciting the 501.4-keV state establishes the spin and parity of the level as $\frac{3}{2}-$. The level at 987.8 keV is depopulated by transitions to the level at 501.4 keV, as well as to the $\frac{1}{2}-[510]$ and $\frac{3}{2}-[512]$ configurations. In this case, the relative photon and electron data fit reasonably well an assignment of $M1$ for transitions of 912, 978, and 988 keV to spin $\frac{1}{2}$, $\frac{3}{2}$, and $\frac{5}{2}$ states, which establishes the 987.8-keV level as $\frac{3}{2}-$.

Some remarks may be made about the gamma-ray de-excitation of these $I=\frac{3}{2}-$ states. The experimental ratios $B(M1:\frac{3}{2}\rightarrow\frac{1}{2})/B(M1:\frac{3}{2}\rightarrow\frac{3}{2})$ are 1.9, 1.2, and 1.0 for decay of the 74.3-, 501.4-, and 987.8-keV $(\frac{3}{2}-)$ states, respectively, to the members of the $K=\frac{1}{2}-$ band. There is surprising consistency in the above ratios, as well as with the predicted ratio of 1.25 calculated for $K_i=\frac{3}{2}$. In line with the ordering of intrinsic states, the expected orbital $\frac{3}{2}-[501]$ is assigned to the 501.4-keV excitation.

D. Ir^{189}(11 day) → Os^{189}

Proton irradiation of Os^{190} produced a source of Ir^{189} activity. Our conversion electron data, compiled in Table XXV, indicates that all of the intense gamma rays are either $E2$ or a mixture of $E2+M1$, except for the 30.8-keV radiation of $M3$ multipole order,[17] which depopulates a 5.7-h isomeric state ($\frac{9}{2}-[505]$). Earlier experiments with Ir^{189} have been reported by Diamond and Hollander[34] and also by Kane,[35] all of whom used high resolution spectrographs. In addition, Kane did photoelectric conversion measurements. Their results, in general, are in agreement with the level scheme shown in Fig. 14, and the relevant transition data summarized in Table XXVI.

The ground-state spin of Os^{189} has been measured as $I_0=\frac{3}{2}$ with a magnetic moment of $\mu=0.65$ nuclear magneton.[17] The ground-state assignment of $\frac{3}{2}-[512]$ is supported by a predicted value of $\mu=0.9$ nm for this orbital.[4] From measured $E2$ transition probabilities, the calculated deformation of Os^{189} is $\delta=0.15$, as compared with $\delta=0.18$ for Os^{187}, and $\delta=0.21$ for W^{183}.[4]

In the decay scheme (Fig. 14), a rotational excitation of the $\frac{3}{2}-$ ground state is postulated at 69.6 keV $(\frac{5}{2}-)$. The level has been Coulomb excited by Durham, Rester,

[35] W. R. Kane, thesis, Harvard University, 1959 (unpublished).

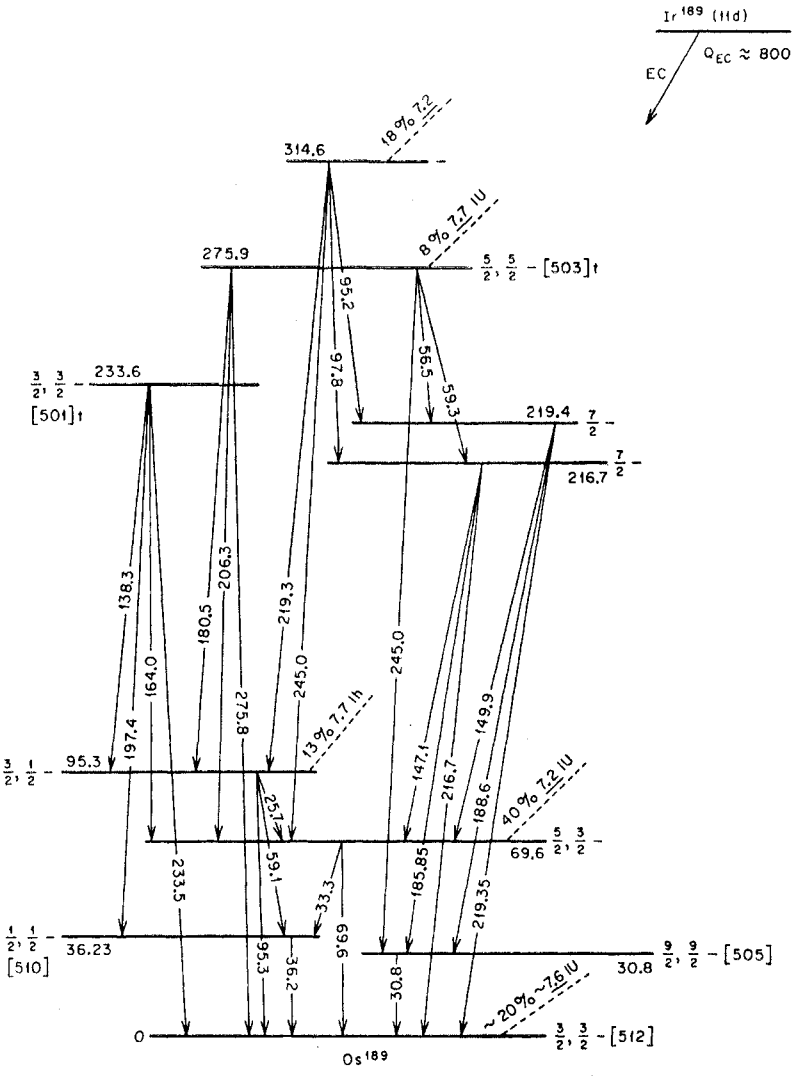

FIG. 14. Levels excited in Os^{189} following decay of Ir^{189} (11 day). *All* observed transitions are placed in the scheme.

and Class,[36] and also observed in the β^- decay of Re^{189} by Crasemann, Emery, and Kane.[37] The intraband transition is an $M1/E2=2.4$ mixture, which is characteristic of the $\frac{3}{2}-[512]$ orbital, and has $3\hbar^2/\mathcal{I}=83.5$ keV.

Another rotational sequence is possibly based on a $\frac{1}{2}-[510]$ level at 36.2 keV, with a rotational excitation at 95.3 keV $(\frac{3}{2}-)$. There appears to be no additional rotational structure in Os^{189} $(N=113)$. The lack of rotations was noted also in Sm^{151} $(N=89)$ at the other end of the deformed region. The intraband radiation of 59.1 keV in the $\frac{1}{2}-[510]$ configuration is described as an $M1/E2=140$ mixture; this is comparable with $M1/E2=135$ in W^{183} and $M1/E2=230$ in Os^{185}. The Coriolis interaction is apparently modifying the inertial properties of the low-lying bands. The trends in experimental data in Table XX indicate that in Os^{189} the level spacing of the upper $K=\frac{1}{2}-$ band is elevated, while the lower $K=\frac{3}{2}-$ band is depressed.

The 233.6-keV $(\frac{3}{2}-)$ state decays to all members of the $K=\frac{1}{2}-$ and $K=\frac{3}{2}-$ bands by mixed $M1+E2$ transitions, and may perhaps be designated as $\frac{3}{2}-[501]$. One may note that the $\Delta I=0$, 1 transitions have low $M1/E2$ ratios (see Table XXVI). This is unexpected, since dipole radiation is K allowed and unhindered in the asymptotic quantum numbers. The electromagnetic transition probability for $M1$ γ rays from the 233.6-keV $(\frac{3}{2}-)$ level to the ground-state $K=\frac{3}{2}-$ sequence is experimentally 0.7, as compared with the theoretical value of 1.5.

The next level at 275.9 keV is de-excited by $M1+E2$ transitions to the ground $(\frac{3}{2}-)$ state, and by pure $E2$ gamma rays to the 30.8-keV $(\frac{9}{2}-)$ state. The multipolarities of the gamma rays suggest $I=\frac{5}{2}-$ for the 275.9-keV level, and one might expect the orbital

[36] F. E. Durham, D. H. Rester, E. M. Class, Bull. Am. Phys. Soc. 4, 98 (1959).
[37] B. Crasemann, G. T. Emery, and W. R. Kane, Bull. Am. Phys. Soc. 7, 353 (1962).

TABLE XXVI. Intensity and multipolarity assigned to transitions depopulating levels shown in decay scheme of Ir^{189}(11 day) $\rightarrow$ Os^{189} (Fig. 14).

Proposed excited states $(I,K\pi)$	(keV)	De-exciting transitions (keV)	Multipole assignment[a]	Calculated relative intensities $N_\gamma+N_{ce}$	N_γ[b]
$(\frac{3}{2},\frac{3}{2}-)$	0				
$(\frac{5}{2},\frac{3}{2}-)$	69.6	33.35	$E2$	205	<1
		69.6	$M1/E2=2.4$	3210	360
$(\frac{9}{2},\frac{9}{2}-)$	30.8	30.8	$M3$	235	<1
$(\frac{1}{2},\frac{1}{2}-)$	36.2	36.23	$M1/E2=250$	640	28
$(\frac{3}{2},\frac{1}{2}-)$	95.3	25.7	$M1+(E2)$	25	0.5
		59.1	$M1/E2=140$	650	113
		95.3	$M1/E2=12$	230	65
$(\frac{7}{2}-)$	216.7	147.1	$M1/E2\approx1$	34	13
		185.85	$(M1+E2)$	44	22
		216.7	$E2$	130	105
$(\frac{7}{2}-)$	219.4	149.9	$E2$	28	14
		188.6	$M1/E2\approx0.5$	30	16
		219.35[c]	$E2$	120	95
$(\frac{3}{2},\frac{3}{2}-)$	233.6	138.3	$M1/E2=3$	28	8
		164.0	$M1+(E2)$	23	10
		197.4	$E2+(M1)$	36	21
		233.5	$M1/E2\approx0.5$	80	60
$(\frac{5}{2},\frac{5}{2}-)$	275.9	56.5	$M1/E2=140$	70	11
		59.3	$M1+E2$	60	10
		180.5	$(M1)$	7.5	3.7
		206.3	$E2$	40	29
		245.0[c]	$E2$	$\sim$200	$\sim$170
		275.8	$M1/E2\approx0.6$	90	70
$(-)$	314.6	95.2	$(M1)$	$\sim$21	$\sim$3
		97.8	$(M1)$	$\sim$13	$\sim$2
		219.3[c]	$E2$	...	...
		245.0[c]	$E2$	$\sim$975	$\sim$830
K x-ray intensity					6000

[a] Multipolarities are assigned either from conversion electron ratios of Table XXV or from consistency with angular momentum selection rules; latter assignments are in parentheses and are shown unmixed since we have no way of estimating mixing ratios.
[b] Estimates of photon intensity are obtained from internal conversion electron data and theoretical conversion coefficients.
[c] Recurring transition is listed twice.

$\frac{5}{2}-[503]$ at about this region of excitation. The experimental $E2$ γ-ray de-excitation from the 275.9-keV state to the $\frac{3}{2}-[512]$ band is

$$B(E2:\ \tfrac{5}{2}\rightarrow\tfrac{3}{2})/B(E2:\ \tfrac{5}{2}\rightarrow\tfrac{5}{2})=0.36,$$

where the intensity rules predict 0.67 for $K_i=\frac{5}{2}$ and 24 for $K_i=\frac{3}{2}$. The existence of an appreciable amount of $E2$ admixture to $M1$ radiation in transitions to low-energy states involving a spin difference of 0 or 1 is observed as for the 233.6-keV state.

Excited states at 216.7 and 219.4 keV are classified as $\frac{7}{2}-$ on the basis of the observed de-excitation and feeding. McGowan *et al.*[38] have observed a level at 219 keV in Os^{189} by Coulomb excitation. There are a number of possible interpretations of the pair of $\frac{7}{2}-$ states: a gamma vibration of the ground state, or a second rotational excitation of the $\frac{3}{2}-[512]$ configuration, or a $\frac{7}{2}-[503]$ single-particle excitation. The experimental $E2$ transition probabilities from the above $\frac{7}{2}-$ states to the ground-state ($K=\frac{3}{2}-$) sequence yields

$$E_i=216.7\text{ keV}:\quad B(E2:\ \tfrac{7}{2}\rightarrow\tfrac{3}{2})/B(E2:\ \tfrac{7}{2}\rightarrow\tfrac{5}{2})=2.4,$$

and

$$E_i=219.4\text{ keV}:\quad B(E2:\ \tfrac{7}{2}\rightarrow\tfrac{3}{2})/B(E2:\ \tfrac{7}{2}\rightarrow\tfrac{5}{2})=1.0.$$

The predicted value for $K_i=\frac{7}{2}$ is 1.5. The existence of a strong quadrupole component in the de-exciting γ rays, as shown in Table XXVI, may be related to the collective excitations described by the unified model (although dipole radiation may be allowed under angular momentum selection rules). Rotational ($\Delta I=1$) transitions in cascade would have low $M1/E2$ mixing ratios associated with the $\frac{3}{2}-[512]$ orbital. Theoretically, of course, dipole radiation is forbidden in vibrational transitions.

It is possible, on the basis of the remaining transitions, to postulate a 314.6-keV state of odd parity. The composite 245.0-keV ($E2$) radiation may proceed from both the 275- and 314-keV states. Consideration of the excitation and de-excitation intensity about the 30.8-keV level determined the apportionment of the transition intensity data.

The decay of $Pt^{189}\rightarrow Ir^{189}$ reported below indicates that Ir^{189} is most likely in a $\frac{3}{2}+[402]$ state. The intensity of the KLL Auger lines is consistent with an estimate of a 20% electron-capture branch to the ground state of Os^{189}. Figure 14 presents the approximate electron-capture branching percentages to levels in Os^{189}, all of odd parity. The transitions are expected to be first forbidden and are observed to have $7.2\leq\log(ft)\leq7.7$.

E. Pt^{189}(11 h) $\rightarrow$ Ir^{189} and Pt^{191}(3 day) $\rightarrow$ Ir^{191}

In this study of excited states in neutron-deficient, odd-Z Ir nuclei, the decay schemes were examined for possible collective effects, as well as for regularities in the energies of single-particle states. Previous investigations of deformed nuclei[6,39] have shown average displacements of about 100 keV between intrinsic proton states populated in odd-A isotopes, where $\Delta A=2$.

Composite sources of Pt($A=189$, 191, and $193m$) were produced by irradiation of natural Ir foils with 22-MeV protons, and subsequent chemical extraction of the Pt.[7] Analysis of the complex spectrum of Pt^{189} was limited by the presence of Pt^{191} and by the low activation yield. No decay from Pt^{193} was observed, aside from transitions (of 12.6 and 135.5 keV) following 4.4-day Pt^{193m} decay.

[38] F. K. McGowan, P. H. Stelson and R. L. Robinson, in *Electromagnetic Lifetimes and Properties of Nuclear States*, Nuclear Science Series 37 (National Academy of Sciences-National Research Council Publication No. 974, Washington, D. C., 1962), p. 119.

[39] N. K. Glendenning and S. G. Nilsson, Bull. Am. Phys. Soc. **6**, 377 (1961).

TABLE XXVII. Conversion electron data in decay of Pt^{191}(3 day) → Ir^{191}.

Transition energy (keV)	K	L_I	L_{II}	L_{III}	M	N	Remarks[a,b]
41.8			35	40	25		$E3$
49.5		~30	c	w			$M1+E2$
82.45		440	850	780	470	110	$M1/E2=1.4$
85.2		13	~4	w			$M1+(E2)$
96.5	>900	300	42	13	70	d	$M1/E2=55$
129.45	670	105	30	18	30	8	$M1/E2=7$
172.3	390	62	c	~1	16	4	$M1$
179.0	80	13.5	5	3.5	5	1.2	$M1/E2=2.5$
187.75	36	5.5			1.7		
213.8	1.4						
219.8[e]	12	c	5.4	<5[d]	2.2		$E2$
221.9	7.7	d					
223.7[e]	6.6	1.1					
268.25[e]	~6	c					
269.1	14.7	c	7.5	2.6	2.6		$E2$
272.0[e]	1.4						
351.5	56	9					$M1$
360.3	100	15.5			3.5		$M1$
409.9	91	14			4		$M1$
457.0	24	4			1.3		
493.0[e]	2						
495.1	2.8						
539.5	60	8.8			2.5		
584.2[e]	0.3						
588.3[e]	0.5	w					
604.6[e]	c						
624.6	4.9	0.8			0.2		
KLL Auger	460						

[a] Multipole assignments are based on K/L and L-subshell ratios.
[b] Intensity data are normalized to the most prominent line. "w" indicates weak line.
[c] Conversion line is partially resolved.
[d] Conversion line is a composite of two different lines.
[e] Not placed in decay scheme.

TABLE XXVIII. Conversion electron data for decay of Pt^{189}(11 h) → Ir^{189}.

Transition energy (keV)	K	L_I	L_{II}	L_{III}	M	N	Remarks[a,b]
71.6		500	100	160	c		$M2$
82.15		~700[e]			d		$M1$
94.25	w	c	1840	1770	900	230	$E2$
113.75	>920	~330[d]	110	70	d		$M1/E2=7$
141.1	1100	220	c		55	16	$M1$
176.4	d	18	c	c			$M1+E2$
181.2[e]	19						
186.65	~240[d]	40					
190.9[e]	14						
204.0	d	10					
223.45	29	c	14	9	8		$E2$
225.9[e]	0.6						
243.6[e]	100	c	70	17	d		$E2$
258.3	11	c	13	6			$E3$
300.6	33	c	12	6			$E2$
317.8	~82[d]	14.5					
404.2	26	5					
541.8[e]	c						
545.5	43	d					
569.3[e]	46	7					
608.1	~39[d]	6					
627.5	~10[e]	w					
721.7	27	5					
736.3[e]	~1.5						
793.2[e]	4.7						
802.0[e]	~1.4						

[a] Multipole assignments are based on K/L and L-subshell ratios.
[b] Intensity data are normalized to 1840 units for the most prominent line. "w" indicates weak line.
[c] Conversion line is partially resolved.
[d] Conversion line is a composite of two different lines.
[e] Not placed in decay scheme.

From the available data[17] (including conversion electron Tables XXVII and XXVIII), it appears that the properties of nuclear levels excited in odd-Ir isotopes are very similar. The eccentricities are $\delta=0.14$ for Ir^{191} and $\delta=0.12$ for Ir^{193}, based on observed $E2$ transition probabilities.[4] Measured spins ($I_0=\frac{3}{2}$) and magnetic moments ($\mu=0.2$ nm) of the above Ir isotopes are consistent with ground-state assignments of $\frac{3}{2}+[402]$.

The rather complete conversion electron data, compiled in Table XXVII for $Pt^{191}\rightarrow Ir^{191}$ decay, allow

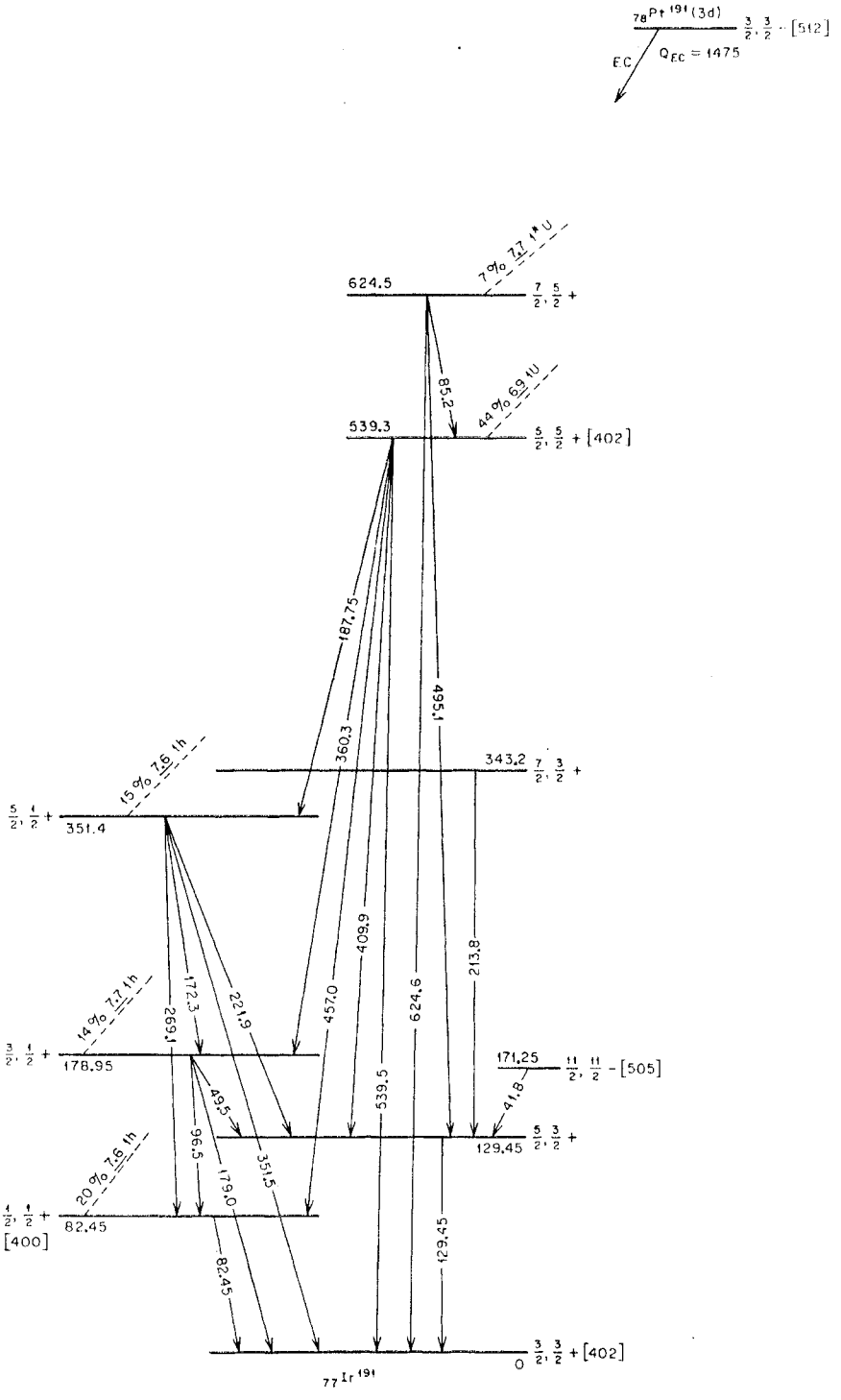

FIG. 15. Electron-capture disintegration of Pt^{191}(3 day) $\rightarrow Ir^{191}$.

TABLE XXIX. Intensity and multipolarity assigned to transitions depopulating levels shown in decay scheme of Pt^{191}(3 day) → Ir^{191} (Fig. 15).

Proposed excited states $(I,K\pi)$	(keV)	De-exciting transitions (keV)	Multipole[a] assignment	Calculated relative intensities $N_\gamma+N_{ce}$	N_γ[b]	Photon data f Smith *et al.*[c] N_γ[c]
$(\frac{3}{2},\frac{3}{2}+)$	0					
$(\frac{5}{2},\frac{3}{2}+)$	129.45	129.45	$M1/E2=7$	1170	310	545
$(\frac{7}{2},\frac{3}{2}+)$	343.2	213.8	$(M1+E2)$	4	2	
$(\frac{1}{2},\frac{1}{2}+)$	82.45	82.45	$M1/E2=1.4$	5880	565	
$(\frac{3}{2},\frac{1}{2}+)$	178.95	49.5	$M1+E2$	57	5	
		96.5	$M1/E2=55$	2620	375	
		179.0	$M1/E2=2.5$	220	112	440
$(\frac{5}{2},\frac{1}{2}+)$	351.4	172.3	$M1$	830	350	
		221.9	$(M1)$	24	14	
		269.1	$E2$	214	185	220
		351.5	$M1$	435	365	1095
$(\frac{5}{2},\frac{5}{2}+)$	539.3	360.3	$M1$	800	680	
		187.75	$(M1)$	85	40	
		409.9	$M1$	985	875	875
		457.0	$(E2)$	1120	1090	220
		539.5	$(M1)$	1270	1200	1860
$(\frac{7}{2},\frac{5}{2}+)$	624.5	85.2	$M1+E2$	112	11	
		495.1	$(M1)$	48	45	
		624.6	$(E2)$	460	453	
(11/2,11/2−)	171.25	41.8	$E3$	108	<1	
K x rays					12 000	

[a] Multipolarities are assigned either from conversion electron ratios of Table XXVII or from consistency with angular momentum selection rules; latter assignments are in parentheses and are shown unmixed since we have no way of estimating mixing ratios.
[b] Estimates of photon intensity are obtained from internal conversion electron data and theoretical conversion coefficients.
[c] Photon data of W. G. Smith and J. M. Hollander, Phys. Rev. **98**, 1258 (1955), are normalized to the 409.9-keV ($M1$) transition. Our scintillation counter measurements are in essential agreement with the previous data except for an increase in the relative intensity of the 457-keV γ ray by a factor of 2.7 observed in our spectrum.

one to expand the decay scheme presented in Nuclear Data Sheets, 1960. The postulated levels shown in Fig. 15 are compatible with the newly included multipolarities assigned in Table XXIX. One may note the agreement of calculated photon intensities (obtained by dividing K-electron intensities by the appropriate theoretical conversion coefficient) with experimental results. Our data and the results of Coulomb excitation[40] are consistent with rotational excitations of 129.4 keV $(\frac{5}{2}+)$ and 343.2 keV $(\frac{7}{2}+)$ belonging to the $\frac{3}{2}+[402]$ ground state. An intensity balance of the proposed decay scheme indicates no appreciable electron-capture branching to the $\frac{3}{2}+[402]$ configuration, and this is somewhat unexpected. The weakly fed isomeric state at 171.2 keV (11/2−) could be associated with the $11/2-[505]$ orbital.

The parent, Pt^{191}, is perhaps in a $\frac{3}{2}-[512]$ state with a disintegration energy of 1475 keV. In the decay scheme of Fig. 15, a $\frac{1}{2}+[400]$ band is shown, consisting of levels at 82.4 keV $(\frac{1}{2}+)$, 179.0 keV $(\frac{3}{2}+)$, and 351.4 keV $(\frac{5}{2}+)$. The energy level spacing of the $K=\frac{1}{2}+$ band has been fitted to the rotational energy formula (see Table XX). In this case, the Coriolis effect is probably making a considerable contribution to the energies. Such an interaction may account for the value of the parameter $B=+0.39$ keV which characterizes the $\frac{3}{2}+[402]$ band. It is estimated that 50% of the electron-capture transitions from Pt^{191} go to the members of the $K=\frac{1}{2}+$ sequence. The transitions are classified as $1h$ and are estimated to have $\log(ft)=7.6$.

At 539.3 keV, there appears a possible $\frac{5}{2}+[402]$ particle state which may have a rotational excitation at 624.5 keV $(\frac{7}{2}+)$. The rotational interpretation is consistent with the $M1/E2$ admixture of the intraband radiation. The $\log(ft)$ values are 6.9 and 7.7, respectively, for the decay to the 539.3- and 624.5-keV states. These are reasonable for the indicated $1u$ and 1^*u transitions to the two states in question.

The proposed decay scheme of Ir^{189} is shown in Fig. 16, and the associated intensities and multipolarities are listed in Table XXX. The Ir^{189} ground state should correspond with the orbital $\frac{3}{2}+[402]$ as in the case for Ir^{191}. The data suggest the development of a rotational sequence at 113.7 keV $(\frac{5}{2}+)$ and 300.5 keV $(\frac{7}{2}+)$ based on the ground $(\frac{3}{2}+)$ state. The percentage of $E2$ admixture in the $\frac{5}{2}\rightarrow\frac{3}{2}$ rotational transition is the same for both Ir^{189} and Ir^{191}. The rotational band in

[40] K. Alder, A. Bohr, T. Huus, B. Mottelson, and A. Winther, Revs. Modern Phys. **28**, 432 (1956).

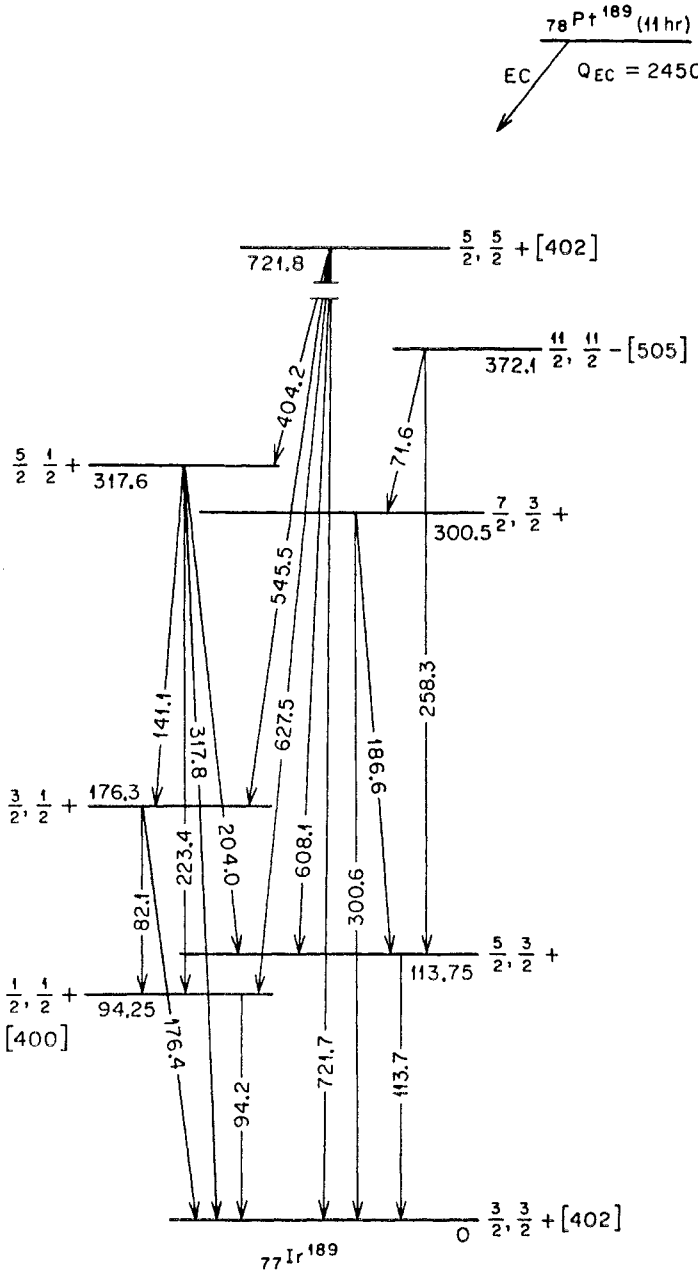

FIG. 16. Levels in Ir^{189} excited by electron-capture decay of Pt^{189} (11 h).

the lighter isotope is described by $3\hbar^2/\mathcal{I}=126.7$ keV and $B=+0.33$ keV compared with $3\hbar^2/\mathcal{I}=143.7$ keV and $B=+0.39$ keV for Ir^{191}. The inertial terms appear to reflect the rapid change in $\mathcal{I}$ for adjacent even-even nuclei. The relevant $2+\rightarrow 0+$ values are 155 keV in Os^{188} and 187 keV in Os^{190}.

The $11/2-[505]$ intrinsic state occurs at 372.1 keV in Ir^{189} and appears to correspond with the isomeric state ($T_{1/2}=4.9$ sec) which occurs in Ir^{191} at 171.2 keV. The nature of the 372.1-keV level is based on the character of the de-exciting γ rays of 71.6 keV ($M2$: $11/2-\rightarrow\frac{7}{2}+$) and 258.3 keV ($E3$: $11/2-\rightarrow\frac{5}{2}+$). The $E3$ competes to the extent of only 8%. The $M2$ and $E3$ multipole assignments are compatible with K/L and L-subshell ratio data. An estimate of the order of magnitude of the half-life of this state is 1 μsec. The mode of population of the $11/2-$ state is unknown, as is the case for the 171.2-keV level in Ir^{191}.

One may construct the levels of the $\frac{1}{2}+[400]$ configuration in Ir^{189} beginning at 94.2 keV ($\frac{1}{2}+$), with successive rotations at 176.3 keV ($\frac{3}{2}+$) and 317.6 keV ($\frac{5}{2}+$). It is apparent that the inertial parameters for

TABLE XXX. Intensity and multipolarity assigned to transitions depopulating levels shown in decay scheme of Pt^{189}(11 h) → Ir^{189} (Fig. 16).

Proposed excited states $(I,K\pi)$	(kev)	De-exciting transitions (kev)	Multipole[a] assignment	Calculated relative intensities $N_\gamma+N_{ce}$	N_γ[b]
$(\frac{3}{2},\frac{3}{2}+)$	0				
$(\frac{5}{2},\frac{3}{2}+)$	113.75	113.75	$M1/E2=7$	~3170	~700
$(\frac{7}{2},\frac{3}{2}+)$	300.5	186.65	($M1$)	560	270
		300.6	$E2$	610	550
$(\frac{1}{2},\frac{1}{2}+)$	94.25	94.25	$E2$	6575	945
$(\frac{3}{2},\frac{1}{2}+)$	176.3	82.15	$M1$	~4900	~540
		176.4	$M1+E2$	~205	~90
$(\frac{5}{2},\frac{1}{2}+)$	317.6	141.1	$M1$	1970	555
		204.0	($M1$)	~160	~85
		223.45	$E2$	285	220
		317.8	($M1$)	~510	~410
(11/2,11/2−)	372.1	71.6	$M2$	1030	17
		258.3	$E3$	80	44
$(\frac{5}{2},\frac{5}{2}+)$	721.8	404.2	($M1$)	275	240
		545.5	($M1$)	950	895
		608.1	($M1$)	1105	1060
		627.5	($E2$)	950	935
		721.7	($M1$)	1170	1135

[a] Multipolarities are assigned either from conversion electron ratios of Table XXVIII or from consistency with angular momentum selection rules; latter assignments are in parentheses and are shown unmixed since we have no way of estimating mixing ratios.
[b] Estimates of photon intensity are obtained from internal conversion electron data and theoretical conversion coefficients.

$K=\frac{1}{2}+$ bands are anomalously large; $3\hbar^2/\mathcal{I}=162$ and 200 keV for Ir^{189} and Ir^{191}, respectively. Here, the Coriolis interaction may be making a contribution of large magnitude. Of course, if the energy levels of the $K=\frac{1}{2}$ band are perturbed, it is difficult to say what the true decoupling parameters are. The intensity balance indicates electron-capture branches of about 20% proceed to the 176.3- and 317.6-keV rotational levels of the $K=\frac{1}{2}+$ band. The decays have $\log(ft)=7.3$ and are classified as $1h$.

In analogy with Pt^{191}, the ground state of Pt^{189} is designated as $\frac{3}{2}-[512]$. The dominant electron-capture branch to the 721.8-keV level is $1u$ with $\log(ft)=6.7$. Electron capture proceeds similarly to the 539.3-keV particle state in Ir^{191}, which suggests a $\frac{5}{2}+[402]$ orbital assignment for the 721.8-keV level. In addition, the experimental $M1$ branching ratios from the above $I=\frac{5}{2}+$ states to members of the $\frac{3}{2}+[402]$ bands are identically 0.6 (see Table XXI).

Pt^{193m} was present in our sources of Pt^{191}. Two transitions of 135.5- and 12.58-keV energy were identified with the isomeric decay $Pt^{193m}(4.4d) \rightarrow Pt^{193}$ (long-lived). The differences in energy of the L_I and M_I conversion electron lines of the 12.58-keV transition are those of Pt. The transition is $M1$ rather than $E1$; the latter would convert primarily to the M_{III} and N_{III} subshells. The 135.5-keV radiation belonging to Pt^{193m} is of $M4$ character. The designation as $M4$ is consistent with the observed ratios: $K/L_I/L_{II}/L_{III}=0.58/0.48/0.15/1$. This is to be compared with the theoretical values of 0.37/0.46/0.11/1 for $M4$ and 2.2/1.1/0.2/1 for $M3$.[8] Similar results have been published previously by Ewan.[41]

IV. DISCUSSION

The purpose of this investigation was to establish more detailed nuclear level schemes and to obtain data on systematic properties of the spectra. In particular, an attempt was made to ascertain the applicability of the Nilsson model. The criteria for construction of decay schemes include transition energy fits, angular momentum selection rules, internal consistency of intensity data, the characteristics of rotational configurations, interband and intraband branching ratios, and $\log(ft)$ estimates. Excited states have been classified as rotational or intrinsic, according to the available evidence and their systematic behavior. The main features of a number of earlier decay schemes have been verified.

In the analysis of nuclear excitation spectra, it is more difficult to establish the character of the high-lying states. The postulation of spins of the upper levels is generally based on the observed decay to the lower bands, and the designation of parity is made on the basis of intensity and multipolarity considerations. The assumption must be made, in general, that pure multipole transitions proceed between bands. In the absence of hindrance factors, dipole radiation which is allowed under angular momentum selection rules should be dominant. The consistency of the $\log(ft)$ values with the asymptotic selection rules proposed by Alaga[10] may allow a test of the level classifications.

This investigation of systematic behavior of energy levels ranges from mass 151 (87 neutrons) to mass 189 (113 neutrons), which expands our previous study in the region of odd-neutron numbers 99 to 107. In addition, some data are presented for two odd-proton nuclei, Ir^{189} and Ir^{191}. As pointed out in the text, the lightest nucleus to which any kind of rotational behavior may possibly be ascribed is Sm^{151} ($N=89$). At the other end of the rare-earth region, neutron number 113 appears to be the limiting case. The understanding of these limiting cases is important for the development of an adequate theory to explain the transition region. Particle states and states of collective character seem to be arranged here in a complicated way, possibly due to the influence of particle-rotation coupling of the many $K=\frac{1}{2}$, $\frac{3}{2}$, and $\frac{5}{2}$ bands in this region.

Considerable data are presented in Tables IV and XX on the nature of collective excitations which give rise to rotational bands. Empirical results from our previous investigation in the region halfway between closed shells are included in Table IV. Relevant data are the inertial parameter $3\hbar^2/\mathcal{I}$, the correction term B for deviations from the $I(I+1)$ energy ratio, as well as the

[41] G. T. Ewan, Can. J. Phys. **35**, 672 (1957).

TABLE XXXI. Summary of intrinsic excitations (in keV) listed according to the Nilsson orbital description for odd-A nuclei in the region of odd neutron numbers 89 to 113.[a] Parentheses are used to designate decreasing reliability of the level assignments; double parentheses designate least certainty.

N	Nucleus	3/2− [532]	3/2+ [402]	1/2+ [660]	3/2+ [651]	3/2− [521]	5/2+ [642]	5/2− [523]	7/2+ [633]	1/2− [521]	5/2− [512]	7/2− [514]	9/2+ [624]	1/2− [510]	3/2− [512]	7/2− [503]
89	Sm^{151}	(344)	((104))	(4)	(0)	((167))	((209))									
89	Gd^{153}	(212)	(109)		(0)	((303))	(129)									
91	Sm^{153}					0										
91	Gd^{155}	((326))	((367))	(247)	(86)	0	(105)	((286))								
93	Gd^{157}					0	(64)									
95	Gd^{159}					0										
95	Dy^{161}					74	0	25								
95	Er^{163}				((415))	(104)	((22))	(0)		(345)						
97	Dy^{163}							0								
97	Er^{165}		((1427))		((853))	(242)	(47)	0	((117))	(297)	(608)					
97	Yb^{167}					((239))	(29)	(0)								
99	Dy^{165}								(0)	(108)						
99	Er^{167}							((585))	0	207	((347))					
99	Yb^{169}							(570)	0	(24)	(191)	((962))				((1465))
101	Yb^{171}								(95)	0	122	(835)	((936))			
101	Hf^{173}									0	((107))					
103	Yb^{173}								351		0	636				
103	Hf^{175}								(207)	125	0	(348)				((1045))
105	Yb^{175}											(0)		((455))		
105	Hf^{177}								(746)		(508)	0	321			(1058)
105	W^{179}											(0)		((221))		
107	Yb^{177}											((104))	(0)	((326))		
107	Hf^{179}											(215)	0	(375)		
107	W^{181}								((953))	((746))	365	((408))	0	((385))	((560))	((807))
107	Os^{183}												0	(170)		
109	W^{183}												((309))	0	208	453
109	Os^{185}													0	127	((356))
111	W^{185}														(0)	
111	Os^{187}													0	(74)	
113	Os^{189}													36	0	((217))

[a] The compilation is based on the assignments of Mottelson and Nilsson (reference 4), our previous work (references 5 and 6), and the present work.

value of a for $K=\frac{1}{2}$ bands. In every case, the particle state is the base state of the rotational band starting with spin $I=K$.

The $M1/E2$ ratios for the first rotational transitions are listed in the above tabulations. The relative $E2$ strengths seem to depend on the details of the odd-particle orbital. Rotational ($\Delta I=1$) transitions in cascade appear to have similar $M1/E2$ mixing ratios, in the absence of strong particle-rotation coupling effects. It is also possible to show a correlation of experimental moments of inertia with the asymptotic quantum number assignments. With reference to $\frac{1}{2}-[510]$ and $\frac{3}{2}-[512]$ bands, the true moments of inertia are obscured by the rapid variation of the adjacent even-even moments in this region and by the Coriolis effect, in which the distortion is found to reflect the magnitude of the spacing of the intrinsic levels.

Figure 9 displays decoupling factors which characterize $\frac{1}{2}-[521]$ bands encountered in odd-N nuclei. The parameter a corresponds to a partial decoupling of the particle motion from the rotating nucleus. The behavior of a is of special interest since it depends on the wave function of the intrinsic motion. Mottelson and Nilsson have explicitly calculated the expected value of a as a function of deformation.[4] There is a good correlation of experiment with theory for orbital $\frac{1}{2}-[521]$, but the situation with regard to orbital $\frac{1}{2}-[510]$ is ambiguous.

The experimental evidence indicates levels which are describable by the unified model,[1] and the positions of intrinsic states which may be correlated with the Nilsson diagram.[2] The relative positions of the postulated intrinsic states in the deformed region may now be examined. Table XXXI is a summary of possible intrinsic levels for odd-N nuclei with neutron numbers 89 to 113. The particle excitations not discussed above are the same as those proposed previously.[4,5] The reliability of the state assignments is indicated by using parentheses around the level energies given in keV. At the far ends of the deformed region, the particle state

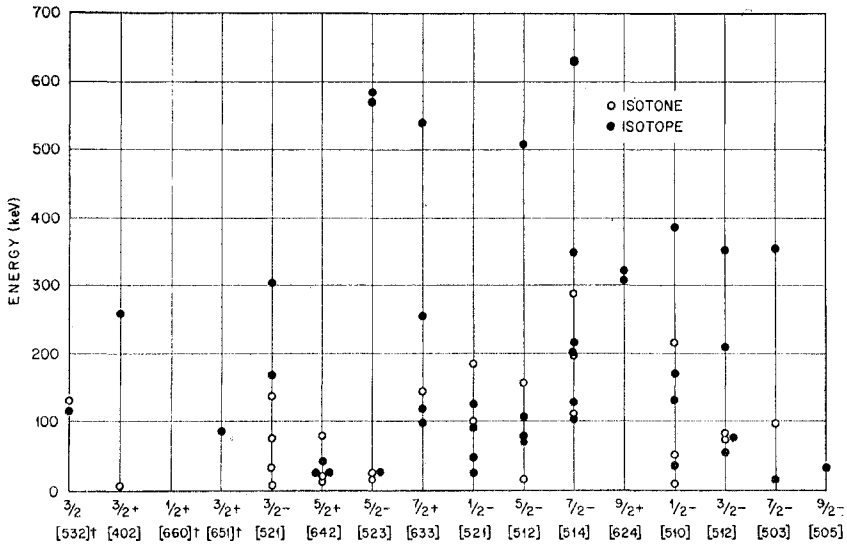

FIG. 17. Empirical energy spacing between common intrinsic states which appear in neighboring isotones and isotopes (see Table XXXI). The open circles represent the values for isotones and the filled circles are for isotopes; in each case $\Delta A = 2$.

assignments are considered less firm, partly due to a lack of evidence of rotational structures. The systematic occurrence of the properties of odd-nucleon orbitals is also less pronounced, possibly reflecting changes in nuclear deformation and of configuration mixing.

One sees a reasonably smooth trend of positions of intrinsic states reproduced by the sequence of Nilsson orbitals appropriate to the strongly deformed region. These are the $\frac{3}{2}-[521]$, $\frac{5}{2}+[642]$, $\frac{5}{2}-[523]$, $\frac{7}{2}+[633]$, $\frac{1}{2}-[521]$, $\frac{5}{2}-[512]$, $\frac{7}{2}-[514]$, $\frac{9}{2}+[624]$, $\frac{1}{2}-[510]$, $\frac{3}{2}-[512]$, $\frac{7}{2}-[503]$, and $\frac{9}{2}-[505]$ neutron orbitals. It is not surprising that the $11/2-[505]$ state is not excited in Gd isotopes since its high spin prevents it from being fed. At large deformation, orbitals $\frac{3}{2}+[402]$ and $\frac{1}{2}+[400]$ may appear; they originate below the 82-neutron shell. The following orbitals associated with smaller eccentricity may be populated: $\frac{3}{2}-[532]$, $\frac{1}{2}+[660]$, and $\frac{3}{2}+[651]$ for light rare earths, and $\frac{3}{2}-[501]$ and $\frac{5}{2}-[503]$ for the Os region.

Isotones of neutron number 95 have different ground state classifications, an unusual circumstance. The $\frac{3}{2}-[521]$, $\frac{5}{2}+[642]$, and $\frac{5}{2}-[523]$ orbitals are assigned to isotones Gd^{159}, Dy^{161}, and Er^{163}, respectively. The experimental results make these assignments fairly certain.

Stephens *et al.*[42] have pointed out the correspondence between empirical energy levels in spectra of odd-proton nuclei with $Z \geq 89$ and Nilsson's single-particle model. For instance, the ground-state levels $\frac{3}{2}+[651]$, $\frac{1}{2}-[530]$, $\frac{5}{2}+[642]$, $\frac{5}{2}-[523]$, and $\frac{3}{2}-[521]$ are observed for proton numbers 89, 91, 93, 95, and 97, respectively. It is interesting to note that the sequence of levels given above is fairly well reproduced in odd-neutron nuclei with $N \geq 89$ except for a displacement of the $\frac{1}{2}-[530]$ state.

[42] F. S. Stephens, F. Asaro, and I. Perlman, Phys. Rev. **113**, 212 (1959).

Figure 17 displays the relative energy shift of single-particle states for a sequence of isotones (open circles) and isotopes (filled circles), where the mass difference is two in each case. Common ground-state orbital assignments are not included. The observed level spacing for successive *isotones* is, for twenty cases, less than 150 keV and they average 60 keV. The remaining five cases are distributed about the 200-keV value. The energy displacement of similar levels in adjacent *isotopes* is found to vary from 20 to 600 keV. The numerical results are not distributed in any particular pattern. The direction of the energy displacement is, however, internally consistent with a few exceptions.

Glendenning and Nilsson[39] have reported similar results in a comparison of energies of analogous intrinsic states for odd-A, odd-Z deformed nuclei. They ascribe the energy shift to differences in the interaction energy of the odd proton on adding a neutron pair.

There remains the possibility of vibrational excitation of the ground or higher-lying intrinsic states. For example, for β vibrations, there should be a rotational band with $K = K_0$, and for γ vibrations, a pair of bands with $K = |K_0 \pm 2|$, where K_0 is the K number for the ground state. It is perhaps too early to conjecture further on these possibilities with the information now available.

To summarize, then, new and more precise data are presented for the decay of Pm^{151}, $Tb^{151,153,155}$, Eu^{157}, $Tm^{163,165}$, Ho^{167}, Re^{183}, $Ir^{185,187,189}$, and $Pt^{189,191,193m}$. In the tables of data, multipolarities are indicated which are based on experimental results (L or K/L ratios, or internal conversion coefficients). Some of the other indicated multipolarities are simply consistent with the decay scheme and selection rules. Tabulated ratios of reduced gamma-ray transition probabilities are based on relative K-conversion line intensities and the appropriate internal conversion coefficients; pure multi-

polarity of the lowest possible order is assumed unless a statement to the contrary is made. The possibility of multipole mixing, as well as admixtures due to the Coriolis effect would affect these ratios. To observe the effect of asymptotic selection rules, gamma-ray transitions proceeding to states of similar spin and parity were compared. Any consistency in the various intensity ratios may point out a systematic behavior which would not be obvious otherwise.

ACKNOWLEDGMENTS

We should like to extend our thanks to R. S. Livingston for his continued interest in this work. The ORNL Isotopes Division supplied the enriched samples. We are also indebted to the operating crew of the ORNL 86-in. cyclotron for a large number of successful irradiations, and to the Y-12 Analytical Chemical Development Group for use of their Leeds and Northrup Microphotometer.